DIPHTHAMIDE BIOSYNTHESIS: CHARACTERIZATION AND MECHANISTIC STUDIES OF AN UNCONVENTIONAL RADICAL SAM ENZYME PHDPH2

A Dissertation

Presented to the Faculty of the Graduate School

of Cornell University

In Partial Fulfillment of the Requirements for the Degree of

Doctor of Philosophy

by

Xuling Zhu

January 2011

DIPHTHAMIDE BIOSYNTHESIS: CHARACTERIZATION AND MECHANISTIC STUDIES OF AN UNCONVENTIONAL RADICAL SAM ENZYME PHDPH2

Xuling Zhu, Ph. D.

Cornell University 2011

Diphthamide, the target of diphtheria toxin, is a unique posttranslational modification on eukaryotic and archaeal translation elongation factor 2 (EF2). The proposed biosynthesis of diphthamide involves three steps. The first step is the formation of a C-C bond between the histidine residue and the 3-amino-3-carboxylpropyl group of S-adenosylmethionine (SAM), which is catalyzed by four enzymes Dph1-Dph4 in eukaryotic or only one enzyme Dph2 in archaea; the second step is the trimethylation of the amino group by Dph5; and the last step is an ATP depended amidation of the carboxyl group by an unknown enzyme.

We have recently found that in an archaeal species Pyrococcus horikoshii (P. horikoshii), the first step uses an S-adenosyl-L-methionine (SAM)-dependent [4Fe–4S] enzyme, PhDph2, to catalyze the formation of a C–C bond. Crystal structure shows that PhDph2 is a homodimer and each monomer contains three conserved cysteine residues that can bind a [4Fe–4S] cluster. In the reduced state, the [4Fe–4S] cluster can provide one electron to reductively cleave the bound SAM molecule. However, different from classical radical SAM enzymes, biochemical evidence suggests that a 3-amino-3-carboxypropyl radical is generated in PhDph2. Further evidence shows that the 3-amino-3-carboxypropyl radical does not undergo hydrogen abstraction reaction, which was observed for the deoxyadenosyl radical in classical radical SAM enzymes. Instead, the 3-amino-3-carboxypropyl radical is added to the

imidazole ring in the pathway towards the formation of the product. Furthermore, the chemistry requires only one [4Fe–4S] cluster to be present in the PhDph2 dimer.

The successful reconstitution of the first step of diphthamide biosynthesis provides the substrate for the second step. We then reconstituted the second step using P. horikoshii PhDph5 in vitro. The results demonstrate that PhDph5 is sufficient to catalyze the mono-, di-, and trimethylation of PhEF2. Interestingly, the trimethylated product from the PhDph5-catalyzed reaction can easily eliminate the trimethylamino group even in the very mild reaction conditions. This unexpected finding on the diphthamide biosynthesis pathway may suggest that the last amidation step occurs very quickly in cells to avoid the elimination reaction or the amidation step occurs before the trimethylation step.

BIOGRAPHICAL SKETCH

Xuling Zhu was born in Tengzhou, Shandong, P.R. China. She graduated from Shandong Normal University, where she majored in Chemistry. She got a M.S. from New York University by studying the mechanism of DNA photolyase repairing cyclobutanen pyrimidine dimer (CPD)-containing DNA under the supervision of Dr. Hans Schelvis. In January 2007, she started graduate school at Cornell University and joined the Prof. Hening Lin group, where she has elucidated the mechanisms of diphthamide biosynthesis.

To my mom,

Caring, invisible and sacrificing,

For whom virtues speak for the silent.

ACKNOWLEDGMENTS

I am truly indebted to my advisor, Prof. Hening Lin, for giving me an opportunity to study in his group and guiding me throughout these years at his lab. Dr. Lin not only provided big pictures of the dissertation projects, walked me through minute experimental details and data analysis processes, but also provided valuable advices and help on matters beyond lab work. To my committee members, Prof. Steven E. Ealick and Prof. Peng Chen, I greatly acknowledge their valuable suggestions and help.

Dr. Hong Jiang used to work in the lab until mid- night, I would like to thank him for his help to stop the LCMS and saving my trips to the lab at night. Also thank Hong for all your critical suggestions. I would like to thank Dr. Jintang Du for all the inspiring, for his helps with experimental techniques and for his kindness for letting me use some buffers he made. Very special thanks go to Xiaoyang Su, my knowledgeable lab mate, for the educational and entertaining talks on both research subjects and a wide range of topics covering science, history and politics. He has been so kind to do me many favors, in and outside the lab, which entails many pages to list. Eileen Wang helped me to make the PhEF2His600A mutant for the activity assay of PhDph2. Jungwoo Kim made the PhDph5 plasmid and did some activity assays. Thank you two for your work on the project. I also thank the rest of the members of the Lin group, present and past– Anita, Saba, Bin, Jon, Diana, Micheal, and Diane, etc. – for all the support, laughter, candy and cookies.

I wish to give thanks to our collaborators: Prof. Ealick, Dr. Yang Zhang, Dr. Andrew T. Torelli and Ms. Rachel M. Koralewski for determining the crystal structure of PhDph2; Prof. Carsten Krebs and Mr. Michael Lee for the Mössbauer spectroscopy study of PhDph2 and Prof. Jack Freed, Dr. Boris Dzikovski for the EPR studies of

PhDph2. Thank you Andrew for helping me freeze protein samples in glovebox and Boris for preparing the adaptors used to seal the EPR tubes in glovebox.

I would also give thanks to Dr. Doris Pun for giving me helpful suggestions on the dissertation writing. To Dr. Abhishek Chatterjee for training me to use glovebox and giving me helpful suggestions on how to deal with oxygen sensitive proteins. To Dr. Sheng Zhang and Robert Sherwood in the Proteomics and Mass Spectrometry of Cornell University for help with the mass analysis.

Finally, I owe so much to my husband Liang, my daughter Zhaoyi and my son Zhaoben, for their being so wonderful themselves, so understanding and supportive . Their love has always been a reliable resource for hope, motivation, strength and warmth. I also thank my parents for their love and for sacrificing themselves to take care of my children. Without their help, I would not have made so far.

TABLE OF CONTENTS

LIST OF FIGURES

LIST OF TABLES

CHAPTER 1

BACKGROUND AND INTRODUCTION

1.1.Posttranslational Modification

The proteome is encoded by the genome in each organism. The human encoding genome contains more than 30, 000 genes, whereas the human proteome consists of more than 1000, 000 molecular species of proteins(1). There are two ways to expand the preteomes: mRNA splicing (2, 3) and protein posttranslational modifications (PTMs).

PTMs play essential roles in the cellular functions and regulations. It accounts for the diversity of proteins beyond encoding by genome by changing the physical and chemical properties, conformations, stabilities and locations of the protein in cell. Histone PTMs such as methylation and demethylation, acetylation and deacetylation can regulate transcription by changing the chromatin structure (4-6). Some PTMs, such as protein phosphorylation, are related to signal transduction. For example, phosphorylation by tyrosine kinases and dephosphorylation by phosphatases of tyrosine transduce signals in the insulin/IGF-1 signaling pathway upon ligand binding to the receptor(7). Protein PTMs usually occur in two ways (1): covalent chemical modifications of a protein after its translation from mRNAs on the side chains of the amino acid residues or chemical cleavage of the peptide backbones. A protein can be modified by covalent additions of some chemical groups, usually electrophilic fragments, to one or more side chains in a protein precursor. 15 out of 20 common proteinogenic amino acids have side chains, usually a nucleophile, that can undergo such diverse modification (Table 1.1)(1). The most commonly identified PTMs include phosphorylation, methylation, acetylation, glycosylation, sulfation, prenylation and ubiquitination. Some PTMs are covalent cleavage of peptide backbones in proteins. The most common example for this kind of PTM involves insulin. Insulin is

translated as a single-chain inactive prohormone that turns to the active two-chain form of insulin by removal of the central part of the proinsulin and subsequent rejoint of the terminals with a disulfide bond (*8*).

Table 1.1. Posttranslational modifications at amino acid side chains[1](*1*)

aa Residue	posttranslational modification	Example
Asp	phosphorylation isomerization to isoAsp	protein tyrosine phosphatases
Glu	methylation carboxylation polyglycination polyglutamylation	chemotaxis receptor proteins Gla residues in blood coagulation tubulin tubulin
Ser	phosphorylation O-glycosylation phosphopantetheinylation autocleavages	serine kinases and phosphatases notch O-glycosylation fatty acid synthase pyruvamidyl enzyme formation
Thr	phosphorylation O-glycosylation	threonine kinases/phosphatases
Tyr	phosphorylation sulfation ortho-nitration TOPA quinone	tyrosine kinases/phosphatases CCR5 receptor maturation inflammatory responses amine oxidase maturation
His	phosphorylation aminocarboxypropylation N-methylation	sensor protein kinases diphthamide formation methyl CoM reductase
Lys	N-methylation N-acylation C-hydroxylation	histone methylation histone acetylation collagen maturation

[1] This table is adapted from C.T. Walsh et al. Protein Posttranslational Modifications: the Chemistry of Proteome Diversifications *Angew. Chem. Int. Ed.* **2005**, 44, 7342 -7372

Table 1.1. Continued

Cys	S-hydroxylation (S-OH) disulfide bond formation phosphorylation S-acylation S-prenylation protein splicing	sulfenate intermediates protein in oxidizing environments PTPases Ras Ras intein excisions
Met	oxidation to sulfoxide	Met sulfoxide reductase
Arg	N-methylation N-ADP-ribosylation	histones GSa
Asn	N-glycosylation N-ADP-ribosylation protein splicing	N-glycoproteins eEF-2 intein excision step
Gln	transglutamination	protein cross-linking
Trp	C-mannosylation	plasma-membrane proteins
Pro	C-hydroxylation	collagen; HIF-1a
Gly	C-hydroxylation	C-terminal amide formation

PTMs, like other biological reactions, require enzymes and sometimes co-substrates. It is worth mentioning that in most cases, PTMs are catalyzed by enzymes and more than 5% of the human geonome (between 1000 to 2000 genes) may encode enzymes dedicated to protein posttranslational modifications. The most common co-substrates involved in posttranslational modifications are small molecules such as ATP/GTP for phosphorylation, NAD for ADP-ribosylation, S-adenosyl-L-methionine (SAM) for methyl transfer and PAPS (phosphoadenosine phosphosulfate) for sulfuryl group transfer, as shown in Figure 1.1. However, some posttranslational modification

enzymes use small proteins as donors of the electrophilic fragments. For example, in the ubiquitylation of proteins, ubiquitin, a 76-residue protein, is used as a co-substrate.

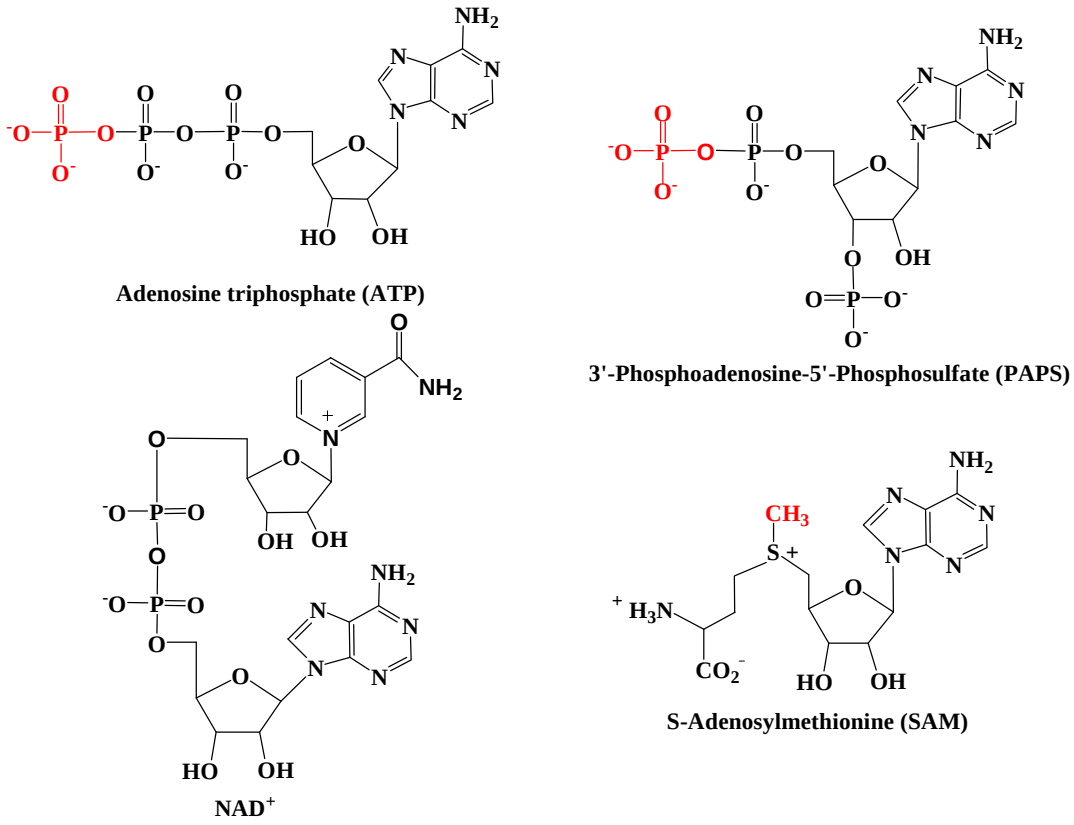

Figure 1.1. Structures of small molecular co-substrate in PTMs.

PTMs can be studied by characterizing the modified products with various techniques. The classic technique to detect the PTMs is thin layer chromatography (TLC) or high performance liquid chromatography (HPLC) after Edman degradation of the modified proteins. Another technique is autoradiography that uses radio-labeled co-substrates to label the modified proteins for detection. Two-dimensional gel electrophoresis detects the subtle difference exhibited by the modified and unmodified proteins in gel electrophoresis. Since most PTMs can result in a change in mass of

modified protein, mass spectrometry is routinely used now to detect PTMs(*9*). The changes in mass in some common PTMs are shown in table 1.2.

Table 1.2. The mass changes in some common PTMs.

PTMs	Nominal mass shift (Da)
Phosphorylation	80
Glycosylation O/N-linked	203, >800
Ubiquitination	>1000
Sumoylation	>1000
Nitration, nTyr	45
Nitrosylation, nSer, nCys	29
Methylation	14
Acetylation	42
Sulfation, sTyr	80
Deamidation	1
Farnesyl	204
Myristoyl	210
Palmitoyl	238
Disulfide bond	-2
Alkylation, aCys	57
Oxidation	16
diphthamide 1st step	101
diphthamide 2nd step	143
diphthamide 3rd step	115

1.2.Diphthamide

Diphtheria was a serious disease with fatality rate up to 20% before the introduction of vaccination. The disease is caused by a gram-positive bacterium, *Corynebacterium diphtheriae*. *C. diphtheriae* kills the host cells by secreting a toxin called diphtheria toxin (DT), which contains two fragments A and B held together by a disulfide bond. Fragment A is a catalytic domain. Fragment B is a recognition subunit and can get access to the host cell by binding to the plasma membrane. Once DT is in the endosome, fragment A will be released from fragment B into the cytosol or

intracellular fluid of the host cell and catalyze the ADP-ribosylation of the eukaryotic elongation factor 2(eEF-2) on a specific modified histidine residue(*10*, *11*). The specific modified histidine residue is a unique protein posttranslational modification on eEF2, which is named diphthamide , since it is the target of diphtheria toxin(*12*). The eEF2 is a GTPase that catalyzes the translocation of the peptidyl-tRNA and mRNA from the ribosome A site to the P site, which is essential for protein biosynthesis. The ADP-ribosylation of diphthamide by DT on eEF-2 inhibits the protein synthesis and leads to host cell death. The diphthamide residue is also a target of Pseudomonas exotoxin A (ETA), which is similar to diphtheria toxin (Figure 1.2)(*13*, *14*).

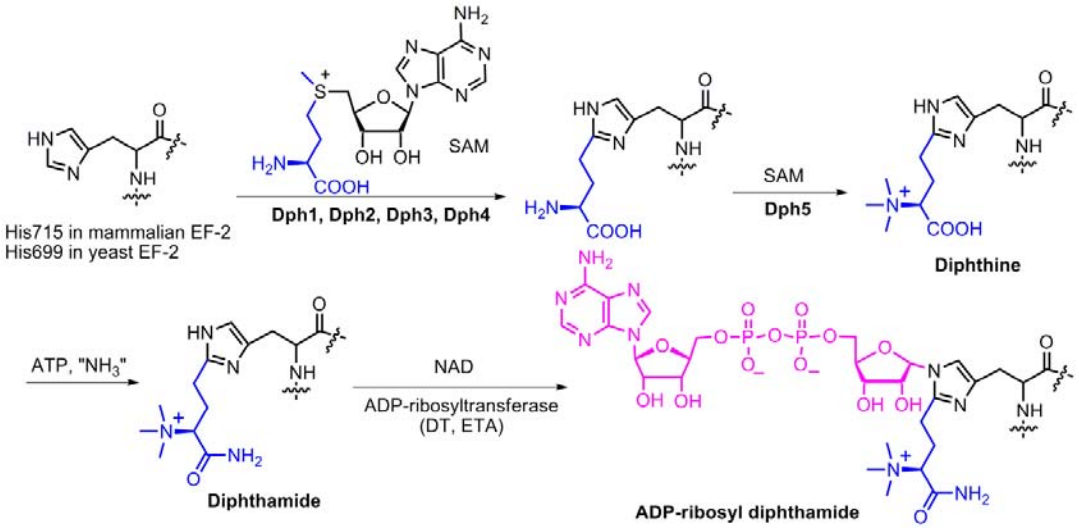

Figure 1.2. The proposed diphthamide biosynthesis pathway and ADP ribosylation ofdiphthamide by bacterial toxins. DT: Diphtheria toxin; ETA: Pseudomonas exotoxin A

Diphthamide is conserved in all eukaryotes and archaea. Although it has been identified for more than three decades, the biosynthesis and biophysical function of diphthamide remain unclear (*15*, *16*). A recent report showed that diphthamide helps

to prevent -1 frame shift in ribosomal protein synthesis(*16*). However, no obvious phenotype can be identified in yeast that lacks diphthamide modification (*12, 17, 18*). Genetic studies over the past three decades revealed that five genes, dph1, dph2, dph3, dph4, and dph5, are required for the biosynthesis of diphthamide (*12, 18-24*). The biosynthesis pathway of diphthamide was proposed based on these studies(*25*). The first step of the biosynthesis is the transfer of 3′-amino-3′-carboxypropyl group from S-adenosyl-L-methionine (SAM) (*26*) to the C-2 position of the imidazole ring of the His residue in eEF-2 (His715 in mammalian eEF-2, His699 in yeast eEF-2 and His600 in archaea *Pyrococcus horikossii*). It is catalyzed by four proteins, Dph1, Dph2, Dph3, and Dph4 in eukaryote and only one protein Dph2 was found by BLAST search in archaeal species. The second step is trimethylation of the amino group catalyzed by Dph5. The last step is ATP-dependent amidation of the carboxyl group catalyzed by unknown enzymes. The first step is particularly intriguing, because carbon-carbon bond formation is rare in posttranslational modification and in the diphthamide case it involves the poorly nucleophillic C-2 position of the imidazole ring.

Interesting questions can be asked here: How can this reaction happen? Why does it need four enzymes in the eukaryotic diphthamide biosynthesis? What are the functions of these enzymes?

Little is known about the four enzymes to date. Bioinformatics suggests that Dph1 and Dph2 are about 20% homologous. Dph1, originally named ovca1since its deletion was found in about 80% of ovarian tumors, was found to be a tumor suppressor gene in human before it was identified as one of the genes involved in diphthamide biosynthesis (*23, 27, 28*). Loss of a dph1 gene was also observed in other types of cancers, such as breast, lung, and brain malignancies (*29-32*). Homozygous dph1 knockout (dph1-/-) mice die before or at birth, while heterozygous dph1 mice (dph1+/-) survived but were prone to develop tumors later in their life(*23, 28*) .

Dph3 and Dph4 both contain a putative CSL zinc finger, which has four Cys residues to coordinate Zn^{2+} (*33*) and the last Cys residue is followed by a Ser and a Leu residue (hence the name CSL zinc finger). However, no function has been assigned to CSL zinc fingers yet. Dph3 is a small protein (~80 aa) that essentially just contains the CSL zinc finger, while Dph4 contains a J domain in addition to the zinc finger domain. The J domain is the 70-residue signature domain of the Hsp40 chaperon family of proteins (such as DnaJ in *E. coli*) and is present in many other proteins(*34*) . Dph3 is required not only for diphthamide biosynthesis, but also for synthesis of 5-methoxycarbonylmethyl (mcm^5) and 5-carbamoylmethyl (ncm^5) groups present on uridines at the wobble position of tRNA(*35*). Dph4 mutations were found in cancers. Why does Dph1 deficiency promote tumor formation? Is there any inherent connection between diphthamide and tumor suppression? In other words, does the deficiency of diphthamide on eEF-2 promote tumor formation in Dph1/Dph4 deficient cells? What is the biological function of diphthamide? These questions remain unanswered. To address these questions, we have to understand better how diphthamide is synthesized and how the biosynthesis is regulated, which is the focus of my thesis.

Originally, our lab tried to reconstitute the biosynthesis of diphthamide in yeast. But the proteins required for the biosynthesis were difficult to express. The expression levels were too low to get enough protein for the reconstitution. Later, we decided to study the diphthamide biosynthesis in a thermorphilic archaeal species, *Pyrococuss horikossii*. As mentioned above, among the four proteins required for the first step of diphthamide biosynthesis, only one is present in *P. horikoshii*. This protein was named Dph2. Here we refer it to PhDph2. We first want to know whether one enzyme, PhDph2, is enough to catalyze the modification. If it is enough, what is the reaction mechanism?

As mentioned in the last section, the first and second steps of diphthamide biosynthesis need SAM as co-substrate. Therefore, the enzymes utilized in diphthamide biosynthesis were expected to exhibit common characteristics of SAM-dependent enzymes. However, we found PhDph2 is different from all the other SAM-dependent enzymes and my thesis work will show that it mediates diphthamide biosynthesis via a novel radical mechanism. To better understand the diphthamide biosynthesis, it is necessary to introduce the SAM-dependent enzyme family in terms of their characteristics and their reaction mechanisms.

1.3. SAM-dependent Enzymes

S-adenosyl-L-methionine (SAM or AdoMet) is the second most widely used enzyme substrate after ATP (*36*) and involved in many essential biochemical processes (*37*). SAM-dependent enzymes are divided into two catalogues based on the reaction mechanism: the general SAM-dependent enzymes, which catalyze the SAM-related reaction by nucleophilic mechanism, and the radical SAM superfamily enzymes.

1.3.1. General SAM-dependent enzymes

SAM is the major methyl donor for various methylation reactions in living organisms, such as methylation of tRNA, histone, hormones and phospholipids. In these reactions, a nucleophile (:Nu) attacks the methyl carbon to heterolyticly cleave the sulfur-carbon (methyl) bond via a S_{N2} mechanism, which results in the transfer of methyl group to the nucleophile to form Nu-CH_3 and the release of S-adenosylhomocysteine (SAH), as shown in Figure1.3.

SAM is also used as a source of ribosyl groups. For example, in the penultimate step of the biosynthetic pathway of queuosine, a hypermodified tRNA nucleoside (*38-41*), SAM is cleaved by enzyme QueA to form the 2,3-epoxy-4,5-

dihydroxycyclopentane ring of the Q precursor epoxyqueosine (oQ), which reacts with tRNA to form tRNA-oQ. The mechanism is shown below (Figure1.4).

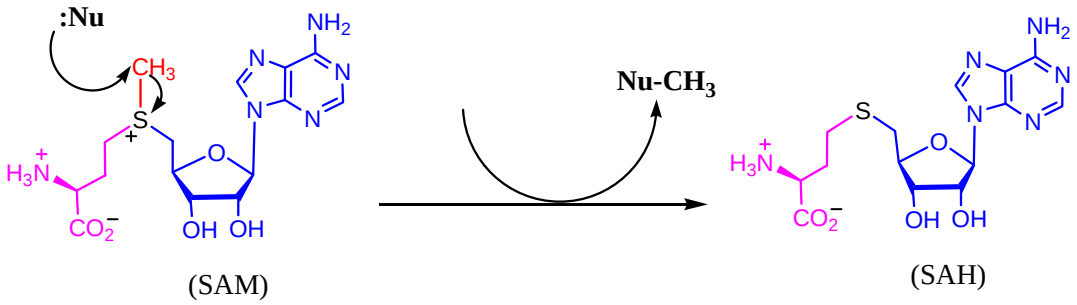

Figure 1.3. Reaction mechanism of SAM as a methyl group donor.

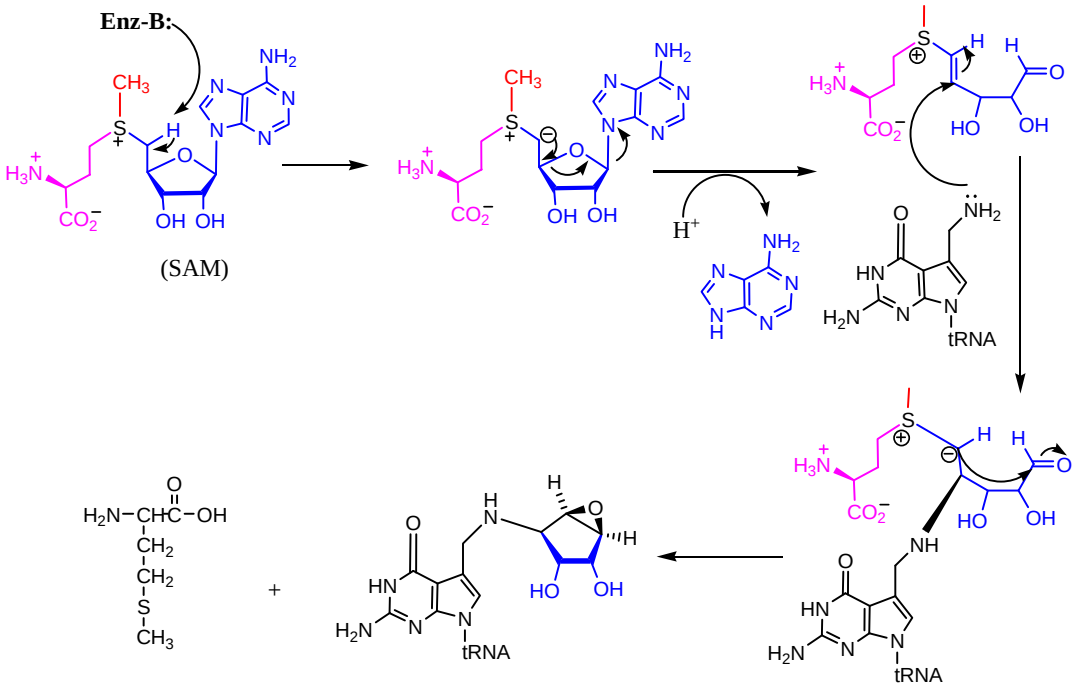

Figure 1.4. Reaction mechanism of SAM as ribosyl group donor**.**

SAM used as an aminopropyl group donor was also found in several biosynthetic pathways, such as the biosynthesis of a β-lactam antibiotic,

norcadicine(*42*), the synthesis of betaine lipid(*43*, *44*), the synthesis of spermidine(*45*) and the synthesis of wybutosine in certain tRNA(*46*) (Figure 1.5) (*42*, *44*). These reactions are believed to occur via an S_{N2}-like mechanism, with either a hydroxyl or an amino group as the nucleophile, except for the reaction in wybutosine biosynthesis (Figure 1.5) (*36*). In fact, SAM can be regarded as a positively charged sulfur atom with three different groups attached: a methyl group, a 5′-deoxyadenosyl group and a 3′-amino-3′-carboxypropyl group. The positively charged sulfur makes the adjacent carbon centers somewhat electrophilic. These carbon centers are susceptible to the attack by nucleophiles, which drives this type of SAM-dependent enzymatic reactions to occur.

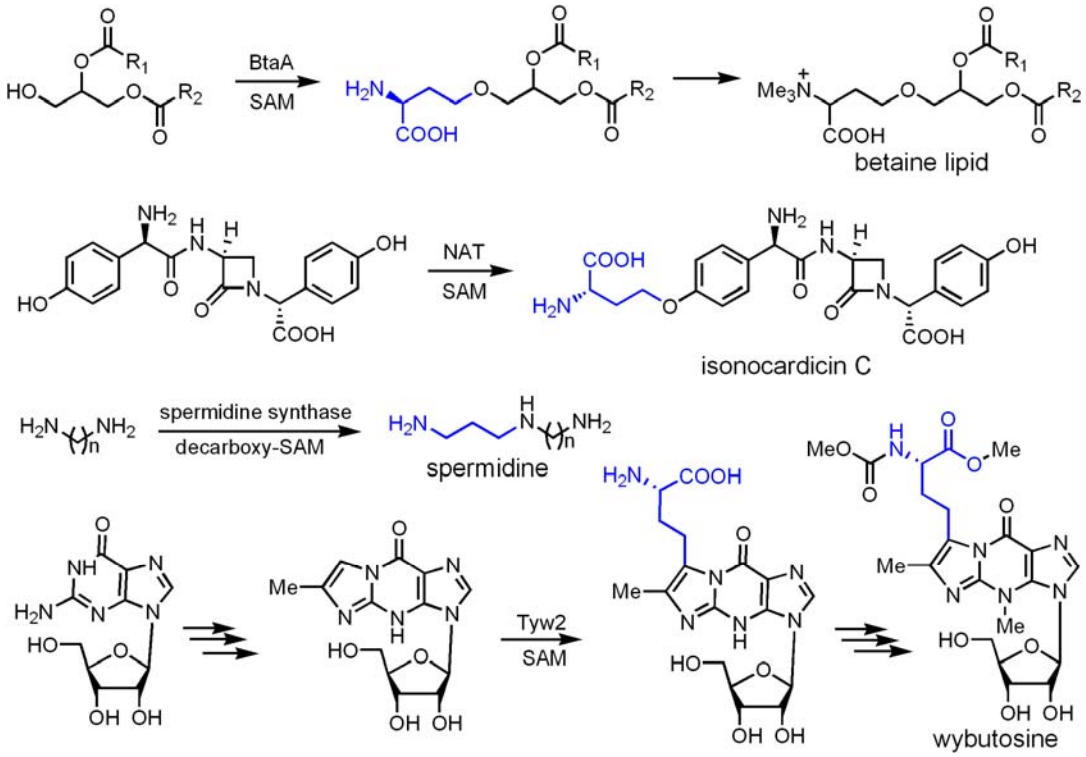

Figure 1.5. Known enzymatic reactions that involve the transfer of the substituted aminopropyl group of SAM or decarboxy-SAM to different acceptor molecules. The reaction in wybutosine biosynthesis is similar to the first step of diphthamide biosynthesis and use a carbon nucleophile.

1.3.2 Radical SAM Superfamily Enzymes

Radical S-adenosyl-L-methionine (SAM) enzymes are of ancient origins. To date, more than 2800 proteins are found by sequence analysis to belong to the radical SAM superfamily, which share a common amino acid sequence motif, CXXXCXXC near the N terminus (Table 1.3). However, recent studies have revealed some variations, such as the CXXCXXXXC motif at C terminus in ThiC, an enzyme involved in thiamine diphosphate biosynthesis in prokaryotes (*47-50*), and the CXXXXCXXC motif in Elp3(*51*) and hmdB(*52*). Therefore, the radical SAM superfamily may be significantly larger than previously imagined, and it is no longer justified to characterize the radical family simply based on the presence of a CXXXCXXC motif in the N-terminal half of a protein sequence. We should also be open to new discoveries that may expand the radical SAM family, as we have learned through this thesis work. Some members of radical SAM superfamily enzymes are listed in Table 1.4 together with the biological functions of the enzymes(*53*).

Table 1.3. Common amino acid sequence motif in classic radical SAM enzymes

LAM	…CSMYCRHC…
PFL activase	…CLMRCLYC…
ARR	…CVHECPGC…
BioB	…CPEDCYKC…
LipA	…CTRRCPFC…
common motif	CXXXCXXC

Since PhDph2 is a radical SAM enzyme, as shown in later chapters of my thesis, the radical SAM enzyme family is the focus of the following discussion, in terms of the binding mode of SAM, the structural motif of enzymes and the reaction mechanism.

Table 1.4. Classic radical SAM enzymes and their function.[2]

Enzymes	Function	Refference
LAM	Lysine 2,3aminomutase	Ruzicka et al., 2000(*54*)
BlsG	Arginine 2,3-aminomutase	Cone et al., 2003(*55*)
Eam	Glutamate 2,3-aminomutase	Ruzicka & Frey, 2007(*56*)
SplB	Spore photoproduct lyase	Rebeil et al., 1998(*57*)
DesII	Desosamine biosynthesis	Trefzer et al.,1999(*58*)
PFL activase	Glycyl radicalization	Wong et al., 1993(*59*)
ARR activase	Glycyl radicalization	Eliasson et al., 1990(*60*)
BioB	Biotin synthase	Duin et al., 1997(*61*)
LipA	Lipoyl synthase	Reed & Cronan, 1993(*62*)
HemN	Coproporphyrinogen III oxidase	Akhtar, 1994(*63*)
MoaA	Molybdopterin biosynthesis	Rieder et al., 1998(*64*)
MiaB	Methylthiolation of tRNA	Esberg et al., 1999(*65*)
TYW1	Wybusine biosynthesis in tRNAPhe	Noma et al.., 2006(*66*)
ThiH	Biogenesis of thiazole in thiamine	Begley et al., 1999(*67*)
NifB	Nitrogenase FeMoCo maturation	Allen et al., 1995(*68*)
AtsB	Formylglycine formation in	Fang et al., 2004(*69*)
CloN6	Clorobicin biosynthesis	Westrich et al., 2003(*70*)
Nclk	Cdk5 activator binding	Ching et al., 2000(*71*)
AviX12	Epimerization in Avilamycin A	Boll et al., 2006(*72*)
Elp3	Elongator complex function	Paraskevopoulou, 2006(*73*)
PcfB	Maturation of propionicin F	Brede et al., 2004(*74*)

1.3.2-1Binding mode of SAM in radical SAM enzymes

SAM binds to one iron of [4Fe-4S] cluster of radical SAM enzymes via the α-amino and α-carboxylate groups of SAM. Radical SAM enzymes use a [4Fe-4S] cluster as the reactive center. The three irons in the [4Fe-4S] cluster are coordinated with three cysteine residues in a CXXXCXXC motif, while the fourth iron is non-coordinated but locked to a certain position in the cubane structure of the [4Fe-4S] cluster. It is this iron that coordinates with the coming SAM molecule. How does SAM bind to the fourth iron? Electron nuclear double resonance (ENDOR) spectroscopy and the X-ray crystal structure make it clear. ^{15}N and ^{17}O- ENDOR

[2] This table is adapted from P. A. Frey *et al* The radical SAM superfamily *Critical Reviews in Biochemistry and Molecular Biology*, 43: 63-88, **2008**

spectroscopy on PFL activase (*75*) implicated that the amino and carboxylate groups of the methionyl moiety in SAM are ligands to the non-coordinated iron (Figure 1.6)(*76*). The x-ray crystal structure of the complex of LAM with PLP, SeSAM, and lysine shows the non-coordinated iron of the [4Fe–4S] cluster to be the nearest neighbor to selenium in SeSAM at a distance of 3.2 Å. Therefore, the fourth iron is chelated to the α-amino and α-carboxylate groups of SAM.

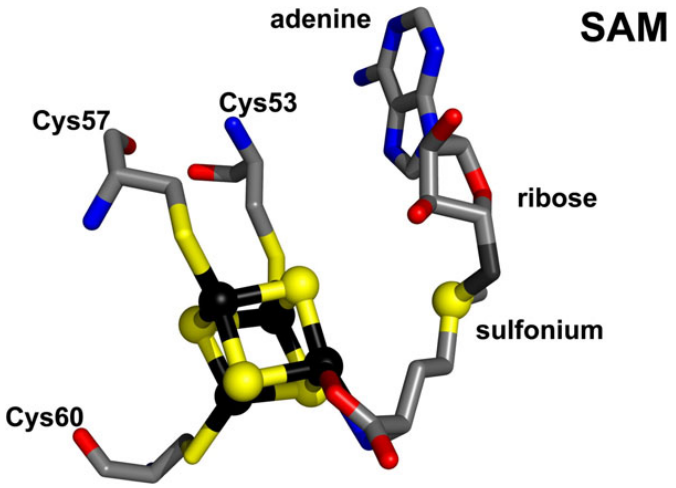

Figure 1.6. Binding mode of SAM in radical SAM enzyme[3] the three irons in the [4Fe-4S] cluster are coordinated with three cysteine residues in a CXXXCXXC motif, while the fourth iron is chelated to the α-amino and α-carboxylate groups of SAM.

1.3.2-2The structural characteristics of radical SAM enzymes

Only a few radical SAM superfamily enzymes have been structurally characterized. All of the solved structures contain a complete $(\beta\alpha)_8$ barrel (BioB and HydE) (Figure 1.7) or a partial incomplete $(\beta\alpha)_6$ barrel (*77-83*).

The crystal structures of the radical SAM enzymes shed light on the radical cleavage reaction at the active site (*84*). Firstly, in all the crystal structures the [4Fe-

[3] This Figure is from Squire J Booker and Tyler L Grove Mechanistic and functional versatility of radical SAM enzymes *F1000 Biol Report* **2010**, 2:52

4S] cluster is located at one end of the barrel with the non-coordinated iron oriented toward the center of the barrel (Figure1.7). This unique iron is coordinated by the amino and carboxyl groups of SAM, which partially seals off the cluster from solvent to protect the oxygen-sensitive cluster from degradation. Secondly, SAM is surrounded by a number of conserved residues and has various non-covalent interactions with them, such as electrostatic, H-bonding, hydrophobic, and π-stacking interactions. This apparently takes tight control of SAM binding for optimal catalytic function in the active site. Finally, several of the radical SAM crystal structures reveal the presence of loops (Figure1.7) that may undergo conformational changes upon substrate binding to help seal off the active sites for optimal radical reaction (*78*).

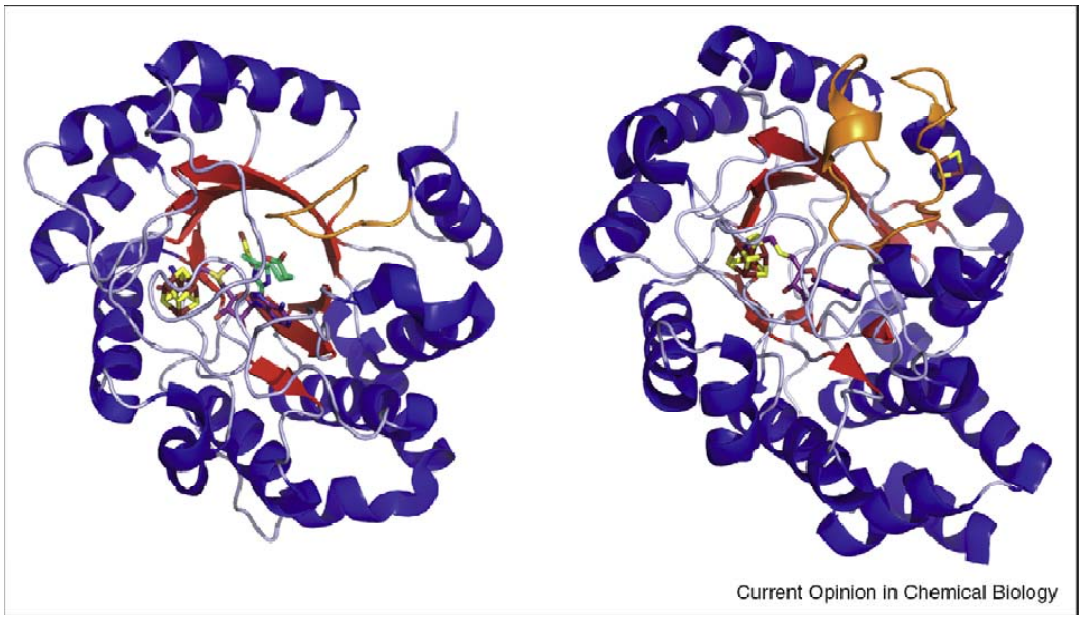

Figure 1.7. [4]X-ray crystal structures of Biotin synthase (BioB, left) with both SAM and dethiobiotin bound and HydE (right) contain a complete TIM $(\beta\alpha)_8$ barrel.

[4] Reuse Figure with permission from Duschene, K.S., Veneziano, S.E., Silver, S.C., Broderick, J.B. *Current Opinion in Chemical Biology* **2009**; *13(1):74-83* Copyright 2009, Elsevier

1.3.2-3 The reaction mechanisms in some radical SAM enzymes

In addition to crystal structure studies mentioned above, spectroscopic and biochemical characterization have also been employed to study the reaction mechanisms catalyzed by radical SAM enzymes. Their $[4Fe\text{-}4S]^{2+}$ clusters, can be reduced by dithionite in vitro to the reduced form $[4Fe\text{-}4S]^{1+}$, which transfers one electron to SAM. Subsequently SAM is cleaved to give the 5-deoxyadenosyl radical and methionine (Figure 1.8).

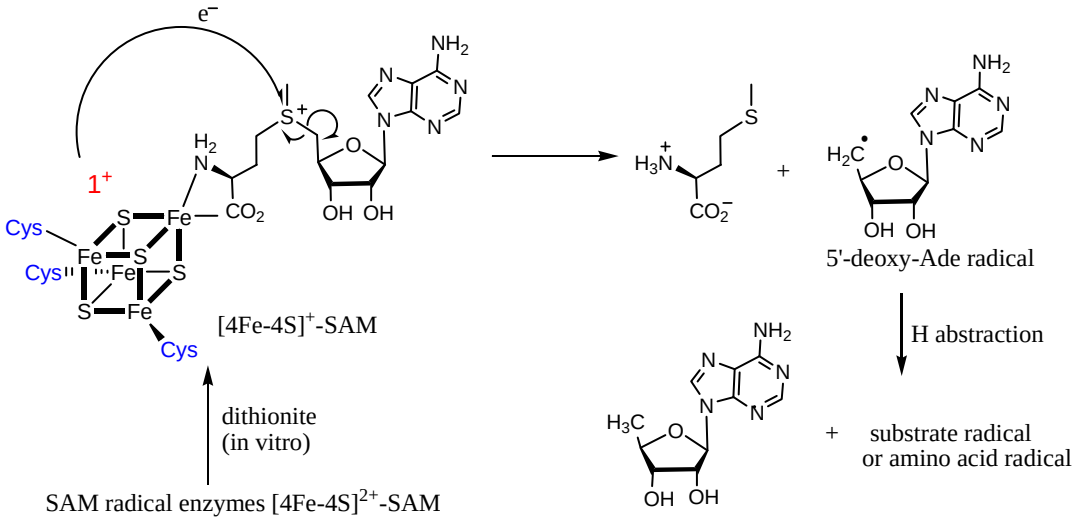

Figure 1.8. The mechanism of SAM cleavage by classic radical SAM enzymes.

Lysine 2, 3-aminomutase

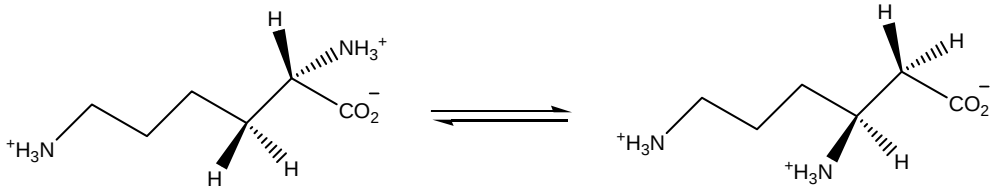

Figure 1.9. The interconversion of L- lysine and L-β-lysine catalyzed by 2, 3-aminomutase (LAM).

The most extensively studied radical SAM enzyme is lysine 2, 3-aminomutase (LAM). This enzyme catalyzes the first step in the metabolism of lysine to acetate, the interconversion of L-lysine and L-β-lysine (Figure 1.9) (*85, 86*). LAM uses pyridoxal 5′-phosphate (PLP) as a cofactor and is sensitive to air. The addition of ferrous iron and PLP increased its activity. EPR analysis indicated the presence of a [4Fe–4S] cluster (*87, 88*). And most importantly, LAM activity absolutely depends on dithionite and S-adenosyl-L-methionine (SAM). In fact, the interconversion of L-lysine and L-β-lysine basically resembles the B12-dependent rearrangement that has been known to follow a radical mechanism. However, instead of using adenosylcobalamin as a substrate, the interconversion of L-lysine and L-β-lysine catalyzed by LAM uses SAM. In addition, the traditional role of PLP in catalysis was to stabilize the amino acid carbanions (*89*), however, its role in the LAM-catalyzed reaction could not be explained, which made it more interesting to study the rearrangement mechanism involving SAM and PLP in LAM-catalyzed reaction. And SAM was later found to be cleaved to form 5′-deoxyadenosyl radical that abstracts hydrogen from the substrate lysine (*90, 91*). The mechanism of hydrogen and amino transfer is shown in Figure 1.10.

Three of the four radical intermediates in the proposed mechanism have been characterized by electron paramagnetic resonance (EPR) spectroscopy *and rapid mix-quench EPR(92)* in the presence of natural substrate, substrate analogue, or cofactor analogue. Product radical **3** (Figure 1.10) is the dominant radical in the steady state and the only one that is stable enough to be detected by EPR spectroscopy when L-lysine is the substrate (*93-96*). Radical stability can be attributed to delocalization of the unpaired electron by the carboxyl group. Radical **1** was identified and characterized by using substrate analogue, 4-thia-L-lysine, which resulted in the most stable radical intermediate under steady state conditions thanks to the adjacent 4-thia

group(*97*, *98*).

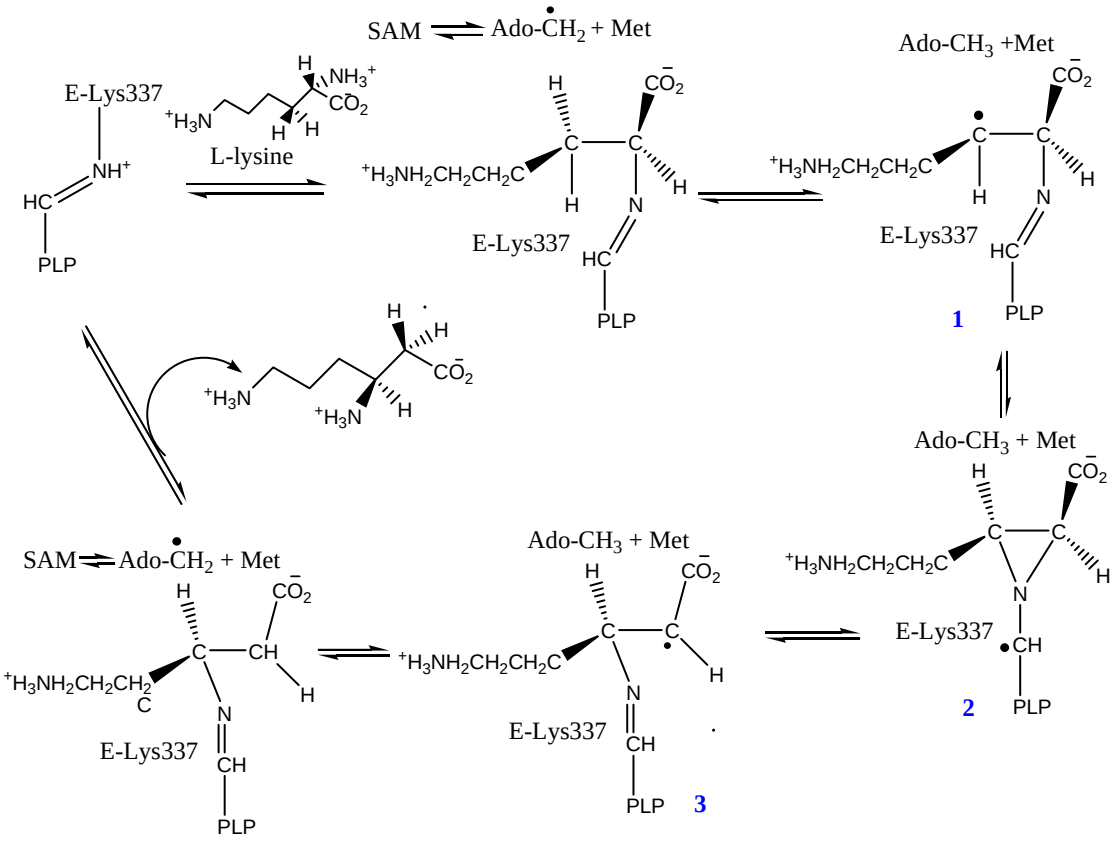

Figure 1.10. Radical reaction mechanism of Lysine 2, 3-aminomutase (LAM). Three radical intermediates (labeled 1, 2 and 3) are generated in the reaction. The radical 3 is the dominant radical in the steady state and the only one that is stable enough to be detected by EPR spectroscopy when L-lysine is the substrate. SAM serves as a coenzyme and is not consumed in the reaction.

By using the same strategy, 5′-deoxyadenosyl radical was identified and characterized using an allylic analogue of the SAM, *anhydro*SAM (*an*SAM,). An allylic radical via reductive cleavage of *an*SAM (*99*) (Figure 1.11) was spin delocalized and stable enough to be detected by EPR spectroscopy.

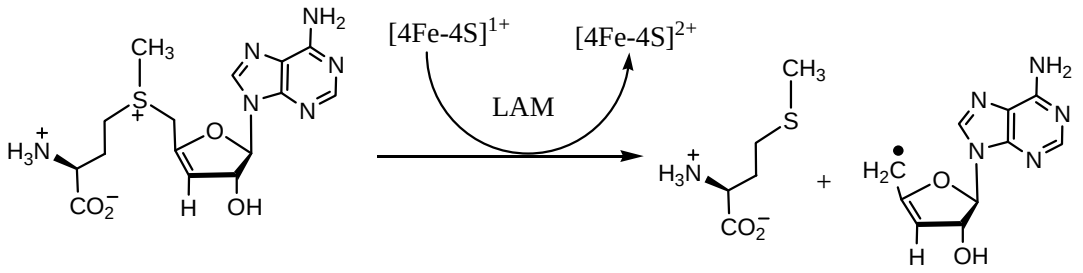

Figure 1.11. An allylic analogue of the SAM, *anhydro*SAM, can be reductively cleaved by LAM to generate a stable allylic radical, which can be detected by EPR spectroscopy.

Pyruvate Formate-Lyase Activase and Pyruvate Formate-Lyase

Pyruvate formate-lyase (PFL) catalyzes the reaction of pyruvate with coenzyme A to generate formate and acetyl-CoA(*100*) (Figure 1.12). The reaction is reversible with the forward rate at 770 sec^{-1} and a backward rate at 260 sec^{-1}(*100*). Aerobically purified PFL did not contain any metals or cofactors and was found to have no activity; anaerobically purified PFL is active in the presence of another enzyme, pyruvate formate-lyase activation enzyme (PFL-activase) (*100, 101*).

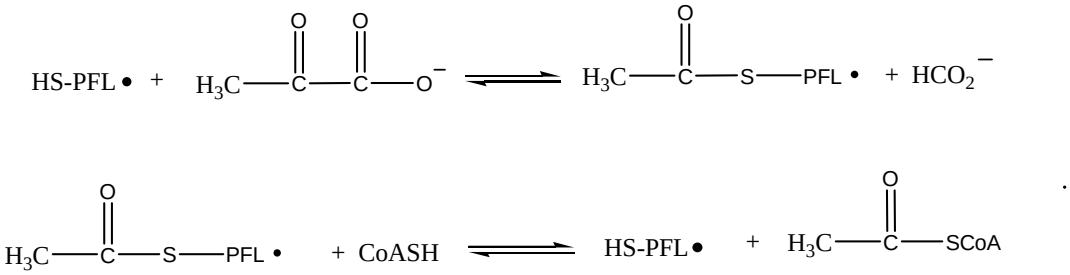

Figure 1.12. Pyruvate formate-lyase (PFL) catalyzes the reaction of pyruvate with coenzyme A to generate formate and acetyl-CoA

PFL-activase, a radical SAM enzyme, activates PFL by using a SAM derived

radical, 5'-deoxyadenosyl radical, generated by the reductive cleavage of SAM. The reaction requires SAM, and a reductant such as 5'-deazaflavin or dithionite or NADPH with the flavodoxin/flavodoxin reductase system (*101, 102*). During the PFL activation process, the 5'-deoxyadenosyl radical stereospecifically abstracts the pro-S hydrogen of Gly734 to generate the glycyl radical and 5'-deoxyadenosine (*103*) (Figure 1.13.). It was found that SAM serves as co-substrate in this reaction, since one equivalent of SAM is homolytically cleaved to generate 5'-deoxyadenosine and methionine (*104*), which is different from its role as a coenzyme in the reaction catalyzed by LAM.

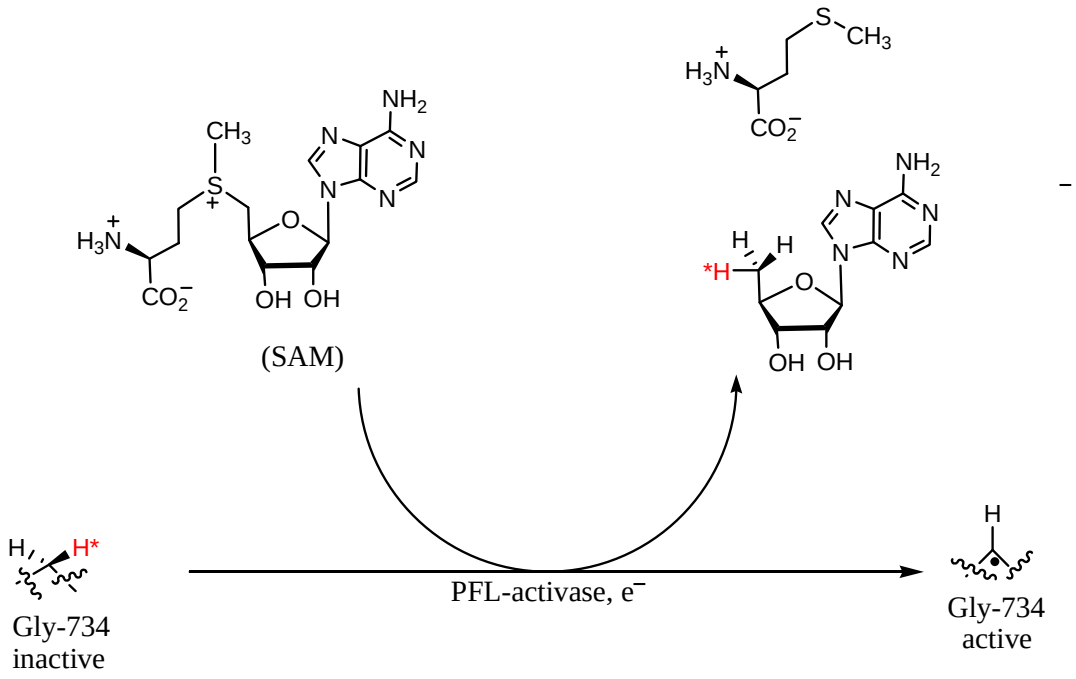

Figure 1.13. The reaction mechanism of PFL-activase. SAM as co-substrate in this reaction was consumed to generate the 5'-deoxyadenosyl radical. This radical abstracts the pro-S hydrogen of Gly734 to generate the glycyl radical and 5'-deoxyadenosine.

A stable radical on the PFL had been observed by EPR (*104*), which was later

assigned to be on the α-carbon of Gly734 (*105*). The α-hydrogen on the glycyl radical on PFL undergoes free solvent exchange as demonstrated in the EPR experiments performed in deuterium oxides (*105, 106*). The combination of mechanism-based inactivation studies and the site-directed mutagenesis showed that the exchange was assisted by Cys419 (*107, 108*). A ping-pong mechanism as shown in Figure1.14 was

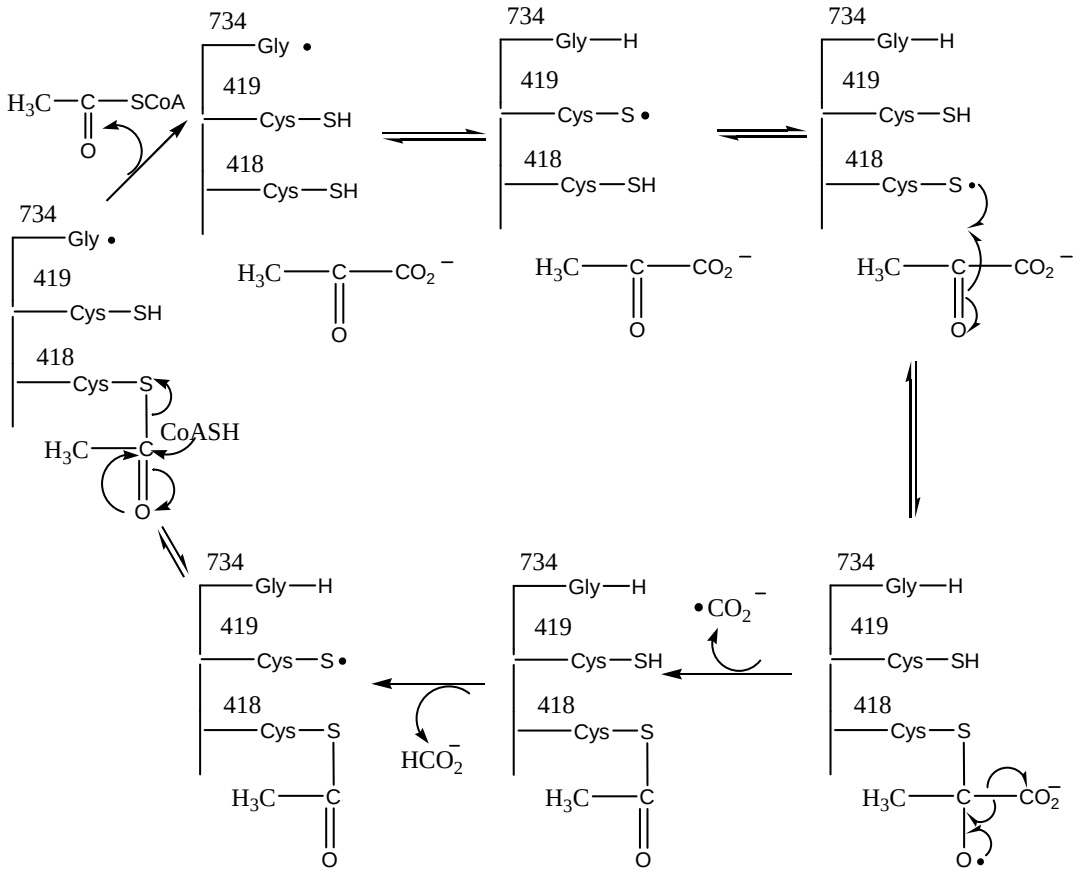

Figure 1.14. The reaction mechanism of Pyruvate formate-lyase (PFL). In this reaction, pyruvate is converted formate and acetyl-CoA

proposed (*100*). PFL incorporates two cysteine residues, Cys418 and Cys419, at its active site. Hydrogen transfers from the Cys419 to the glycyl radical to generate an intermediate cysteine-thiyl radical. The thiyl radical on Cys418 transferred from

Cys419 then produces a formyl radical, which abstracts a hydrogen atom fromCys419 to form formate and regenerate the glycyl radical. Finally, coenzyme A is acetylated by the acetyl group transferred from Cys418 (Figure 1.14).

Biotin Synthase

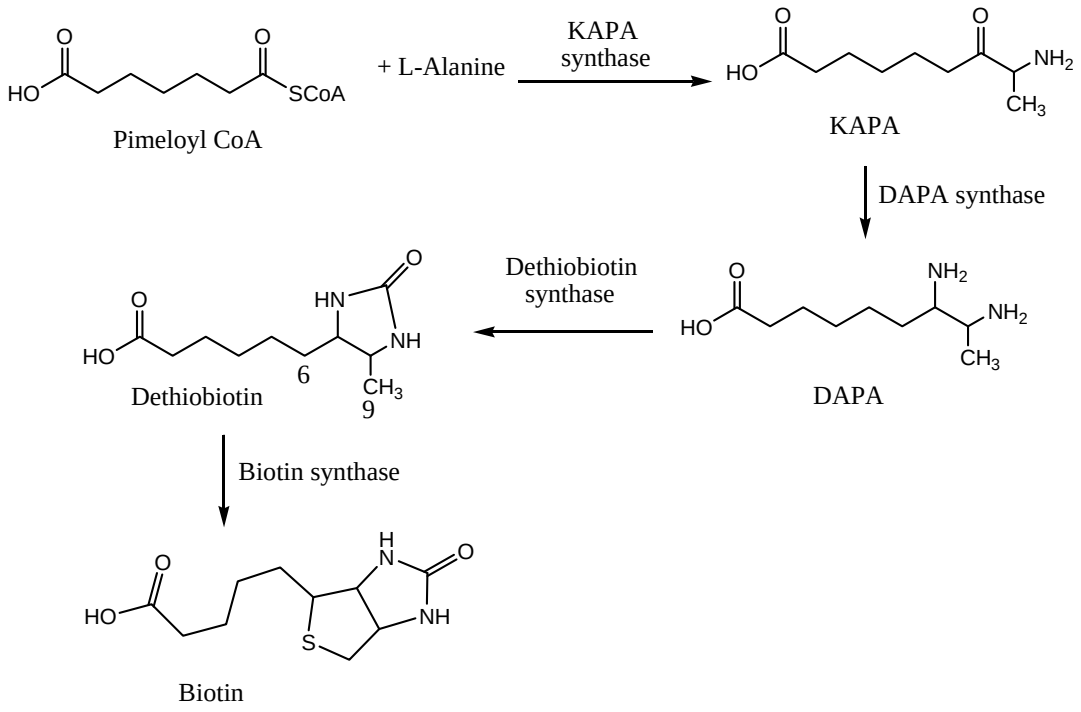

Figure 1.15. The biotin biosynthesis pathway.

The biosynthesis of biotin in plants and most bacteria includes four steps each catalyzed by one enzyme: BioF (KAPA synthase), BioA (DAPA synthase), BioD (dethiobiotin synthase) and BioB (biotin synthase) (*109*) (Figure 1.15) The convertion of dethiobiotin to biotin catalyzed by biotin synthase is the most chemically difficult one in the pathway. In this step two unreactive hydrogen atoms at carbon 6 and 9 of dethiobiotin are abstracted and a sulfur atom is inserted between these two carbons

(Figure 1.16). The reaction requires a SAM and a reducing system consisting of flavodoxin, flavodoxin reductase and NADPH (*110*).

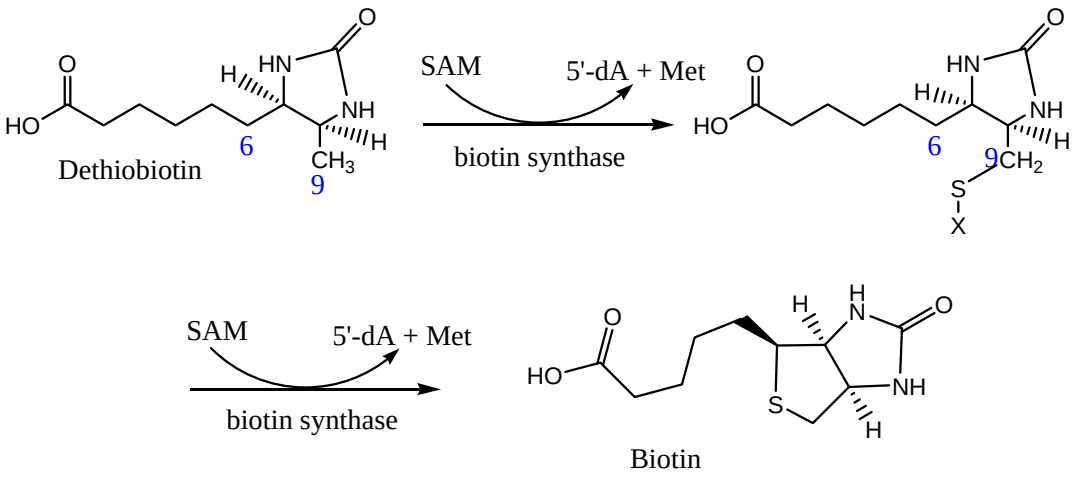

Figure 1.16. The interconversion of dethiobiotin to biotin.

The crystal structure of E. coli biotin synthase containing the SAM cofactor and the substrate dethiobiotin, is the first crystal structure of the radical SAM enzymes that has been determined (*78*). The protein is homodimeric and each monomer adopts an $(\alpha\beta)_8$ barrel. SAM, dethiobiotin, a [4Fe-4S] and a [2Fe-2S] cluster were observed in the active site. The [4Fe-4S] cluster is coordinated by three highly conserved Cys residues (Cys53, Cys57 and Cys 60), While the [2Fe-2S] cluster is coordinated by an atypical metal ligand, arginine 260 and three Cys residues (Cys97, Cys128, and Cys188) (*78*). Arg260 is not crucial for the catalysis of biotin synthase as suggested by mutagenic studies (*111*).

What is the function of the [2Fe-2S]? The [2Fe-2S] was found in the aerobically purified biotin synthase. Recent biophysical studies including UV-vis, EPR, Mössbauer, and resonance Raman spectroscopies have suggested that the sulfur atoms in biotin were derived from the [2Fe-2S] cluster (*112-114*).

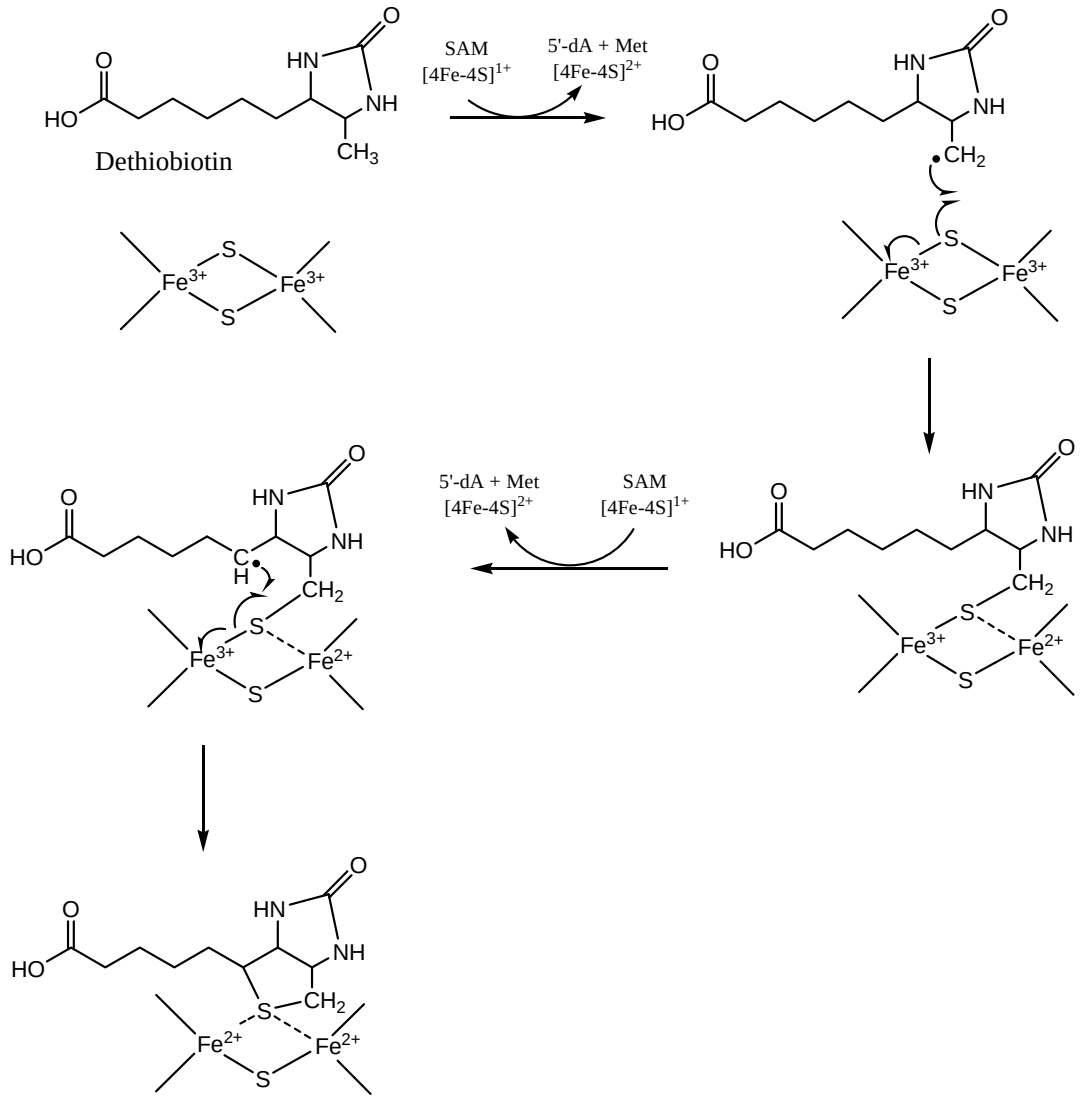

Figure 1.17. Mechanism of biotin synthesis.

The current working model for the reaction mechanism is shown in Figure 1.17. (*112*). The 5'-deoxyadenosyl radical abstracts a hydrogen atom at carbon 9 of dethiobiotin to generate 5'-deoxyadenosine, methionine, and a C-9-centered substrate radical, which subsequently attacks a bridging μ-sulfido atom of the [2Fe-2S] cluster to generate the sulfur-containing intermediate. In the next step, the 5'-deoxyadenosyl radical derived from another molecule of SAM abstracts the hydrogen on C- 6 atom of

the 9- mercaptodethiobiotin intermediate to generate the C-6-centered radical intermediate. This radical attacks the sulfur atom of the intermediate to form the thiophane ring in biotin with reduction of the coordinated FeIII to FeII. The abstraction of the hydrogen atom at C-9 occurs prior to that at C-6, which was proven by feeding the cells with ^{35}S labeled 9-mercapto dethiobiotin experiments where ^{35}S was transferred into biotin by *B. sphaericus*, while no labeled biotin was found in the same experiment with ^{35}S labeled 6-mercapto dethiobiotin (*115*).

1.4 Dissertation Statement

My dissertation investigates diphthamide biosynthesis in an archaea species Pyrocuccus horrikoshii. The proposed diphthamide biosynthesis includes three steps: the first step is the transfer of 3-amino-3-carboxylpropyl group to an histidine residue on Elongation Factor 2 (EF2) catalyzed by four enzymes in eukaryotes and one enzyme in archaea; the second step is trimethylation of the amino group and the third step is amidation of the carboxyl group. My goal is to reconstitute the diphthamide biosynthesis in vitro and investigate the mechanisms with autoradiography, spectroscopies (UV-Vis, NMR), MALDI-MS and HPLC techniques.

In Chapter 2, I will present the biochemical and spectroscopic characterization of PhDph2 and the detection of a novel radical generated by reductive cleavage of SAM by PhDph2. For the first time, we found that PhDph2 is sensitive to oxygen and determined that it contains a [4Fe-4S] cluster with x-ray crystallography, UV-vis, EPR and Mössbauer spectroscopy, suggesting that PhDph2 may use a radical mechanism. We also tried to detect the radical products with biochemical techniques such as autoradiography, MALDI-MS and HPLC. The autoradiography experiment shows that in the present of PhEF2, PhDph2 can transfer 3′-amino-3′-carboxypropyl from SAM to PhEF2. The MALDI-MS of digested PhEF2 after reaction further confirmed the

modification on PhEF2. An HPLC assay demonstrated that PhDph2 can cleave SAM to form 5′-deoxy-5′-methylthioadenosine (MTA) in the presence of a reductant dithionite. Two possible mechanisms of the first step of diphthamide biosynthesis, the radical mechanism and the nucleophilic attacking mechanism, were proposed based on the SAM cleavage product of MTA. The other product of SAM cleavage, 2′-aminobutiric acid (ABA), was identified by NMR and also detected by LCMS after dansyltion reaction monitored by LCMS. Therefore, PhDph2 is a novel radical SAM enzyme and catalyzes the first step of diphthamdie biosynthesis via a 3′-amino-3′-carboxyl radical through a radical mechanism.

In Chapter 3, detailed mechanistic studies of the first step of diphthamide biosynthesis were presented. We found that 3′-amino-3′-carboxyl radical was added directly to the C2 of imidozole ring, instead of abstracting one hydrogen to produce an amino acid radical. Furthermore, only one [4Fe-4S] cluster instead of both of the clusters in the homodimer is needed to facilitate the enzymatic reaction.

The last chapter of my dissertation shows the work on the reconstitution of the second step of diphthamide biosynthesis. Successful reconstitution of the first step of the diphthamide biosynthesis in vitro set stage for the reconstitution of the second step by providing the substrate for the second step reaction. We found that PhDph5 is sufficient to catalyze the mono-, di- and trimethylation of PhEF2. In addition, the trimethylated product can easily eliminate the trimethylamino group even in very mild reaction conditions in vitro, which may suggest that the last step of diphthamide biosynthesis may occur very fast to prevent the elimination reaction from happening in vivo.

REFERENCES

1. Walsh, C. T., Garneau-Tsodikova, S., and Gatto, G. J., Jr. (2005) Protein posttranslational modifications: the chemistry of proteome diversifications, *Angew Chem Int Ed Engl 44*, 7342-7372.

2. Maniatis, T., and Tasic, B. (2002) Alternative pre-mRNA splicing and proteome expansion in metazoans, *Nature 418*, 236-243.

3. Black, D. L. (2003) Mechanisms of alternative pre-messenger RNA splicing, *Annu Rev Biochem 72*, 291-336.

4. Strahl, B. D., and Allis, C. D. (2000) The language of covalent histone modifications, *Nature 403*, 41-45.

5. Jenuwein, T., and Allis, C. D. (2001) Translating the histone code, *Science 293*, 1074-1080.

6. Roth, S. Y., Denu, J. M., and Allis, C. D. (2001) Histone acetyltransferases, *Annu Rev Biochem 70*, 81-120.

7. Tagwerker, C., Flick, K., Cui, M., Guerrero, C., Dou, Y., Auer, B., Baldi, P., Huang, L., and Kaiser, P. (2006) A tandem affinity tag for two-step purification under fully denaturing conditions: application in ubiquitin profiling and protein complex identification combined with in vivocross-linking, *Mol Cell Proteomics 5*, 737-748.

8. Dodson, G., and Steiner, D. (1998) The role of assembly in insulin's biosynthesis, *Curr Opin Struct Biol 8*, 189-194.

9. Farley, A. R., and Link, A. J. (2009) Identification and quantification of protein posttranslational modifications, *Methods Enzymol 463*, 725-763.

10. Van Ness, B. G., Howard, J. B., and Bodley, J. W. (1980) ADP-ribosylation of elongation factor 2 by diphtheria toxin. Isolation and properties of the novel ribosyl-amino acid and its hydrolysis products, *J. Biol. Chem. 255*, 10717-10720.

11. Van Ness, B. G., Howard, J. B., and Bodley, J. W. (1980) ADP-ribosylation of elongation factor 2 by diphtheria toxin. NMR spectra and proposed structures of ribosyl-diphthamide and its hydrolysis products, *J. Biol. Chem. 255*, 10710-10716.

12. Liu, S., Milne, G. T., Kuremsky, J. G., Fink, G. R., and Leppla, S. H. (2004) Identification of the proteins required for biosynthesis of diphthamide, the target of bacterial ADP-ribosylating toxins on translation elongation factor 2, *Mol. Cell. Biol. 24*, 9487-9497.

13. Perentesis, J. P., Miller, S. P., and Bodley, J. W. (1992) Protein toxin inhibitors of protein-synthesis, *Biofactors 3*, 173-184.

14. Walsh, C. T. (2006) *Posttranslational modifications of proteins: Expanding nature's inventory*, Roberts and Company Publishers, Englewood, Colorado.

15. Gomez-Lorenzo, M. G., Spahn, C. M. T., Agrawal, R. K., Grassucci, R. A., Penczek, P., Chakraburtty, K., Ballesta, J. P. G., Lavandera, J. L., Garcia-Bustos, J. F., and Frank, J. (2000) Three-dimensional cryo-electron microscopy localization of EF2 in the *Saccharomyces cerevisiae* 80S ribosome at 17.5 Å resolution, *EMBO J. 19*, 2710-2718.

16. Ortiz, P. A., Ulloque, R., Kihara, G. K., Zheng, H., and Kinzy, T. G. (2006) Translation elongation factor 2 anticodon mimicry domain mutants affect fidelity and diphtheria toxin resistance, *J. Biol. Chem. 281*, 32639-32648.

17. Phan, L. D., Perentesis, J. P., and Bodley, J. W. (1993) Saccharomyces cerevisiae elongation factor 2. Mutagenesis of the histidine precursor of diphthamide yields a functional protein that is resistant to diphtheria toxin, *J. Biol. Chem. 268*, 8665-8668.

18. Mattheakis, L. C., Sor, F., and Collier, R. J. (1993) Diphthamide synthesis in *Saccharomyces cerevisiae*: structure of the DPH2 gene, *Gene 132*, 149.

19. Moehring, J. M., Moehring, T. J., and Danley, D. E. (1980) Posttranslational modification of elongation factor 2 in diphtheriatoxin-resistant mutants of CHO-K1 cells, *Proc. Natl. Acad. Sci. USA 77*, 1010-1014.

20. Moehring, T. J., Danley, D. E., and Moehring, J. M. (1984) In vitro biosynthesis of diphthamide, studied with mutant Chinese hamster ovary cells resistant to diphtheria toxin, *Mol. Cell. Biol. 4*, 642-650.

21. Chen, J. Y., Bodley, J. W., and Livingston, D. M. (1985) Diphtheria toxin-resistant mutants of *Saccharomyces cerevisiae.*, *Mol. Cell. Biol. 5*, 3357-3360.

22. Mattheakis, L., Shen, W., and Collier, R. (1992) DPH5, a methyltransferase gene required for diphthamide biosynthesis in Saccharomyces cerevisiae., *Mol. Cell. Biol. 12*, 4026-4037.

23. Phillips, N. J., Ziegler, M. R., and Deaven, L. L. (1996) A cDNA from the ovarian cancer critical region of deletion on chromosome 17p13.3, *Cancer Lett. 102*, 85.

24. Schultz, D. C., Balasara, B. R., Testa, J. R., and Godwin, A. K. (1998) Cloning and localization of a human diphthamide biosynthesis-like protein-2 gene,DPH2L2, *Genomics 52*, 186.

25. Chen, J. Y., and Bodley, J. W. (1988) Biosynthesis of diphthamide in Saccharomyces cerevisiae. Partial purification and characterization of a specific S-adenosyl-L-methionine:elongation factor 2 methyltransferase, *J Biol Chem 263*, 11692-11696.

26. Dunlop, P. C., and Bodley, J. W. (1983) Biosynthetic labeling of diphthamide in Saccharomyces cerevisiae, *J Biol Chem 258*, 4754-4758.

27. Chen, C.-M., and Behringer, R. R. (2005) OVCA1: tumor suppressor gene, *Curr. Opin. Genet. Dev. 15*, 49.

28. Phillips, N. J., Ziegler, M. R., Radford, D. M., Fair, K. L., Steinbrueck, T., Xynos, F. P., and Donis-Keller, H. (1996) Allelic deletion on chromosome 17p13.3 in early ovarian cancer, *Cancer Res. 56*, 606-611.

29. Konishi, H., Takahashi, T., Kozaki, K., Yatabe, Y., Mitsudomi, T., Fujii, Y., Sugiura, T., and Matsuda, H. (1998) Detailed deletion mapping suggests the involvement of a tumor suppressor gene at 17p13.3, distal to p53, in the pathogenesis of lung cancers, *Oncogene 17*, 2095-2100.

30. Phelan, C. M., Borg, A., Cuny, M., Crichton, D. N., Baldersson, T., Andersen, T. I., Caligo, M. A., Lidereau, R., Lindblom, A., Seitz, S., Kelsell, D., Hamann, U., Rio, P., Thorlacius, S., Papp, J., Olah, E., Ponder, B., Bignon, Y. J., Scherneck, S., Barkardottir, R., Borresen-Dale, A. L., Eyfjord, J., Theillet, C., Thompson, A. M., Larsson, C., and et al. (1998) Consortium study on 1280 breast carcinomas: allelic loss on chromosome 17 targets subregions associated with family history and clinical parameters, *Cancer Res 58*, 1004-1012.

31. Liscia, D. S., Morizio, R., Venesio, T., Palenzona, C., Donadio, M., and Callahan, R. (1999) Prognostic significance of loss of heterozygosity at loci on chromosome 17p13.3-ter in sporadic breast cancer is evidence for a putative tumour suppressor gene, *Br J Cancer 80*, 821-826.

32. Hoff, C., Mollenhauer, J., Waldau, B., Hamann, U., and Poustka, A. (2001) Allelic imbalance and fine mapping of the 17p13.3 subregion in sporadic breast carcinomas, *Cancer Genet Cytogenet 129*, 145-149.

33. Sun, J., Zhang, J., Wu, F., Xu, C., Li, S., Zhao, W., Wu, Z., Wu, J., Zhou, C.-Z., and Shi, Y. (2005) Solution structure of Kti11p from *Saccharomyces cerevisiae* reveals a novel zinc-binding module, *Biochemistry 44*, 8801-8809.

34. Kelley, W. L. (1998) The J-domain family and the recruitment of chaperone power, *Trends Biochem. Sci. 23*, 222-227.

35. Huang, B. O., Johansson, M. J. O., and Bystrom, A. S. (2005) An early step in wobble uridine tRNA modification requires the Elongator complex, *RNA 11*, 424-436.

36. Fontecave, M., Atta, M., and Mulliez, E. (2004) S-adenosyl-L-methionine: nothing goes to waste, *Trends Biochem Sci 29*, 243-249.

37. Cantoni, G. L. (1975) Biological methylation: selected aspects, *Annu Rev Biochem 44*, 435-451.

38. Grimm, C., Klebe, G., Ficner, R., and Reuter, K. (2000) Screening orthologs as an important variable in crystallization: preliminary X-ray diffraction studies of the tRNA-modifying enzyme S-adenosyl-methionine:tRNA ribosyl transferase/isomerase, *Acta Crystallogr D Biol Crystallogr 56*, 484-488.

39. Iwata-Reuyl, D. (2003) Biosynthesis of the 7-deazaguanosine hypermodified nucleosides of transfer RNA, *Bioorg Chem 31*, 24-43.

40. Van Lanen, S. G., and Iwata-Reuyl, D. (2003) Kinetic mechanism of the tRNA-modifying enzyme S-adenosyl-L-methionine:tRNA ribosyltransferase-isomerase (QueA), *Biochemistry 42*, 5312-5320.

41. Van Lanen, S. G., Kinzie, S. D., Matthieu, S., Link, T., Culp, J., and Iwata-Reuyl, D. (2003) tRNA modification by S-adenosyl-L-methionine:tRNA ribosyltransferase-isomerase. Assay development and characterization of the recombinant enzyme, *J Biol Chem 278*, 10491-10499.

42. Reeve, A. M., Breazeale, S. D., and Townsend, C. A. (1998) Purification, characterization, and cloning of an S-adenosyl-L-methionine-dependent 3-amino-3-carboxypropyltransferase in nocardicin biosynthesis, *J. Biol. Chem. 273*, 30695-30703.

43. Klug, R. M., and Benning, C. (2001) Two enzymes of diacylglyceryl-O-4'-(N,N,N,-trimethyl)homoserine biosynthesis are encoded by btaA and btaB in the purple bacterium Rhodobacter sphaeroides, *Proc. Natl. Acad. Sci. USA 98*, 5910-5915.

44. Riekhof, W. R., Andre, C., and Benning, C. (2005) Two enzymes, BtaA and BtaB, are sufficient for betaine lipid biosynthesis in bacteria, *Arch. Biochem. Biophys. 441*, 96-105.

45. Ikeguchi, Y., Bewley, M. C., and Pegg, A. E. (2006) Aminopropyltransferases: function, structure and genetics, *J. Biochem. 139*, 1-9.

46. Noma, A., Kirino, Y., Ikeuchi, Y., and Suzuki, T. (2006) Biosynthesis of wybutosine, a hyper-modified nucleoside in eukaryotic phenylalanine tRNA, *EMBO J. 25*, 2142–2154.

47. Chatterjee, A., Li, Y., Zhang, Y., Grove, T. L., Lee, M., Krebs, C., Booker, S. J., Begley, T. P., and Ealick, S. E. (2008) Reconstitution of ThiC in thiamine pyrimidine biosynthesis expands the radical SAM superfamily, *Nat Chem Biol 4*, 758-765.

48. Martinez-Gomez, N. C., and Downs, D. M. (2008) ThiC is an [Fe-S] cluster protein that requires AdoMet to generate the 4-amino-5-hydroxymethyl-2-methylpyrimidine moiety in thiamin synthesis, *Biochemistry 47*, 9054-9056.

49. Martinez-Gomez, N. C., Poyner, R. R., Mansoorabadi, S. O., Reed, G. H., and Downs, D. M. (2009) Reaction of AdoMet with ThiC generates a backbone free radical, *Biochemistry 48*, 217-219.

50. Raschke, M., Burkle, L., Muller, N., Nunes-Nesi, A., Fernie, A. R., Arigoni, D., Amrhein, N., and Fitzpatrick, T. B. (2007) Vitamin B1 biosynthesis in plants requires the essential iron sulfur cluster protein, THIC, *Proc Natl Acad Sci U S A 104*, 19637-19642.

51. Okada, Y., Yamagata, K., Hong, K., Wakayama, T., and Zhang, Y. A role for the elongator complex in zygotic paternal genome demethylation, *Nature 463*, 554-558.

52. McGlynn, S. E., Boyd, E. S., Shepard, E. M., Lange, R. K., Gerlach, R., Broderick, J. B., and Peters, J. W. Identification and characterization of a novel member of the radical AdoMet enzyme superfamily and implications for the biosynthesis of the Hmd hydrogenase active site cofactor, *J Bacteriol 192*, 595-598.

53. Frey, P. A., Hegeman, A. D., and Ruzicka, F. J. (2008) The Radical SAM Superfamily, *Crit Rev Biochem Mol Biol 43*, 63-88.

54. Ruzicka, F. J., Lieder, K. W., and Frey, P. A. (2000) Lysine 2,3-aminomutase from Clostridium subterminale SB4: mass spectral characterization of cyanogen bromide-treated peptides and cloning, sequencing, and expression of the gene kamA in Escherichia coli, *J Bacteriol 182*, 469-476.

55. Cone, M. C., Yin, X., Grochowski, L. L., Parker, M. R., and Zabriskie, T. M. (2003) The blasticidin S biosynthesis gene cluster from Streptomyces griseochromogenes: sequence analysis, organization, and initial characterization, *Chembiochem 4*, 821-828.

56. Ruzicka, F. J., and Frey, P. A. (2007) Glutamate 2,3-aminomutase: a new member of the radical SAM superfamily of enzymes, *Biochim Biophys Acta 1774*, 286-296.

57. Rebeil, R., Sun, Y., Chooback, L., Pedraza-Reyes, M., Kinsland, C., Begley, T. P., and Nicholson, W. L. (1998) Spore photoproduct lyase from Bacillus subtilis spores is a novel iron-sulfur DNA repair enzyme which shares features with proteins such as class III anaerobic ribonucleotide reductases and pyruvate-formate lyases, *J Bacteriol 180*, 4879-4885.

58. Trefzer, A., Salas, J. A., and Bechthold, A. (1999) Genes and enzymes involved in deoxysugar biosynthesis in bacteria, *Nat Prod Rep 16*, 283-299.

59. Wong, K. K., Murray, B. W., Lewisch, S. A., Baxter, M. K., Ridky, T. W., Ulissi-DeMario, L., and Kozarich, J. W. (1993) Molecular properties of pyruvate formate-lyase activating enzyme, *Biochemistry 32*, 14102-14110.

60. Eliasson, R., Fontecave, M., Jornvall, H., Krook, M., Pontis, E., and Reichard, P. (1990) The anaerobic ribonucleoside triphosphate reductase from Escherichia coli requires S-adenosyl-L-methionine as a cofactor, *Proc Natl Acad Sci U S A 87*, 3314-3318.

61. Duin, E. C., Lafferty, M. E., Crouse, B. R., Allen, R. M., Sanyal, I., Flint, D. H., and Johnson, M. K. (1997) [2Fe-2S] to [4Fe-4S] cluster conversion in Escherichia coli biotin synthase, *Biochemistry 36*, 11811-11820.

62. Reed, K. E., and Cronan, J. E., Jr. (1993) Lipoic acid metabolism in Escherichia coli: sequencing and functional characterization of the lipA and lipB genes, *J Bacteriol 175*, 1325-1336.

63. Akhtar, M. (1994) The modification of acetate and propionate side chains during the biosynthesis of haem and chlorophylls: mechanistic and stereochemical studies, *Ciba Found Symp 180*, 131-151; discussion 152-135.

64. Rieder, C., Eisenreich, W., O'Brien, J., Richter, G., Gotze, E., Boyle, P., Blanchard, S., Bacher, A., and Simon, H. (1998) Rearrangement reactions in the biosynthesis of molybdopterin--an NMR study with multiply 13C/15N labelled precursors, *Eur J Biochem 255*, 24-36.

65. Esberg, B., Leung, H. C., Tsui, H. C., Bjork, G. R., and Winkler, M. E. (1999) Identification of the miaB gene, involved in methylthiolation of isopentenylated A37 derivatives in the tRNA of Salmonella typhimurium and Escherichia coli, *J Bacteriol 181*, 7256-7265.

66. Noma, A., Kirino, Y., Ikeuchi, Y., and Suzuki, T. (2006) Biosynthesis of wybutosine, a hyper-modified nucleoside in eukaryotic phenylalanine tRNA, *EMBO J 25*, 2142-2154.

67. Begley, T. P., Xi, J., Kinsland, C., Taylor, S., and McLafferty, F. (1999) The enzymology of sulfur activation during thiamin and biotin biosynthesis, *Curr Opin Chem Biol 3*, 623-629.

68. Allen, R. M., Chatterjee, R., Ludden, P. W., and Shah, V. K. (1995) Incorporation of iron and sulfur from NifB cofactor into the iron-molybdenum cofactor of dinitrogenase, *J Biol Chem 270*, 26890-26896.

69. Fang, Q., Peng, J., and Dierks, T. (2004) Post-translational formylglycine modification of bacterial sulfatases by the radical S-adenosyl-L-methionine protein AtsB, *J Biol Chem 279*, 14570-14578.

70. Westrich, L., Heide, L., and Li, S. M. (2003) CloN6, a novel methyltransferase catalysing the methylation of the pyrrole-2-carboxyl moiety of clorobiocin, *Chembiochem 4*, 768-773.

71. Ching, Y. P., Qi, Z., and Wang, J. H. (2000) Cloning of three novel neuronal Cdk5 activator binding proteins, *Gene 242*, 285-294.

72. Boll, R., Hofmann, C., Heitmann, B., Hauser, G., Glaser, S., Koslowski, T., Friedrich, T., and Bechthold, A. (2006) The active conformation of avilamycin A is conferred by AviX12, a radical AdoMet enzyme, *J Biol Chem 281*, 14756-14763.

73. Paraskevopoulou, C., Fairhurst, S. A., Lowe, D. J., Brick, P., and Onesti, S. (2006) The Elongator subunit Elp3 contains a Fe4S4 cluster and binds S-adenosyl-L-methionine, *Mol Microbiol 59*, 795-806.

74. Brede, D. A., Faye, T., Johnsborg, O., Odegard, I., Nes, I. F., and Holo, H. (2004) Molecular and genetic characterization of propionicin F, a bacteriocin from Propionibacterium freudenreichii, *Appl Environ Microbiol 70*, 7303-7310.

75. Walsby, C. J., Ortillo, D., Broderick, W. E., Broderick, J. B., and Hoffman, B. M. (2002) An anchoring role for FeS clusters: chelation of the amino acid moiety of S-adenosyl-L-methionine to the unique iron site of the [4Fe-4S] cluster of pyruvate formate-lyase activating enzyme, *J Am Chem Soc 124*, 11270-11271.

76. Chen, D., Walsby, C., Hoffman, B. M., and Frey, P. A. (2003) Coordination and mechanism of reversible cleavage of S-adenosyl-L-methionine by the [4Fe-4S] center in lysine 2,3-aminomutase, *J Am Chem Soc 125*, 11788-11789.

77. Layer, G., Moser, J., Heinz, D. W., Jahn, D., and Schubert, W. D. (2003) Crystal structure of coproporphyrinogen III oxidase reveals cofactor geometry of Radical SAM enzymes, *EMBO J 22*, 6214-6224.

78. Berkovitch, F., Nicolet, Y., Wan, J. T., Jarrett, J. T., and Drennan, C. L. (2004) Crystal structure of biotin synthase, an S-adenosyl-L-methionine-dependent radical enzyme, *Science 303*, 76-79.

79. Hanzelmann, P., and Schindelin, H. (2004) Crystal structure of the S-adenosyl-L-methionine-dependent enzyme MoaA and its implications for molybdenum cofactor deficiency in humans, *Proc Natl Acad Sci U S A 101*, 12870-12875.

80. Lepore, B. W., Ruzicka, F. J., Frey, P. A., and Ringe, D. (2005) The x-ray crystal structure of lysine-2,3-aminomutase from Clostridium subterminale, *Proc Natl Acad Sci U S A 102*, 13819-13824.

81. Hanzelmann, P., and Schindelin, H. (2006) Binding of 5'-GTP to the C-terminal FeS cluster of the radical S-adenosyl-L-methionine enzyme MoaA provides insights into its mechanism, *Proc Natl Acad Sci U S A 103*, 6829-6834.

82. Nicolet, Y., Rubach, J. K., Posewitz, M. C., Amara, P., Mathevon, C., Atta, M., Fontecave, M., and Fontecilla-Camps, J. C. (2008) X-ray structure of the [FeFe]-hydrogenase maturase HydE from Thermotoga maritima, *J Biol Chem 283*, 18861-18872.

83. Vey, J. L., Yang, J., Li, M., Broderick, W. E., Broderick, J. B., and Drennan, C. L. (2008) Structural basis for glycyl radical formation by pyruvate formate-lyase activating enzyme, *Proc Natl Acad Sci U S A 105*, 16137-16141.

84. Duschene, K. S., Veneziano, S. E., Silver, S. C., and Broderick, J. B. (2009) Control of radical chemistry in the AdoMet radical enzymes, *Curr Opin Chem Biol 13*, 74-83.

85. Chirpich, T. P., Zappia, V., Costilow, R. N., and Barker, H. A. (1970) Lysine 2,3-aminomutase. Purification and properties of a pyridoxal phosphate and S-adenosyl-L-methionine-activated enzyme, *J Biol Chem 245*, 1778-1789.

86. Zappia, V., and Barker, H. A. (1970) Studies on lysine-2,3-aminomutase. Subunit structure and sulfhydryl groups, *Biochim Biophys Acta 207*, 505-513.

87. Petrovich, R. M., Ruzicka, F. J., Reed, G. H., and Frey, P. A. (1991) Metal cofactors of lysine-2,3-aminomutase, *J Biol Chem 266*, 7656-7660.

88. Petrovich, R. M., Ruzicka, F. J., Reed, G. H., and Frey, P. A. (1992) Characterization of iron-sulfur clusters in lysine 2,3-aminomutase by electron paramagnetic resonance spectroscopy, *Biochemistry 31*, 10774-10781.

89. Eliot, A. C., and Kirsch, J. F. (2004) Pyridoxal phosphate enzymes: mechanistic, structural, and evolutionary considerations, *Annu Rev Biochem 73*, 383-415.

90. Moss, M., and Frey, P. A. (1987) The role of S-adenosyl-L-methionine in the lysine 2,3-aminomutase reaction, *J Biol Chem 262*, 14859-14862.

91. Baraniak, J., Moss, M. L., and Frey, P. A. (1989) Lysine 2,3-aminomutase. Support for a mechanism of hydrogen transfer involving S-adenosyl-L-methionine, *J Biol Chem 264*, 1357-1360.

92. Frey, P. A., and Magnusson, O. T. (2003) S-adenosyl-L-methionine: a wolf in sheep's clothing, or a rich man's adenosylcobalamin?, *Chem Rev 103*, 2129-2148.

93. Ballinger, M. D., Frey, P. A., and Reed, G. H. (1992) Structure of a substrate radical intermediate in the reaction of lysine 2,3-aminomutase, *Biochemistry 31*, 10782-10789.

94. Ballinger, M. D., Reed, G. H., and Frey, P. A. (1992) An organic radical in the lysine 2,3-aminomutase reaction, *Biochemistry 31*, 949-953.

95. Ballinger, M. D., Frey, P. A., Reed, G. H., and LoBrutto, R. (1995) Pulsed electron paramagnetic resonance studies of the lysine 2,3-aminomutase substrate radical: evidence for participation of pyridoxal 5'-phosphate in a radical rearrangement, *Biochemistry 34*, 10086-10093.

96. Chang, C. H., Ballinger, M. D., Reed, G. H., and Frey, P. A. (1996) Lysine 2,3-aminomutase: rapid mix-freeze-quench electron paramagnetic resonance studies establishing the kinetic competence of a substrate-based radical intermediate, *Biochemistry 35*, 11081-11084.

97. Wu, W., Lieder, K. W., Reed, G. H., and Frey, P. A. (1995) Observation of a second substrate radical intermediate in the reaction of lysine 2,3-aminomutase: a radical centered on the beta-carbon of the alternative substrate, 4-thia-L-lysine, *Biochemistry 34*, 10532-10537.

98. Miller, J., Bandarian, V., Reed, G. H., and Frey, P. A. (2001) Inhibition of lysine 2,3-aminomutase by the alternative substrate 4-thialysine and characterization of the 4-thialysyl radical intermediate, *Arch Biochem Biophys 387*, 281-288.

99. Magnusson, O. T., Reed, G. H., and Frey, P. A. (2001) Characterization of an allylic analogue of the 5'-deoxyadenosyl radical: an intermediate in the reaction of lysine 2,3-aminomutase, *Biochemistry 40*, 7773-7782.

100. Knappe, J., Blaschkowski, H. P., Grobner, P., and Schmitt, T. (1974) Pyruvate formate-lyase of Escherichia coli: the acetyl-enzyme intermediate, *Eur J Biochem 50*, 253-263.

101. Knappe, J., Schacht, J., Mockel, W., Hopner, T., Vetter, H., Jr., and Edenharder, R. (1969) Pyruvate formate-lyase reaction in Escherichia coli. The enzymatic system converting an inactive form of the lyase into the catalytically active enzyme, *Eur J Biochem 11*, 316-327.

102. Conradt, H., Hohmann-Berger, M., Hohmann, H. P., Blaschkowski, H. P., and Knappe, J. (1984) Pyruvate formate-lyase (inactive form) and pyruvate formate-lyase activating enzyme of Escherichia coli: isolation and structural properties, *Arch Biochem Biophys 228*, 133-142.

103. Frey, M., Rothe, M., Wagner, A. F., and Knappe, J. (1994) Adenosylmethionine-dependent synthesis of the glycyl radical in pyruvate formate-lyase by abstraction of the glycine C-2 pro-S hydrogen atom. Studies of [2H]glycine-substituted enzyme and peptides homologous to the glycine 734 site, *J Biol Chem 269*, 12432-12437.

104. Knappe, J., Neugebauer, F. A., Blaschkowski, H. P., and Ganzler, M. (1984) Post-translational activation introduces a free radical into pyruvate formate-lyase, *Proc Natl Acad Sci U S A 81*, 1332-1335.

105. Wagner, A. F., Frey, M., Neugebauer, F. A., Schafer, W., and Knappe, J. (1992) The free radical in pyruvate formate-lyase is located on glycine-734, *Proc Natl Acad Sci U S A 89*, 996-1000.

106. Unkrig, V., Neugebauer, F. A., and Knappe, J. (1989) The free radical of pyruvate formate-lyase. Characterization by EPR spectroscopy and involvement in catalysis as studied with the substrate-analogue hypophosphite, *Eur J Biochem 184*, 723-728.

107. Parast, C. V., Wong, K. K., Kozarich, J. W., Peisach, J., and Magliozzo, R. S. (1995) Electron paramagnetic resonance evidence for a cysteine-based radical in pyruvate formate-lyase inactivated with mercaptopyruvate, *Biochemistry 34*, 5712-5717.

108. Parast, C. V., Wong, K. K., Lewisch, S. A., Kozarich, J. W., Peisach, J., and Magliozzo, R. S. (1995) Hydrogen exchange of the glycyl radical of pyruvate formate-lyase is catalyzed by cysteine 419, *Biochemistry 34*, 2393-2399.

109. Webb, M. E., Marquet, A., Mendel, R. R., Rebeille, F., and Smith, A. G. (2007) Elucidating biosynthetic pathways for vitamins and cofactors, *Nat Prod Rep 24*, 988-1008.

110. Sanyal, I., Cohen, G., and Flint, D. H. (1994) Biotin synthase: purification, characterization as a [2Fe-2S]cluster protein, and in vitro activity of the Escherichia coli bioB gene product, *Biochemistry 33*, 3625-3631.

111. Broach, R. B., and Jarrett, J. T. (2006) Role of the [2Fe-2S]2+ cluster in biotin synthase: mutagenesis of the atypical metal ligand arginine 260, *Biochemistry 45*, 14166-14174.

112. Ugulava, N. B., Sacanell, C. J., and Jarrett, J. T. (2001) Spectroscopic changes during a single turnover of biotin synthase: destruction of a [2Fe-2S] cluster accompanies sulfur insertion, *Biochemistry 40*, 8352-8358.

113. Jameson, G. N., Cosper, M. M., Hernandez, H. L., Johnson, M. K., and Huynh, B. H. (2004) Role of the [2Fe-2S] cluster in recombinant Escherichia coli biotin synthase, *Biochemistry 43*, 2022-2031.

114. Tse Sum Bui, B., Mattioli, T. A., Florentin, D., Bolbach, G., and Marquet, A. (2006) Escherichia coli biotin synthase produces selenobiotin. Further evidence of the involvement of the [2Fe-2S]2+ cluster in the sulfur insertion step, *Biochemistry 45*, 3824-3834.

115. Marquet, A., Frappier, F., Guillerm, G., Azoulay, M., Florentin, D., and Tabet, J. C. (1993) Biotin biosynthesis: synthesis and biological evaluation of the putative intermediate thiols, *Journal of the American Chemical Society 115*, 2139-2145.

CHAPTER 2

DIPHTHAMIDE BIOSYNTHESIS REQUIRES AN ORGANIC RADICAL GENERATED BY AN IRON-SULPHUR ENZYME*

Abstract

Archaeal and eukaryotic translation elongation factor 2 contain a unique posttranslationally modified histidine residue called "diphthamide", the target of diphtheria toxin. The biosynthesis of diphthamide was proposed to involve three steps, with the first step being the formation of a C-C bond between the histidine residue and the 3-amino-3-carboxypropyl group of S-adenosyl-L-methionine (SAM). However, details of the biosynthesis have remained unknown. In this chapter, I present biochemical evidence showing that the first step of diphthamide biosynthesis in the archaeon *Pyrococcus horikoshii* uses a novel iron-sulfur cluster enzyme, Dph2. X-ray crystal structure shows that Dph2 is a homodimer and each monomer contains a [4Fe-4S] cluster. Biochemical data suggest that unlike the enzymes in the radical SAM superfamily, Dph2 does not form the canonical 5´-deoxyadenosyl radical. Instead, it breaks the $C_{\gamma,Met}$-S bond of SAM and generates a 3′-amino-3′-carboxylpropyl radical. This work suggests that *Pyrococcus horikoshii* Dph2 represents a novel SAM-dependent [4Fe-4S]-containing enzyme that catalyzes unprecedented chemistry.

Introduction

Corynebacterium diphtheriae is a pathogenic bacterium that causes the infectious disease diphtheria in humans(*1*). This bacterium kills host cells by secreting a protein factor, diphtheria toxin(*2*), which catalyzes the ADP-ribosylation of a posttranslationally modified histidine residue (Figure 2. 1) in eukaryotic translation elongation factor 2 (eEF2).(*3*) Because this posttranslational modification is the target of diphtheria toxin, it was named "diphthamide". eEF2 is a GTPase required for the translocation step of ribosomal protein synthesis.(*4*) The diphthamide modification is conserved in all eukaryotes and archaea and is important for ribosomal protein synthesis.(*4*, *5*) Although diphthamide was identified more than three decades ago, its biosynthesis has remained an enigma.(*6*) Five genes required for diphthamide biosynthesis were identified in eukaryotes, Dph1, Dph2, Dph3, Dph4, and Dph5,(*3*, *7*-*13*) and a biosynthetic pathway has been proposed (Figure 2.1).

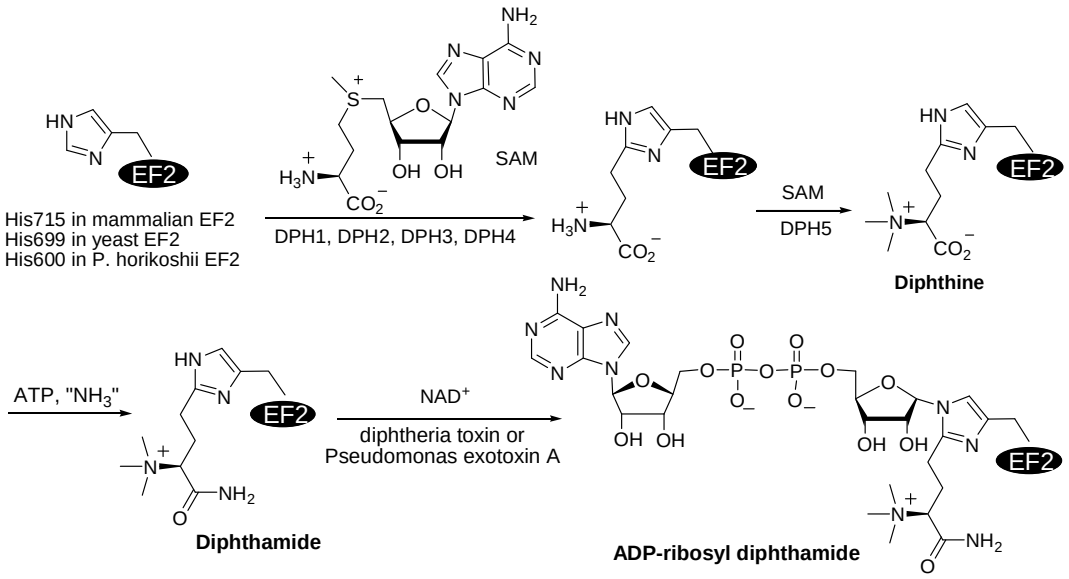

Figure 2.1. The structure of diphthamide and its proposed biosynthesis pathway. The diphthamide residue is the target of bacterial ADP-ribosyltransferases, diphtheria toxin and Pseudomonas exotoxin A.

The first step of diphthamide biosynthesis is the transfer of the 3′-amino-3′-carboxypropyl (ACP) group from S-adenosyl-L-methionine (SAM) to the C-2 position of the imidazole ring of the target histidine residue in eEF2 and is catalyzed by Dph1-4 in eukaryotes. This step is followed by a trimethylation, catalyzed by Dph5, and an amidation, catalyzed by an unidentified enzyme. The first step is particularly interesting for several reasons. First, SAM is generally a methyl donor, but in the first step the ACP group is transferred from SAM. Second, protein posttranslational modifications that involve C-C bond formation are rare(*6*) and in diphthamide biosynthesis the C-C bond formation involves the poorly nucleophilic C-2 of the imidazole ring. Third, in eukaryotes, this reaction requires four proteins, Dph1-4, raising questions about the function of each protein.

Dph1 and Dph2 share about 20% sequence identity, but are not similar to any other protein with known function. Iterative BLAST searches(*14*) starting with *Saccharomyces cerevisiae* Dph1 or Dph2 generate both proteins from other eukaryotic species. In contrast, BLAST searches identify only one protein, Dph2, in archaeal species. Archaeal Dph2s are more similar to eukaryotic Dph1 than to Dph2. Eukaryotic Dph3 and Dph4 have no orthologs in archaea based on BLAST searches. To better understand diphthamide biosynthesis, we initially attempted to reconstitute the first step using *Pyrococcus horikoshii* Dph2 (PhDph2) and translation elongation factor 2 (PhEF2) under aerobic conditions without success. The X-ray crystal structure of PhDph2 revealed an intriguing constellation of three conserved cysteine residues -- each from a different structural domain -- suggestive of an iron-sulfur cluster. Subsequently, PhDph2 activity was reconstituted in the presence of dithionite under anaerobic conditions. A crystal structure of reconstituted PhDph2 along with UV-Vis, EPR, and Mössbauer spectroscopies confirmed the presence of a [4Fe-4S] cluster.

Detailed biochemical characterization suggests that the PhDph2-catalyzed reaction involves a 3′-amino-3′-carboxypropyl radical intermediate. The data suggest that PhDph2 is a novel SAM-dependent [4Fe-4S]-containing enzyme(*15*) that catalyzes unprecedented chemistry.

Results

PhDph2 is aerobically inactive

PhDph2 and PhEF2 were expressed in *Escherichia coli* and purified under aerobic conditions. No activity was observed when using these proteins to reconstitute the first step of diphthamide biosynthesis. One explanation for the lack of activity is that the reaction requires an oxygen-sensitive cofactor and another is that additional proteins or small molecules are required. In the latter case the additional proteins might be orthologs of eukaryotic Dph3 and Dph4; however, attempts to reconstitute activity under similar conditions using yeast Dph1-4 and eEF2 were also unsuccessful.

PhDph2 can modify PhEF2 in E. coli cells

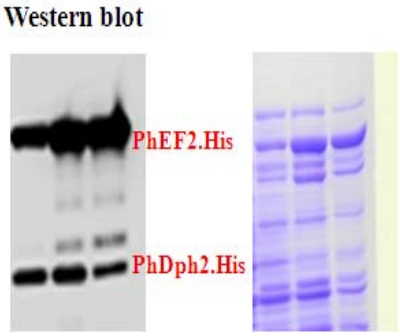

Figure 2.2. Coexpression of PhDph2 and PhEF2 in *E. coli*. The coexpression is confirmed by western blot against His_6 tag.

PhDph2 and PhEF2 were coexpressed in *E. coli* to determine if PhDph2 is

enough to catalyze the diphthamide modification on PhEF2. The expression of both PhDph2 and PhEF2 were confirmed by western blot against His6 tag (Figure 2.2). The modification on coexpressed PhEF2 was analyzed by MALDI-MS (Figure 2.3)

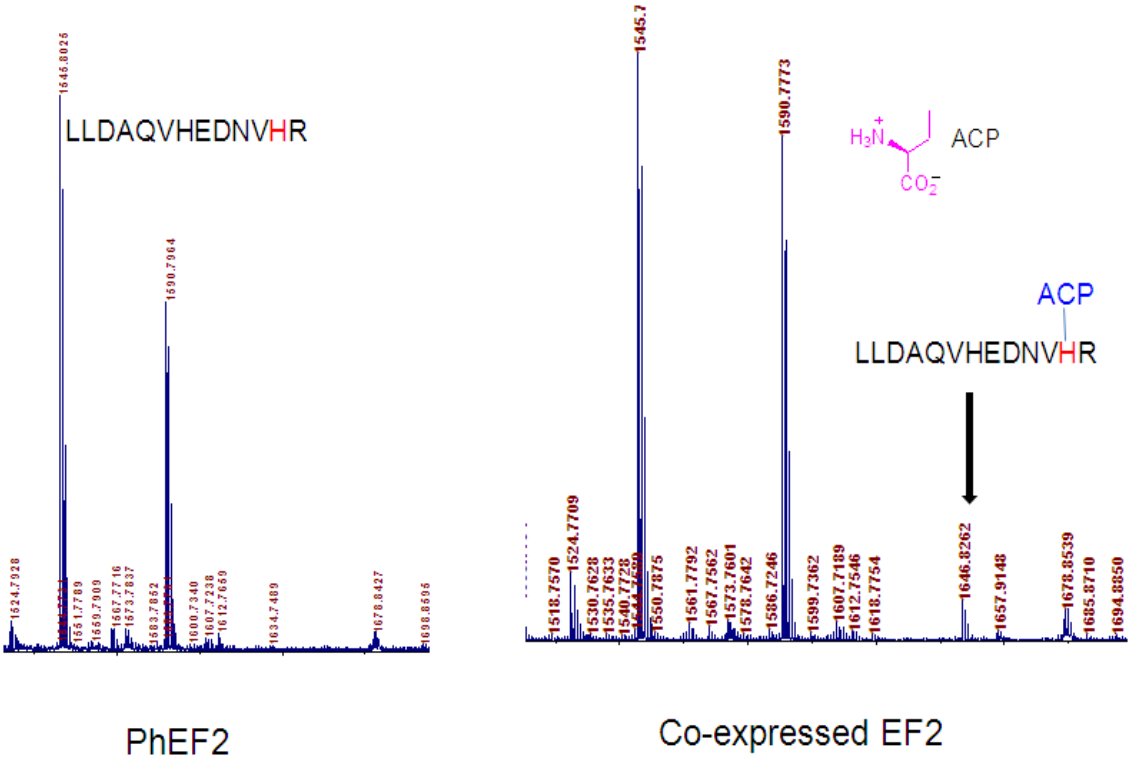

Figure 2.3. The MALDI-MS spectra of PhEF2 expressed alone in E. coli (left) and PhEF2 coexpressed with PhDph2 in E. coli (right). The mass of polypeptide with unmodified histidine and ACP-modified histidine are 1546 (m/z) and 1647, respectively. ACP: 3′-amino-3′-carboxypropyl group.

It shows that PhDph2 can modify PhEF2 in *E. coli* cell. Therefore the explanation for the lack of activity of the aerobically purified PhDph2 is that the reaction may require an oxygen-sensitive cofactor.

Crystal structure of PhDph2

To provide structural insight into the catalytic mechanism of PhDph2, we

determined its X-ray crystal structure at 2.3 Å resolution using selenomethionine (SeMet) single anomalous diffraction (SAD) phasing. The structure showed that

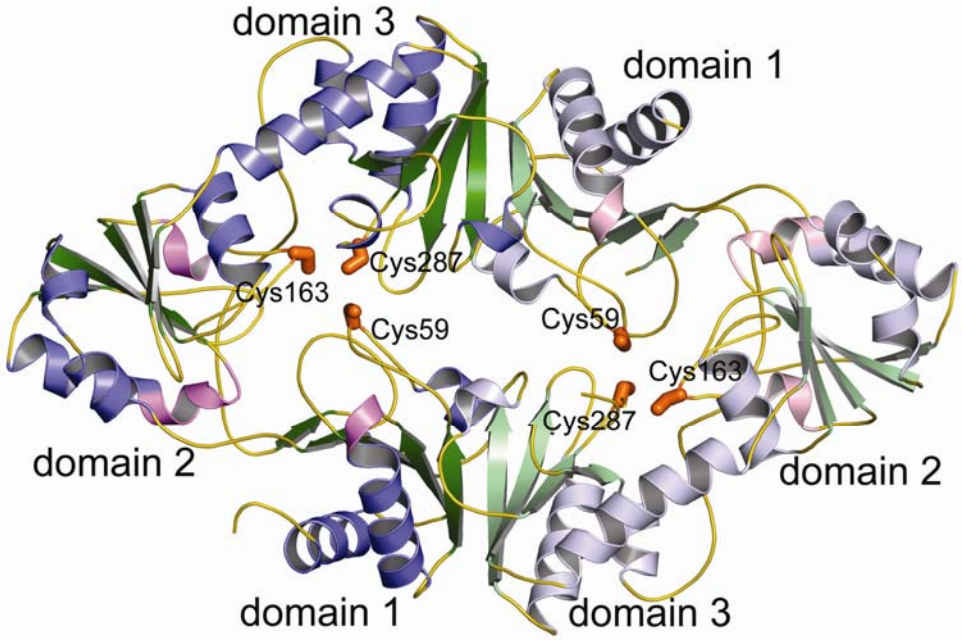

Figure 2.4. [5]Structure of PhDph2 homodimer. The PhDph2 homodimer is shown in the ribbon diagram with one monomer in dark color and the other in light color. Each monomer is also color by secondary structure. The three conserved cysteine residues for each monomer are shown in the stick representation.

PhDph2 is a homodimer (Figure 2.4). Each PhDph2 monomer consists of three domains with all three domains sharing the same overall fold. The basic domain fold is a four-stranded parallel β-sheet with three flanking α-helices (or two α-helices and one 3_{10} helix in the case of domain 2) (Figure 2.5). The two -sheets in domain 1 and 2 each contains an additional β-strand that is antiparallel to the rest of the -sheet. Domains 2 and 3 have two additional α-helices. Domain 1 of one monomer and domain 3 of the adjacent monomer form the dimer interface, creating an extended

[5] X-ray crystal structure of apo PhDph2 was resolved by Dr. Yang Zhang.

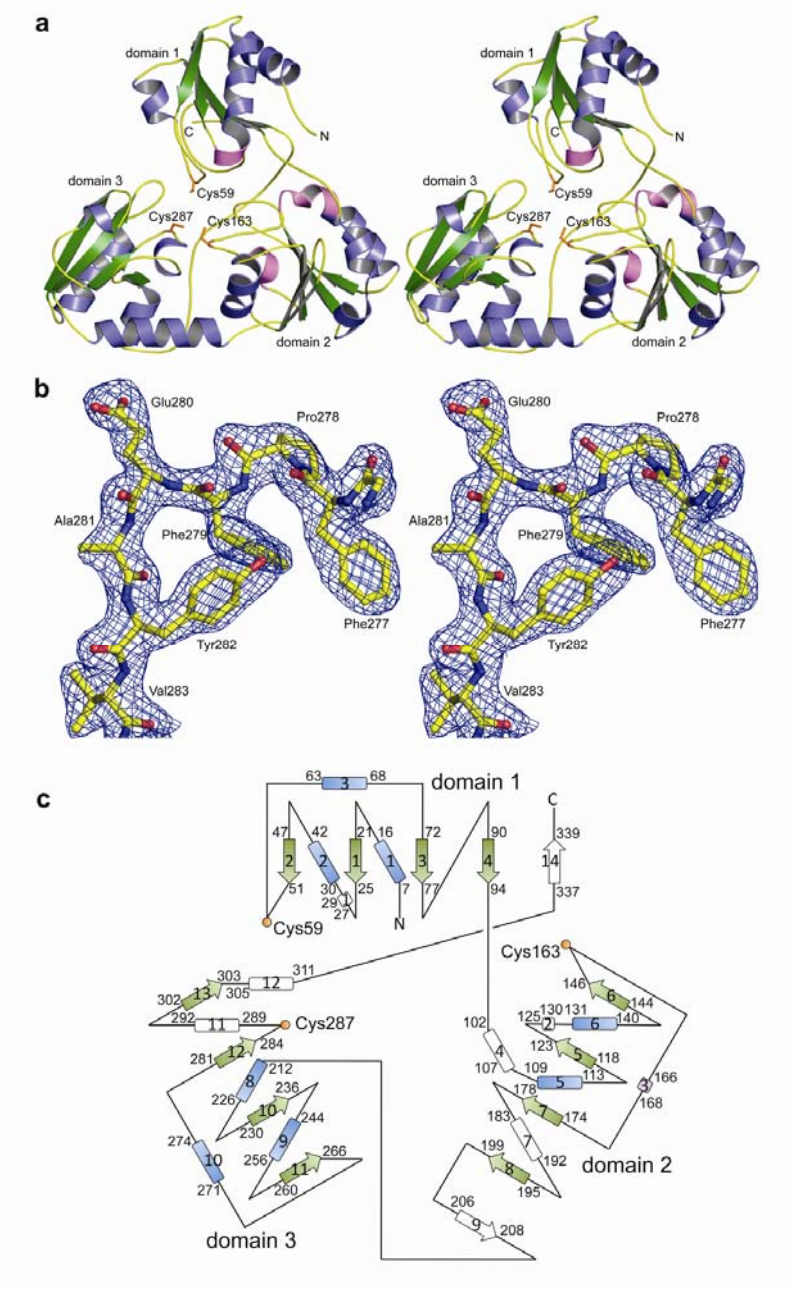

Figure 2.5. Three-dimensional structure of *Ph*Dph2. a, *Ph*Dph2 monomer colored by secondary structure. The locations of the three conserved cysteine residues are indicated. b, Representative region of a 2Fo-Fc composite omit electron density map and the final atomic model for residues 277-283. The map was calculated at 2.1 Å resolution and is contoured at 1 σ. c, Topology diagram of *Ph*Dph2. The conserved secondary structures of the three domains are colored blue for α- helices, lavender for a 310-helix, and green for β-strands.

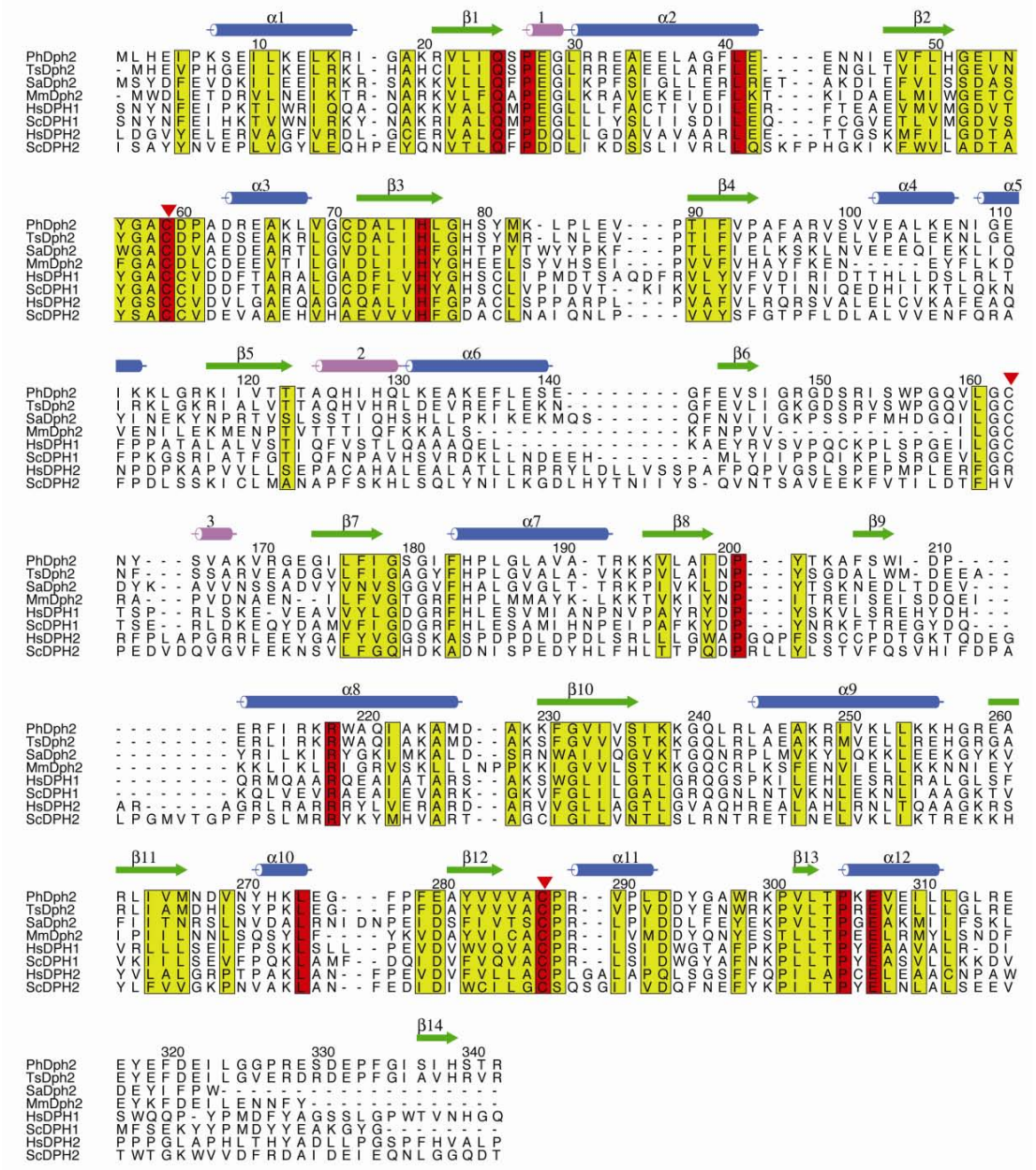

Figure 2.6. Sequence alignment for PhDph2 and orthologs. Three additional archaeal orthologs are included for comparison: *Thermococcus* sp. AN4 (Ts), *Sulfolobus acidocaldarius* (Sa) and *Methanococcus maripaludis* (Mm). Also included are the *Homo sapiens* (Hs) and *Saccharomyces cerevisiae* (Sc) orthologs of PhDph2: *Hs*Dph1, *Sc*Dph1, *Hs*Dph2 and *Sc*Dph2. Secondary structural elements are shown above each row and are based on the structure of PhDph2. Residues conserved in all eight sequences are highlighted in red. Residues with conservative changes are highlighted in yellow. The three conserved cysteine residues that bind to the [4Fe-4S] cluster of PhDph2 are indicated by red triangles.

nine-stranded β-sheet. The domain folds and their arrangement resemble the structure of quinolinate synthase(*16*); however, the orientations of the domains with respect to each other are different in the two enzymes. Three conserved cysteine residues (Cys59, Cys163 and Cys287), each coming from a different structural domain, are clustered together in the center of the PhDph2 monomers. All three cysteine residues are conserved in eukaryotic Dph1s. The first and third cysteine residues are conserved in eukaryotic Dph2s (Figure 2.6).

Reconstitution of PhDph2 activity

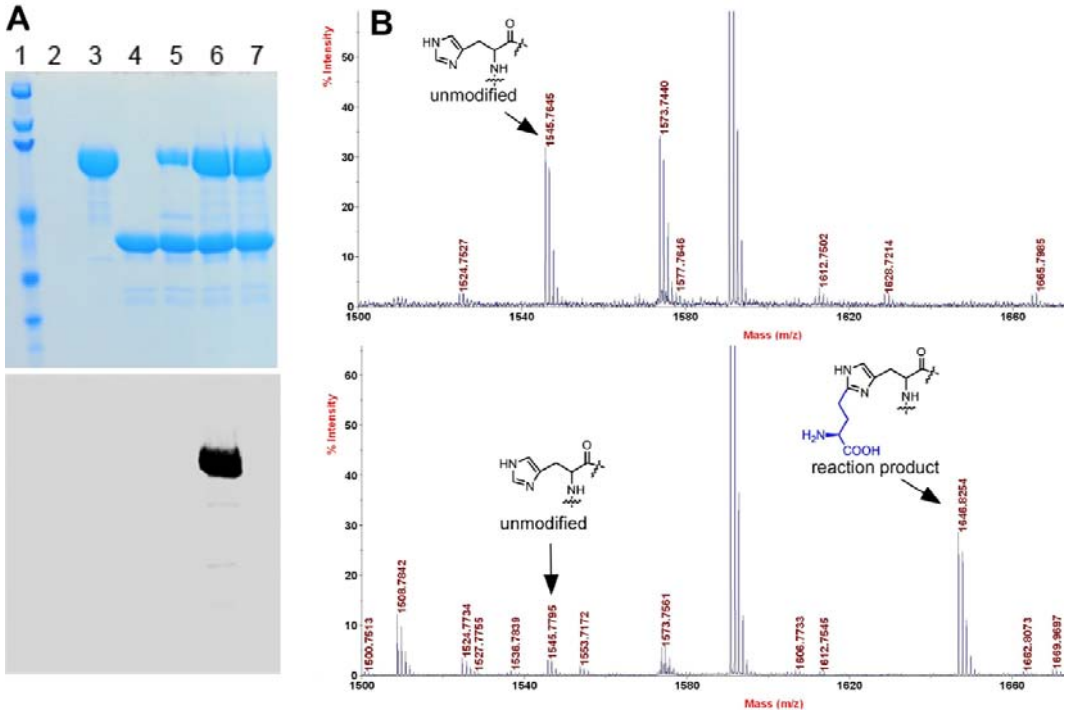

Figure 2.7. *In vitro* reconstitution of PhDph2 activity. a, Activity assay using carboxy-^{14}C SAM. Top panel shows the Coomassie blue-stained gel; bottom panel shows the autoradiography. Lane 1: Protein standard; 2: Blank lane; 3: PhEF2 + SAM, negative control; 4: PhDph2 + SAM, negative control; 5: PhEF2 H600A + PhDph2 + SAM, negative control; 6: PhEF2 + PhDph2 + SAM + dithionite; 7: PhEF2 + PhDph2 + SAM, no dithionite, negative control. b, The MALDI-MS spectra of PhEF2 unmodified (top) and modified by PhDph2 in an *in vitro* reaction (bottom).

The clustering of the three cysteine residues in the crystal structure and the requirement for SAM raised the possibility that PhDph2 utilizes a [4Fe-4S] cluster (*15*). Radical SAM enzymes harbor a [4Fe-4S] cluster coordinated by three cysteines in a CX_3CX_2C motif(*17*), although variations of this motif have been reported (*18*), (*19*) to generate a 5´-deoxyadenosyl radical. Since [4Fe-4S] clusters are typically oxygen-sensitive, PhDph2 was purified and assayed anaerobically. Using ^{14}C-SAM, we showed that PhEF2 can be labeled in the presence of PhDph2 (Figure 2.7a, lane 6), but not in the absence of PhDph2 (lane 3) or dithionite (lane 7). When His600 of PhEF2, the site of the diphthamide modification, was changed to alanine, no reaction occurred in the presence of PhDph2 (lane 5). MALDI-MS of the PhEF2 protein confirmed that an ACP group was added after the reaction (Figure 2.7 b). These results suggest the possibility that PhDph2 is a SAM-dependent Fe-S enzyme and demonstrate that no other enzyme is required for the first step of diphthamide biosynthesis *in vitro*.

Characterization of the [4Fe-4S] cluster

The anaerobically purified PhDph2 contains 1.3 ± 0.2 and 1.9 ± 0.2 equivalents of iron and sulfur per polypeptide, respectively, and displays a broad absorption band at ~400 nm, which disappears upon reduction by 0.5 mM dithionite (Figure 2.8a). The 400 nm absorption is typical of a $[4Fe\text{-}4S]^{2+}$ cluster. Quantification based on the 400 nm absorption suggests the presence of ~0.3 $[4Fe\text{-}4S]^{2+}$ per PhDph2. EPR spectra of dithionite-reduced PhDph2 are shown in Figure 2.8b. The *g*-values (2.03, 1.92, and 1.86) and the temperature-dependence are typical of a $[4Fe\text{-}4S]^{+}$ cluster.(*20-23*) Quantification of the EPR spectrum suggests the presence of ~0.3 $[4Fe\text{-}4S]^{+}$ per PhDph2. The ^{57}Fe-enriched anaerobically-isolated PhDph2 contains 2.0 ± 0.2 and 2.1 ± 0.2 equivalents of iron and sulfur per polypeptide, respectively. The 4.2-K/53-mT Mössbauer spectrum (Figure 2.8c) is dominated by a quadrupole doublet

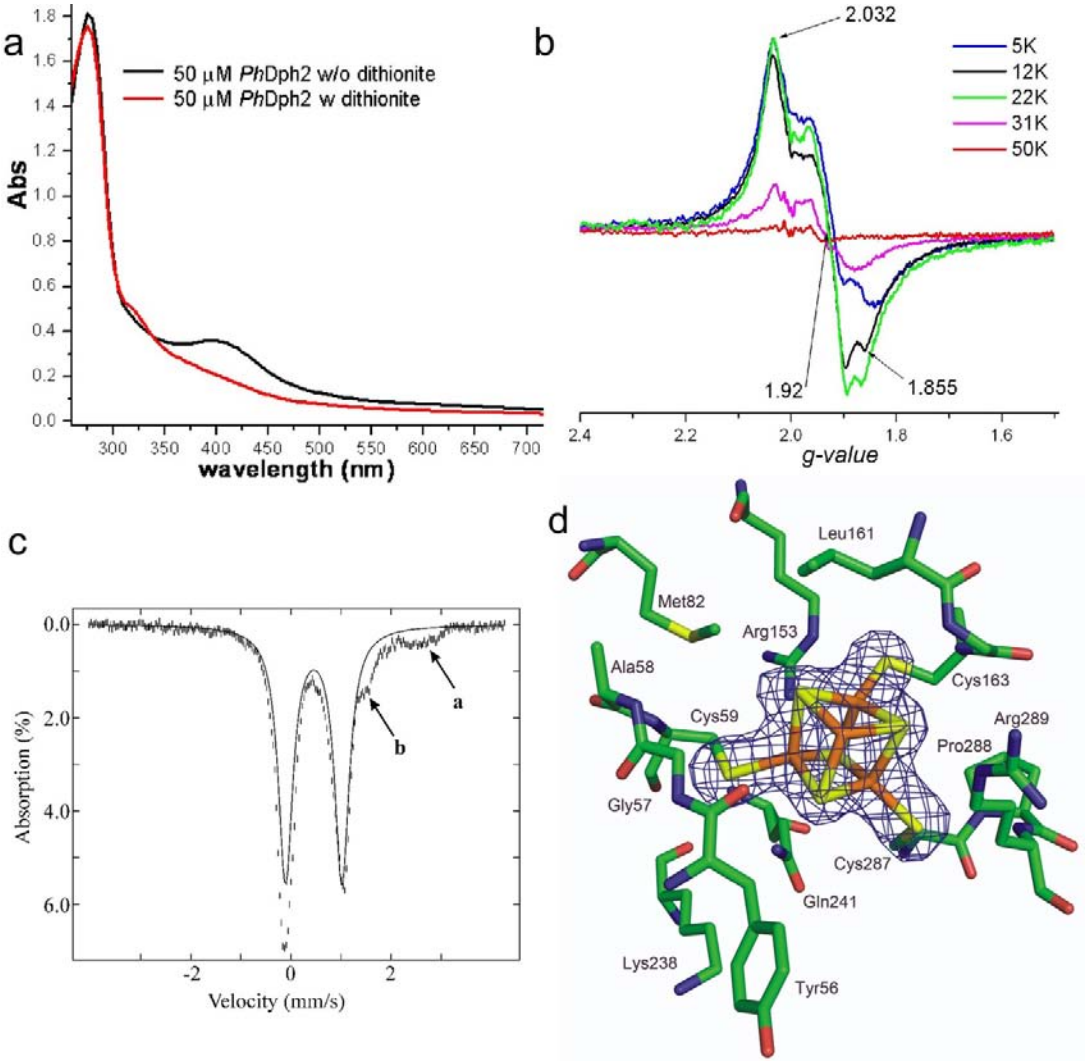

Figure 2. 8. [6]Spectroscopic characterization of the [4Fe-4S] cluster in PhDph2. a, UV-vis absorption spectra of anaerobically-isolated and dithionite-reduced PhDph2. b, X-band EPR spectra of dithionite-reduced PhDph2 at different temperature. c, 4.2-K/53-mT Mössbauer spectrum of anaerobically-isolated ^{57}Fe-labeled PhDph2 expressed in *E. coli*. d, Structure of PhDph2 with [4Fe-4S] cluster.

[6] Data of EPR spectra was collected and analyzed by Dr. Boris Dzikovski; Micheal Lee performed the Mössbauer spectrum; Dr. Andrew T. Torelli determined the crystal structure of PhDph2with iron-sulfur cluster.

with parameters (isomer shift (δ) of 0.43 mm/s and quadrupole splitting parameter ΔE_Q) of 1.13 mm/s) typical of $[4Fe\text{-}4S]^{2+}$ clusters (solid line in Figure 2.8 c, 73% of total intensity). The weak absorption peak labeled (a) suggests the presence of a small amount (~10%) of high-spin Fe (II), which is presumably nonspecifically bound to the protein. The shoulder labeled (b) belongs to a quadrupole doublet (~15% intensity), the left line of which contributes to the prominent peak at -0.2 mm/s. Although the nature of the Fe species that gives rise to this absorption is not known, similar spectral features were observed for a sample of *P. horikoshii* quinolinate synthase,(*24*) which is structurally similar to PhDph2 and also harbors a [4Fe-4S] cluster (Figure 2.8d). Thus, all the spectroscopic data indicate that PhDph2 contains a [4Fe-4S] cluster.

Brown crystals of the anaerobically purified PhDph2 were obtained that belong to the same space group as the inactive PhDph2. A crystal structure determined to 2.1 Å resolution showed clear electron density for a [4Fe-4S] cluster. Refinement of the PhDph2 structure with a [4Fe-4S] cluster included gave final *R* and R_{free} values of 20.4% and 25.2%, respectively.

Reaction mechanism

To explore the PhDph2 reaction mechanism, HPLC was used to analyze the reaction products. In the reaction that contained SAM, PhDph2, PhEF2 and dithionite, most SAM molecules were converted to 5´-deoxy-5´-methylthioadenosine (MTA) In control reactions without PhDph2 or dithionite, only low levels of MTA were observed and most SAM molecules were left intact. This is consistent with the activity assay results shown in Figure 2.9. Cleavage of the C5´-S bond of SAM did not occur

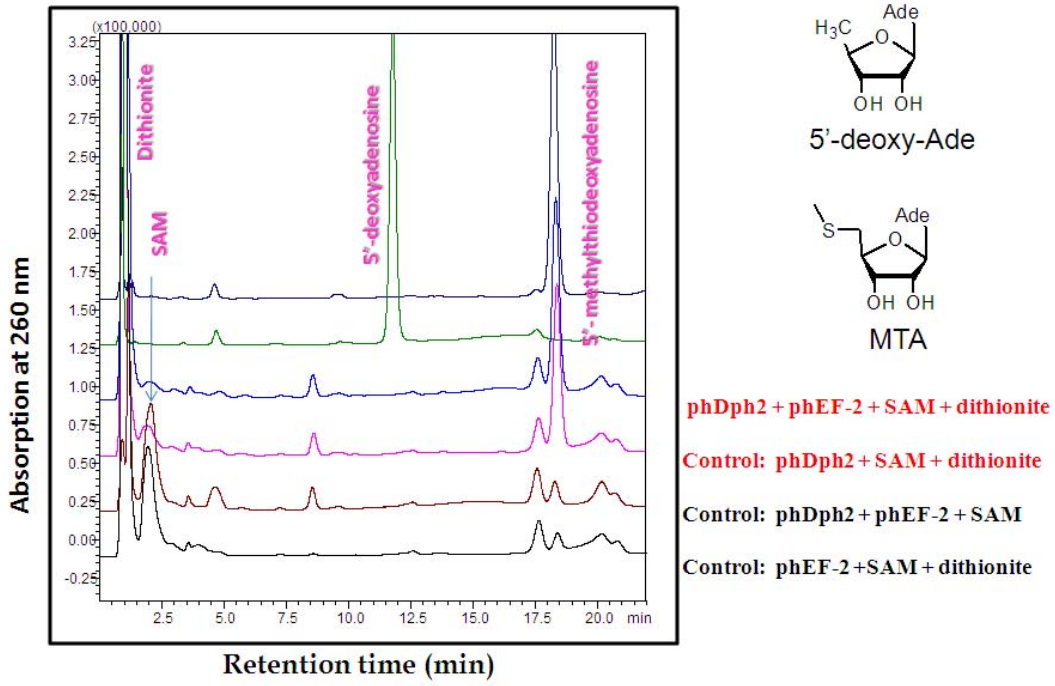

Figure 2. 9. HPLC analysis of reaction products suggests PhDph2 does not form 5´-deoxyadenosine, instead of MTA structure is shown at the right side.

because the formation of 5´-deoxyadenosine (the most likely product of the adenosyl moiety) was not observed. Collectively, the results suggest that PhDph2 catalyzes the cleavage of the $C_{\gamma,Met}$-S bond of SAM only in the presence of reductant, transfers the ACP group to PhEF2, and releases the remaining MTA.

Two different mechanisms can be proposed for the PhDph2-catalyzed cleavage of the $C_{\gamma,Met}$-S bond of SAM. One is that the $[4Fe\text{-}4S]^{+}$ cluster provides one electron to reductively cleave the $C_{\gamma,Met}$-S bond of SAM, forming MTA, an ACP radical, and the oxidized $[4Fe\text{-}4S]^{2+}$ cluster (Figure 2.11a). Alternatively, the [4Fe-4S] cluster in PhDph2 binds SAM and orients it correctly for nucleophilic attack by the C2 of the

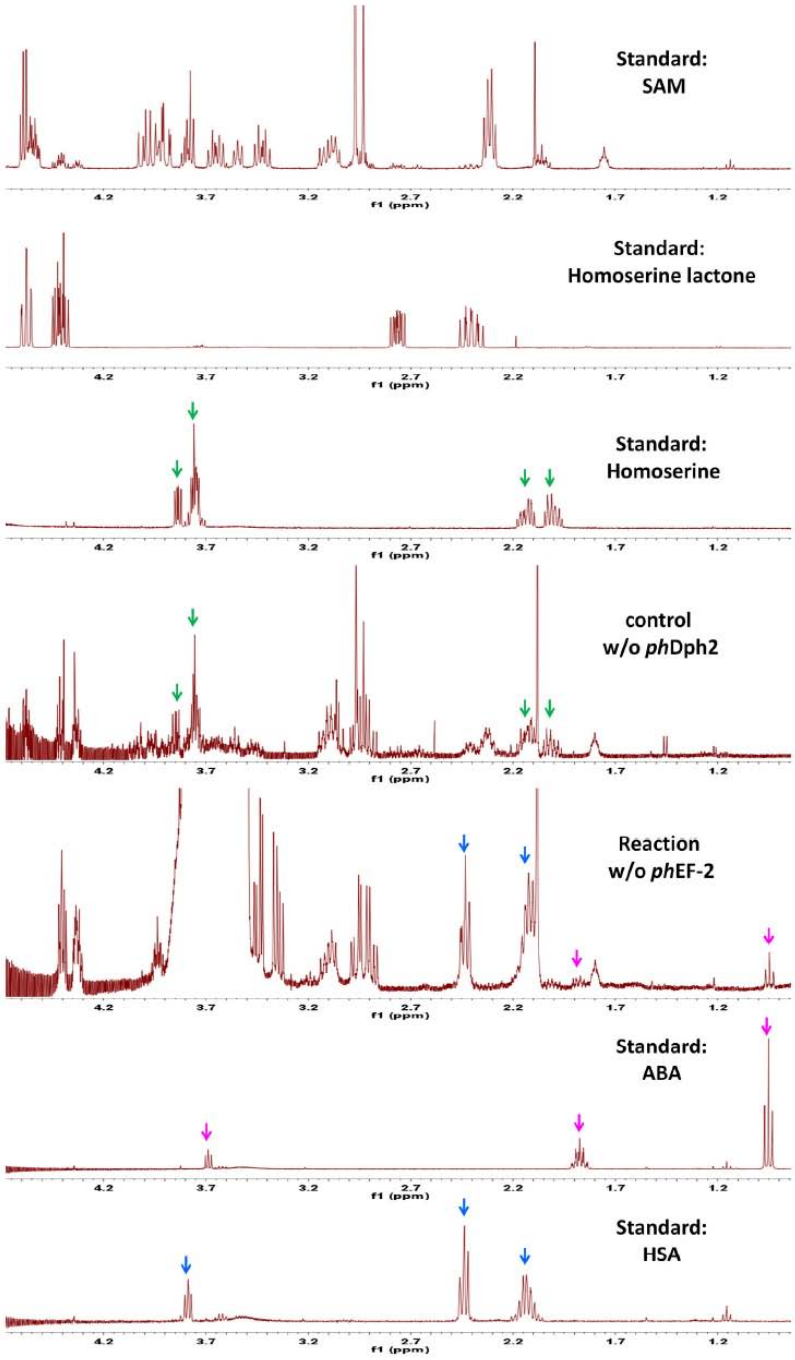

Figure 2.10. NMR spectra of standard compounds, products from PhDph2 reaction, and products from the control reaction without PhDph2. These spectra are overlaid so that it is easy to tell which compound is present in the reaction or control. Homoserine lactone (peaks marked with green arrows) and unreacted SAM were the major identifiable compounds present in the control reaction without PhDph2. In the reaction with PhDph2, the major identifiable compounds are HSA (peaks marked by cyan arrows) and ABA (peaks marked by magenta arrows).

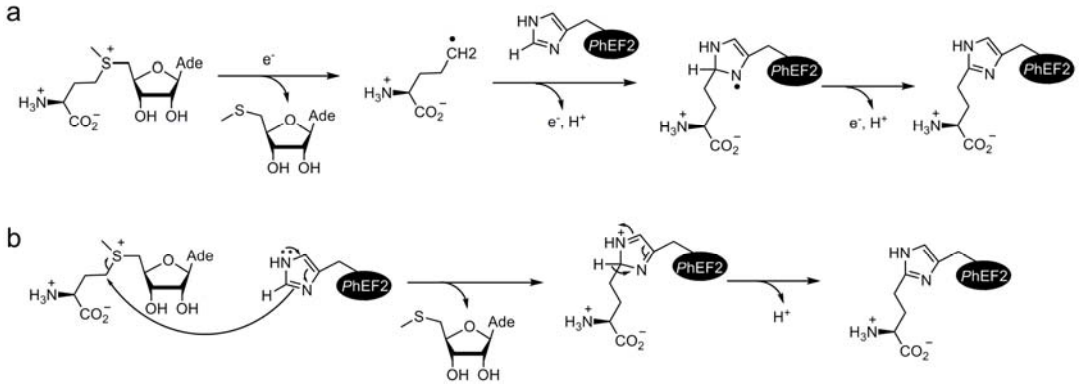

Figure 2.11. Two possible reactions mechanisms proposed for PhDph2 based on the observation made in Figure 5a. (a) A radical mechanism. The $[4Fe\text{-}4S]^{+}$ cluster provides an electron to reductively break the $C_{\gamma,Met}$-S bond of SAM, generating a 3-amino-3-carboxypropyl radical, which then adds to the imidazole ring. The resulting radical then loses one electron and one proton to give the product. (b) A nucleophilic mechanism. The $[4Fe\text{-}4S]^{+}$ serves to anchor SAM in the right position and orientation for nucleophilic attack by the C2 position of the imidazole ring. Deprotonation of the resulting adduct then gives the product.

imidazole ring (Figure 2.11b), leading to the formation of products. Further evidence to differentiate these two possibilities was provided by the identification of the product derived from the ACP group in the reaction without PhEF2. In the absence of PhEF2, PhDph2 can still cleave the $C_{\gamma,Met}$-S bond of SAM, generating MTA (Figure 2.9). The fate of the ACP group was interrogated by ^{1}H-NMR (Figure 2.10). In the reaction containing PhDph2, SAM, and dithionite, several new peaks were observed, which were not observed in control samples without dithionite or PhDph2 (Figure 2.10). These peaks were assigned to two products: 2-aminobutyric acid (ABA) and homocysteine sulfinic acid (HSA). The NMR spectra of authentic samples of ABA and HSA confirmed these assignments (Figure 2.10). In Figure 2.10, these NMR spectra were compared to those of homoserine, homoserine lactone, and SAM, ruling out the possibility that PhDph2 catalyzes the formation of homoserine or homoserine

lactone via a nucleophilic mechanism.

To further validate these results, the reaction mixtures were purified by TLC, dansylated, and subsequently analyzed by LCMS. The structures and molecular weights of the dansylated compounds are shown in Figure 2.12. In the control reaction without PhDPh2, the formation of dansylated homoserine (m/z 337, MH^+, retention time 18.35 min) was observed (Figure 2.13), which is consistent with the NMR results (Figure 2.10). In the reaction with PhDph2, SAM, and dithionite, the formation of dansylated homoserine was suppressed compared with the control. Instead, dansylated ABA (*m/z* 337, MH^+, 23.60 min) and HSA (*m/z* 401, MH^+, 16.65 min) were observed (Figure 2.13). Dansylated homoserine lactone and ABA have the same retention time, but can be differentiated by their *m/z*-values (337 and 335 for ABA and homoserine lactone, respectively). During the TLC purification and dansylation reaction, HSA was partially oxidized to homocysteine sulfonic acid, as evidenced by the ion with *m/z* 417 (MH^+, Figure 2.13).

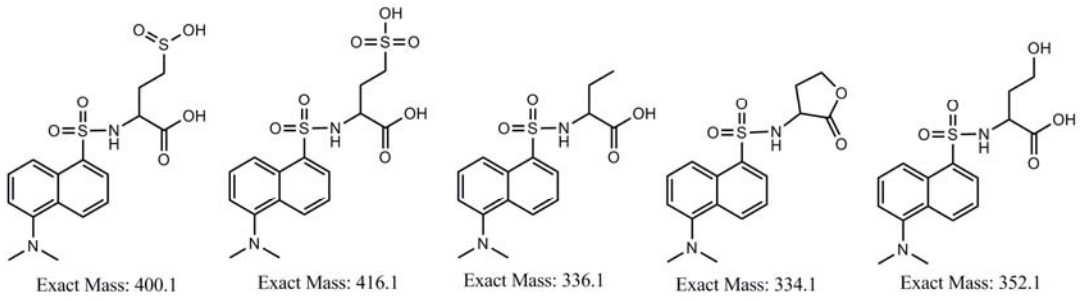

Figure 2. 12. The structures and molecular weights of the dansylated compounds that can possibly form in the PhDph2-catalyzed cleavage of SAM. Whether these compounds were produced or not were checked by LCMS in Figure 2.13c.

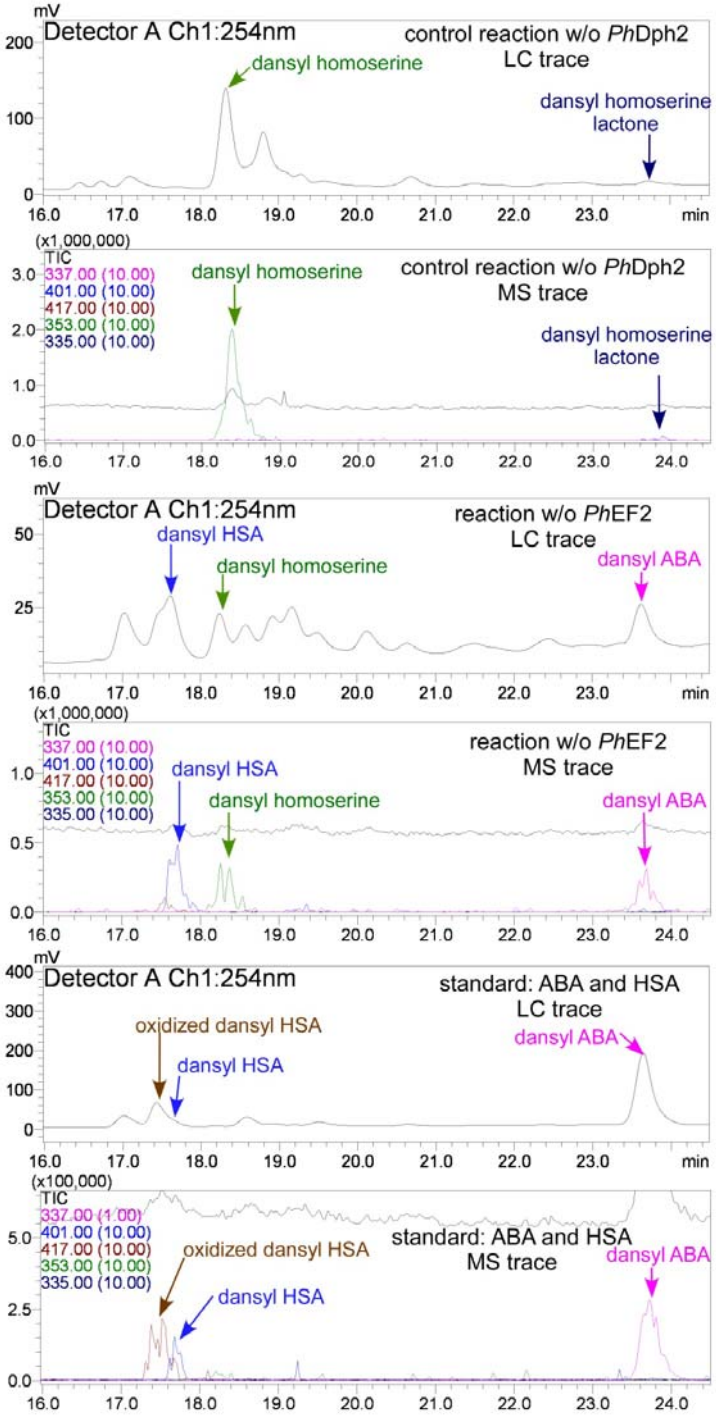

Figure 2. 13. Detection of dansylated reaction products by LCMS. The MS traces (total ion counts and ion counts for specific compounds) were shown for the reaction with PhDph2, control reaction without PhDph2, and ABA and HSA standards

Overall, the results from the LCMS analysis and NMR analysis demonstrate that PhDph2 catalyzes the formation of ABA and HAS in the absence of PhEF2. The formation of ABA and HSA can be best explained by the generation of an ACP radical followed by hydrogen extraction to give ABA or quenching by dithionite to give HSA.

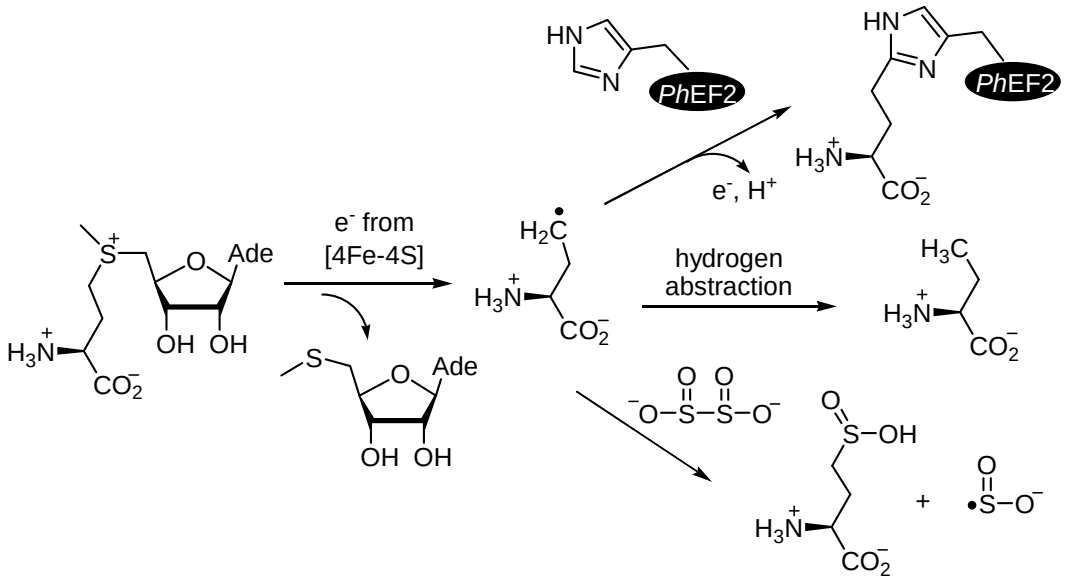

Figure 2.14. The proposed reaction mechanism for PhDph2. The formation of ABA and HSA can be best explained by a 3-amino-3-carboxypropyl radical intermediate. The radical can be generated by electron transfer from the [4Fe-4S] cluster, similar to the generation of 5´-deoxyadenosyl radical in other radical SAM enzymes. In the presence of PhEF2, the radical will react with PhEF2 to form the modified PhEF2 product. In the absence of PhEF2, the radical can either abstract a hydrogen atom to form ABA or be quenched by dithionite to give HSA.

Discussion

The biochemical, structural and spectroscopic data presented here establish that PhDph2 is a novel [4Fe-4S] cluster enzyme. PhDph2 cleaves the $C_{\gamma,Met}$-S bond of SAM to MTA and transfers the ACP group to His600 of PhEF2. This reaction is strictly dependent on the presence of reductant. In the absence of the natural substrate,

PhEF2, the ACP moiety is trapped either as ABA or as HSA, which suggests the intermediacy of an ACP radical. The reductive cleavage of SAM to a thioether and an alkyl radical by a reduced $[4Fe\text{-}4S]^{+}$ cluster is the hallmark feature of the superfamily of radical SAM enzymes.(*15*) However, there are two crucial differences between the radical SAM enzymes and PhDph2. First, the radical SAM enzymes exclusively cleave the C5´-S bond to generate methionine and a 5´-deoxyadenosyl radical, which is used for a variety of downstream C-H cleavage reactions. Second, the radical SAM superfamily is characterized by a conserved CX_3CX_2C motif(*17*) (or CX_2CX_4C in ThiC(*18*), or CX_5CX_2C in HmdA(*19*)) that binds the [4Fe-4S] cluster. This motif is not present in *Ph*Dph2. Instead the three conserved cysteine residues are located in separate structural domains and are separated by more than 100 residues in the sequence. Consequently, the three-dimensional structure of PhDph2 is distinct from the structures of the known radical SAM enzymes BioB,(*25*) HemN,(*26*) LAM,(*27*) MoaA,(*28*) PFL-AE,(*29*) and ThiC(*18*), which all have β-barrel or modified β-barrel folds. PhDph2 is structurally similar to quinolinate synthase,(*16*) which is also composed of three structurally homologous domains in a triangular arrangement. The triangular arrangement of domains in PhDph2 positions the three conserved cysteine residues in the central cavity to bind the [4Fe-4S] cluster. In quinolinate synthase, the three conserved cysteine residues required to bind the cluster are also widely separated in the amino acid sequence and located in different domains.(*30*),(*23*) However, quinolinate synthase is not SAM-dependent and its proposed role is in the dehydration of the penultimate precursor of quinolinate.(*23*) In addition, the IspH enzyme in the non-mevalonate pathway for isoprenoid biosynthesis also uses a similar triangular arrangement to bind a [3Fe-4S] cluster.(*31*)

It is likely that the different reaction outcome, i.e. cleavage of the C5´-S bond in the radical SAM enzymes vs. cleavage of the $C_{\gamma,Met}$-S bond in *Ph*Dph2, is controlled

by different orientations of SAM relative to the [4Fe-4S] cluster. In the radical SAM enzymes, the amino and carboxyl groups of SAM coordinate to the non-cysteine-ligated Fe site of the [4Fe-4S] cluster.(*32*) Future structural and spectroscopic studies are required to investigate how SAM is bound at the active site of PhDph2.

Our data demonstrated that PhDph2 is the only gene product required to catalyze the first step of diphthamide biosynthesis *in vitro*. In contrast, biosynthesis of diphthamide in eukaryotes requires four gene products, Dph1-4. Studies on PhDph2 provide important insight into the functions of eukaryotic Dph1-4. The crystal structure shows that PhDph2 is a homodimer. Eukaryotic Dph1 and Dph2 are both homologous to each other and to archaeal Dph2. In addition, Dph1 and Dph2 in eukaryotes form a heterodimer.(*3, 33-35*) Therefore it is possible that the eukaryotic Dph1-Dph2 heterodimer is structurally homologous to the PhDph2 homodimer. The three cysteine residues required to bind the cluster are conserved in Dph1 and two of the cysteine residues are conserved in Dph2. Thus the heterodimer of Dph1-Dph2 should at least bind one [4Fe-4S] cluster and may be sufficient to catalyze the first step *in vitro*. Dph2, which only has two of the conserved Cys residues, could either have a different catalytic function than Dph1 or could be regulatory. *In vivo*, Dph3 and Dph4 are also required for diphthamide biosynthesis.(*3*) These gene products may be required to keep the [4Fe-4S] cluster in a reduced state. This hypothesis is supported by the observation that Dph3 can bind iron and is redox active.(*36*) Alternatively Dph3 and Dph4 may be required for proper assembly of the [4Fe-4S] clusters. The Fe-S cluster assembly pathways in bacteria and mitochondria of eukaryotes are known to involve J domain-containing co-chaperone proteins, such as bacterial HscB and yeast JAC1(*37, 38*), that are similar to Dph4. Confirmation of these functional assignments awaits detailed biochemical and structural studies.

Experimental

Cloning, expression and purification of PhDph2 under anaerobic conditions

The gene encoding *P. horikoshii* Dph2 was amplified by PCR from *Pyrococcus horikoshii* genomic DNA and inserted into pENTR^{TM}/TEV/D-TOPO® entry vector (Invitrogen), followed by recombination with pDESTF1 destination vector to create expression clones with an N-terminal His_6 tag. The plasmids were transformed into the *E. coli* expression strain BL21(DE3) with pRARE. The cells were grown in LB media with 100 g/ml ampicillin at 37 °C and were supplemented with $FeCl_3$, $Fe(NH_4)_2(SO_4)_2$ and L-cysteine to final concentrations of 50 µM, 50 µM and 400 µM, respectively, when the absorbance of the cell culture reached an OD_{600} of 0.8. The cells were induced at an OD_{600} of 0.8 – 1.0 with 0.1 mM isopropyl-β-D-thiogalactopyranoside (IPTG), at which point the culture flasks were sealed to limit the amount of oxygen in the system. The induced cells were incubated in a shaker (New Brunswick Scientific Excella E25) at 37 °C and 200 rpm for 3 h before being transferred to the 4 °C cold room, where they were kept overnight without agitation. Cells were harvested the second day by centrifugation at 6,371 g (Beckman Coulter Avanti J-E), 4 °C for 10 min. Purification of PhDph2 was performed in an anaerobic chamber (Coy Laboratory Products) except for the centrifugation step. Cell pellets (from 2 l LB culture) were re-suspended in 30 mL lysis buffer (500 mM NaCl, 10 mM $MgCl_2$, 5 mM imidazole, 1 mM DTT and 20 mM Tris-HCl at pH 7.4). Cells were lysed by incubating with 0.3% (w/v) lysozyme (Fisher) at 26 °C for 1 h, followed by freezing in liquid nitrogen and thawing at 26 °C once. Cell debris was removed by centrifugation at 48,384 g (Beckman Coulter Avanti J-E) for 30 min. The supernatant was incubated for 1 h with 1.2 ml Ni-NTA resin (Invitrogen) pre-equilibrated with the lysis buffer. The resin after incubation was loaded onto a polypropylene column and washed with 20 ml lysis buffer. PhDph2 was eluted from the column with elution

buffers (100 mM or 150 mM imidazole in the lysis buffer, 3 ml each). The brown-colored elution fractions were buffer exchanged to 150 mM NaCl, 1 mM DTT, and 200 mM Tris-HCl at pH 7.4 using a Bio-Rad 10–DG desalting column. The protein was further purified by heating at 95 °C for 10 min and centrifugation at 48,384 g to remove the precipitate. Purified PhDph2 was concentrated using Amicon Ultra-4 centrifugal filter devices (Millipore).

Expression and purification of SeMet substituted PhDph2

PhDph2.pDESTF1 was transformed into the methionine-auxotrophic *E. coli* strain B834(DE3) pRARE that was obtained by transforming pRARE plasmid into B834(DE3). Cells were grown in M9 minimal medium supplemented with all amino acids (0.04 mg/mL) except L-methionine, 50 mg/l L-SeMet, 1x MEM vitamin solution, 0.4% (w/v) glucose, 2 mM $MgSO_4$, 25 mg/ml $FeSO_4$ and 0.1 mM $CaCl_2$. The SeMet substituted PhDph2 was overexpressed and purified similarly as described above except aerobically and no additional iron and cysteine were added to the media.

Expression and purification of ^{57}Fe-labeled PhDph2 for Mössbauer spectroscopy.

E. coli BL21pRARE cells transformed with PhDph2.pDESTF1 were grown in M9 minimal medium supplemented with 0.2% (w/v) glucose, 2 mM $MgSO_4$ and 0.1 mM $CaCl_2$ at 37 °C. The ^{57}Fe stock solution was prepared by dissolving ^{57}Fe powder (Isoflex USA) in HCl to final concentrations of 1 M iron and 2.5 M chloride. The ^{57}Fe stock solution and L-Cys were added to M9 media to final concentrations of 100 µM and 400 µM, respectively, before induction. The cells were induced at an OD_{600} of 0.8 with 100 µM IPTG and incubated at 20 °C for an additional 20 h. ^{57}Fe labeled PhDph2 was anaerobically purified by following the same procedure used for the native protein purification. The final protein concentration, determined by Bradford protein assay (Bio-Rad), was 30 mg/ml (~800 µM). Iron was quantified by using the commercial Quantichrom iron assay kit (DIFE-250, Bioassay systems).

Cloning, expression and purification of PhEF2

Cloning of PhEF2 followed the same protocol as that of PhDph2. The plasmid was transformed into the *E. coli* expression strain, BL21 (DE3) with a pRARE plasmid. The cells were grown in LB media at 37 °C and induced at an OD600 of 1.0 with 0.1 mM IPTG. Cells were harvested after 3 h of induction by centrifugation at 6,000 rpm for 10 min. PhEF2 was purified through Ni-NTA affinity chromatography following the same protocol for PhDph2. The protein was further purified by heating at 95 °C for 10 min and subsequent FPLC purification using a Superdex 200 gel filtration column and a Q6 anion exchange column (Bio-Rad).

Anaerobic reconstitution of PhDph2 activity and mass characterization of PhEF2

The reaction components, 12 μM PhEF2, 24 μM PhDph2, and 10 mM dithionite were added to 150 mM NaCl, 1 mM DTT, and 200 mM Tris-HCl at pH 7.4 to a final volume of 15 μl in the anaerobic chamber under strictly anaerobic conditions. The reaction vials were sealed before taking out of the anaerobic chamber. ^{14}C-SAM (2μL, final concentration of 267 μM) was injected into each reaction vial to start the reaction. The reaction mixtures were vortexed briefly to mix and incubated at 65 °C for 40 min. The reaction was stopped by adding protein loading dye to the reaction mixture and subsequent heating at 100 °C for 10 min, followed by 12% SDS-PAGE electrophoresis. The dried gel was exposed to a PhosphorImaging screen (GE Healthcare, Piscataway, NJ) and the radioactivity was detected using a STORM860 phosphorimager (GE Healthcare, Piscataway, NJ).

Enzymatic reactions with normal SAM followed the same procedure, except that normal SAM was introduced in the anaerobic chamber. The PhEF2 band from the Coomassie blue-stained SDS-PAGE gel was cut out and digested by trypsin. Digestion products were extracted and cleaned using a Millipore Ziptip C4, then characterized by MALDI-MS at the Proteomics and Mass Spectrometry Facility of Cornell

University.

Analysis of reaction products with HPLC

Under anaerobic conditions, reactions were set up that contained 30 µM PhEF2, 30 µM PhDph2, 10 mM dithionite, 31 µM SAM, 150 mM NaCl, 1 mM DTT, and 200 mM Tris-HCl at pH 7.4 in a final volume of 64 µl. The mixture was incubated at 65 °C for 5 min, and then frozen at -20 °C. The reaction mixture was ice-thawed and TFA was added to a final concentration of 5%, followed by centrifugation to separate the precipitated proteins and the supernatant. The precipitated proteins were re-dissolved and PhEF2 was checked by MALDI-MS as described above to make sure the reaction had occurred. The supernatant was analyzed by HPLC (Shimadzu) on a C18 column (HαSprite) monitored at 260 nm absorbance, using a linear gradient from 0 to 40% buffer B in 20 min at a flow rate of 0.3 ml min^{-1} (buffer A: 50 mM ammonium acetate, pH 5.4; buffer B, 50% (v/v) methanol/water).

^{1}H NMR of reaction mixture

A complete reaction (260 µM PhDph2, 10 mM dithionite and 1000 µM SAM, in 1 ml of 100 mM phosphate buffer with 150 mM sodium chloride, pH=7.4) and control (without PhDph2 or without dithionite) were set up anaerobically. After incubation at 65 °C for 40 min, PhDPh2 was removed using a Millipore YM-10 Microcon filter unit. The flow-through was lyophilized overnight to dryness and then dissolved in 300 µL D_2O for NMR. Shigemi D_2O matched NMR tube was used. ^{1}H NMR spectra were obtained on an INOVA 400 spectrometer. Compared with controls, four new peaks were identified on ^{1}H NMR: *a*. 0.95 ppm (t, 1H, J = 7.6 Hz), *b*. 1.88 ppm (m, 1H), *c*. 2.12 ppm (m, 2H) and *d*. 2.43 ppm (t, 1H, J = 7.5 Hz). H-H DQCOSY 2D NMR spectrum (data not shown) showed that peak a is coupled to b, peak c is coupled to d and another peak (3.78 ppm) that is hidden under the huge signal from buffer. NMR data were analyzed by MestReNova (version 6.0.1).

Dansylation reaction to detect the MS of the reaction products by LC-MS

NMR samples were desalted and purified by TLC silica gel $60F_{254}$ (EMD Chemicals Inc.) with developing solvent (n-butanol : acetic acid : water = 2:1:1). The desired product bands (Rf 0.15 -0.65, below the Rf value of 5´-deoxy-5´-methylthioadenosine) were cut off the TLC plates and the products were washed off the silica gel by water and lyophilized overnight to dryness. The lyophilized products were dissolved with 50 mM sodium bicarbonate to a final concentration approximately 5 times of that of the NMR reaction. The solution was adjusted to pH 9-10 by 12% NaOH. Dansylation reactions were initiated by adding 0.5 volume of 50 mM dansyl chloride in acetonitrile to the solution and the reactions were carried out at room temperature in the dark for 30 min. Dansylated products were separated and analyzed by LC-MS with a linear gradient 0-80% solvent B in 33 min, at a flow rate of 0.8 ml/min. LC-MS experiments were carried out on a SHIMADZU LCMS-QP8000α with C18 column (250 × 4.6 mm, 10 μm, Grace Davison Discovery Sciences Headquarters) monitoring at 254 and 335 nm with positive mode for mass detection. Solvents for LC-MS were water with 0.1% formic acid (solvent A) and acetonitrile with 0.1% formic acid (solvent B).

Sample preparation for Mössbauer spectroscopy and EPR

Anaerobically purified ^{57}Fe-labeled PhDph2 was dialyzed into a buffer containing 200 mM Tris-HCl (pH 7.4), 150 mM NaCl, 1 mM DTT and 10% glycerol, and concentrated to 25 – 30 mg/mL. The sample was frozen in liquid nitrogen in the anaerobic chamber for Mössbauer spectroscopy.

For EPR measurements, PhDph2 (700 μM, with 15% glycerol) with and without 16 mM dithionite were incubated for 30 min before loading into an EPR quartz tube in the glovebox.

Crystallization and structure determination of iron-free PhDph2

Aerobically purified iron-free PhDph2 proteins were dialyzed to 10 mM sodium acetate at pH 4.6 and concentrated to 12 mg/ml for the crystallization experiments. The native protein was subjected to a series of sparse matrix screens (Hampton Research, Emerald Biostructures) using the hanging drop vapor-diffusion method at 18 °C in order to determine initial crystallization conditions. Best crystals for both SeMet substituted and native PhDph2 were obtained from 6 – 8% PEG 4000, 0.1 M ammonium acetate, 0.2 M KCl, 2% ethylene glycol, and 0.05 M sodium citrate at pH 5.1 – 5.3. These crystals belong to the space group $P2_12_12_1$ with typical unit cell dimensions of a = 58.5 Å, b = 82.0, and c = 160.0 Å. Each asymmetric unit contains two monomers, corresponding to a solvent content of 50.3% and Matthews coefficient of 2.47 $Å^3$/Da.

The PhDph2 SeMet crystals were briefly transferred into a solution containing 6% glycerol, 16% ethylene glycol, 10% PEG 4000, 0.2 M ammonium acetate, 0.2 M KCl, and 0.1 M sodium citrate at pH 5.3 for cryoprotection. The crystals were allowed to soak in the cryo-solution for 30 – 45 s before plunging them into liquid nitrogen. In an attempt to reconstitute the iron sulfur clusters in crystals, native crystals were soaked in 10% PEG 4000, 100 mM citrate pH 5.3, 200 mM ammonium acetate, 200 mM KCl, 10% ethylene glycol, 8 mM SAM, 4 mM $Fe(NH_4)_2(SO_4)_2$, 4 mM NaS, and 40 mM DTT for 1 h prior to the same cryoprotection and freezing procedure described above.

Data sets were collected at the Advanced Photon Source beamlines 24-ID-C and 24-ID-E using ADSC Quantum 315 CCD detectors. For the single wavelength SeMet data set, the energy was selected to maximize Δf" of the incorporated selenium (12661.5 eV, 0.97922 Å). Data sets were integrated and scaled using HKL2000(*39*). Data processing statistics are summarized in Supplementary Table 1.

Eight selenium atom positions were determined using HKL2MAP(*40*). These

sites were used for SAD phasing using MLPHARE(*41*) at 2.5 Å resolution. Initial phases were further improved through density modification, twofold noncrystallographic symmetry averaging, and phase extension for the 2.3 Å resolution native data using RESOLVE.(*42*, *43*) The resulting map was readily interpretable and an initial model was built using the interactive graphics program Coot(*44*). The model refinement was carried out through alternating cycles of manually rebuilding using Coot, restrained refinement and water picking using Refmac5(*45*) and Phenix(*46*).

Crystallization and structure determination of reconstituted PhDph2.

Reconstituted PhDph2 protein was dialyzed to 100 mM NaCl, 1 mM DTT, and 10 mM sodium acetate at pH 4.6, concentrated to 20 mg/ml, and crystallized anaerobically at 26 °C in the glove box using the hanging drop vapor diffusion method. Anoxic sparse matrix screening solutions (Hampton Research, Emerald Biostructures) were used for initial crystallization screens. The optimized crystallization condition is as follows: drops were set up with 1.3 µl protein and an equal volume of 25 – 30% PEG 400, 0.2 M lithium sulfate and 0.1 M MES at pH 6.5, and were equilibrated against a reservoir solution of 0.6 M lithium chloride. Crystals appeared in a week and belonged to the same space group as that of the iron-free structure ($P2_12_12_1$ with averaged unit cell dimensions of a = 55.7 Å, b = 80.5 Å and c = 162.1 Å). Prior to the data collection experiment, crystals were cryoprotected with 2.5 – 5% ethylene glycol, 25 – 30% PEG 400, 0.2 M lithium sulfate, and 0.1 M MES at pH 6.5, then plunged directly into liquid nitrogen in the glove box. A total of 200° of data were recorded at an energy of 12662.0 eV on an ADSC Quantum 315 CCD detector. The data were integrated and scaled to 2.1 Å resolution using HKL2000(*39*). The previously solved structure of PhDph2 lacking the iron sulfur cluster was used to generate phases by Fourier synthesis. A difference Fourier map was calculated and averaged for the two monomers to improve the electron density, and the resulting map

was used to model the [4Fe-4S] cluster. A 2.8 Å resolution anomalous difference Fourier map calculated from a data set collected at 7150 eV (1.73405 Å) was also used as a reference for positioning the [4Fe-4S] cluster (not shown). The structure was refined using CNS(*47*).

UV-Vis spectroscopy.

Samples of PhDph2 (50 µM), with and without dithionite, were prepared anaerobically in 150 mM NaCl and 200 mM Tris-HCl at pH 7.4. The sample treated with dithionite was allowed to incubate for 30 min after adding the reducing agent at a final concentration of 0.5 mM. The samples were sealed in a Quartz cell (100 µl each) before taking out from the anaerobic chamber. UV-Vis spectra were obtained on a Cary 50 Bio UV-Visible spectrophotometer (Varian), scanning from 200 nm to 800 nm. The baseline was corrected with the buffer used to prepare the samples.

EPR spectroscopy.

ESR spectra were recorded at ACERT on a Bruker EMX spectrometer at a frequency of 9.24 GHz under standard conditions in 4 mm ID quartz tubes. The tubes were filled with PhDph2 solutions in an oxygen-free atmosphere and sealed under vacuum at 77 K. ESR measurements at 5-50 K were carried out using a liquid helium cryostat, ESR-10 (Oxford Instruments Ltd, England). The spectrometer settings were: modulation frequency 100 kHz, modulation amplitude 8 G, microwave power 0.63 mW.

Mössbauer spectroscopy.

Mössbauer spectra were recorded on a spectrometer from WEB research (Edina, MN) operating in the constant acceleration mode in transmission geometry. Spectra were recorded with the temperature of the sample maintained at 4.2 K using a SVT-400 cryostat from Janis (Wilmington, MA) in an externally applied magnetic field of 53 mT oriented parallel to the γ-beam. The quoted isomer shifts are relative to

the centroid of the spectrum of a foil of α-Fe metal at room temperature. Data analysis was performed using the program WMOSS from WEB research.

REFERENCES

1. (2005) Diphtheria, p http://www.cdc.gov/ncidod/DBMD/diseaseinfo/diptheria_t.htm.
2. Collier, R. J. (2001) Understanding the mode of action of diphtheria toxin: a perspective on progress during the 20th century, *Toxicon 39*, 1793-1803.
3. Liu, S., Milne, G. T., Kuremsky, J. G., Fink, G. R., and Leppla, S. H. (2004) Identification of the proteins required for biosynthesis of diphthamide, the target of bacterial ADP-ribosylating toxins on translation elongation factor 2, *Mol. Cell. Biol. 24*, 9487-9497.
4. Gomez-Lorenzo, M. G., Spahn, C. M. T., Agrawal, R. K., Grassucci, R. A., Penczek, P., Chakraburtty, K., Ballesta, J. P. G., Lavandera, J. L., Garcia-Bustos, J. F., and Frank, J. (2000) Three-dimensional cryo-electron microscopy localization of EF2 in the *Saccharomyces cerevisiae* 80S ribosome at 17.5 Å resolution, *EMBO J. 19*, 2710-2718.
5. Ortiz, P. A., Ulloque, R., Kihara, G. K., Zheng, H., and Kinzy, T. G. (2006) Translation elongation factor 2 anticodon mimicry domain mutants affect fidelity and diphtheria toxin resistance, *J. Biol. Chem. 281*, 32639-32648.
6. Walsh, C. T. (2006) *Posttranslational modifications of proteins: Expanding nature's inventory*, Roberts and Company Publishers, Englewood, Colorado.
7. Moehring, J. M., Moehring, T. J., and Danley, D. E. (1980) Posttranslational modification of elongation factor 2 in diphtheriatoxin-resistant mutants of CHO-K1 cells, *Proc. Natl. Acad. Sci. USA 77*, 1010-1014.
8. Moehring, T. J., Danley, D. E., and Moehring, J. M. (1984) In vitro biosynthesis of diphthamide, studied with mutant Chinese hamster ovary cells resistant to diphtheria toxin, *Mol. Cell. Biol. 4*, 642-650.

9. Chen, J. Y., Bodley, J. W., and Livingston, D. M. (1985) Diphtheria toxin-resistant mutants of *Saccharomyces cerevisiae.*, *Mol. Cell. Biol. 5*, 3357-3360.

10. Mattheakis, L., Shen, W., and Collier, R. (1992) DPH5, a methyltransferase gene required for diphthamide biosynthesis in *Saccharomyces cerevisiae*., *Mol. Cell. Biol. 12*, 4026-4037.

11. Mattheakis, L. C., Sor, F., and Collier, R. J. (1993) Diphthamide synthesis in *Saccharomyces cerevisiae*: structure of the DPH2 gene, *Gene 132*, 149.

12. Phillips, N. J., Ziegler, M. R., and Deaven, L. L. (1996) A cDNA from the ovarian cancer critical region of deletion on chromosome 17p13.3, *Cancer Lett. 102*, 85.

13. Schultz, D. C., Balasara, B. R., Testa, J. R., and Godwin, A. K. (1998) Cloning and localization of a human diphthamide biosynthesis-like protein-2 gene,DPH2L2, *Genomics 52,* 186.

14. Altschul, S. F., Gish, W., Miller, W., Myers, E. W., and Lipman, D. J. (1990) Basic local alignment search tool, *J. Mol. Biol. 215*, 403-410.

15. Frey, P. A., Hegeman, A. D., and Ruzicka, F. J. (2008) The radical SAM superfamily, *Crit. Rev. Biochem. Mol. Biol. 43*, 63 - 88.

16. Sakuraba, H., Tsuge, H., Yoneda, K., Katunuma, N., and Ohshima, T. (2005) Crystal structure of the NAD biosynthetic enzyme quinolinate synthase, *J. Biol. Chem. 280*, 26645-26648.

17. Sofia, H. J., Chen, G., Hetzler, B. G., Reyes-Spindola, J. F., and Miller, N. E. (2001) Radical SAM, a novel protein superfamily linking unresolved steps in familiar biosynthetic pathways with radical mechanisms: functional characterization using new analysis and information visualization methods, *Nucl. Acids Res. 29*, 1097-1106.

18. Chatterjee, A., Li, Y., Zhang, Y., Grove, T. L., Lee, M., Krebs, C., Booker, S. J., Begley, T. P., and Ealick, S. E. (2008) Reconstitution of ThiC in thiamine pyrimidine biosynthesis expands the radical SAM superfamily, *Nat. Chem. Biol. 4*, 758-765.

19. McGlynn, S. E., Boyd, E. S., Shepard, E. M., Lange, R. K., Gerlach, R., Broderick, J. B., and Peters, J. W. (2010) Identification and characterization of a novel member of the radical AdoMet enzyme superfamily and implications for the biosynthesis of the Hmd hydrogenase active site cofactor, *J. Bacteriol. 192*, 595-598.

20. Makinen, G. B., and Wells, M. W. (1987) Application of EPR saturation methods to paramagnetic metal ions in proteins, in *ENDOR, EPR and electron spin echo for probing coordination spheres* (Sigel, H., and Sigel, A., Eds.), pp 129-204.

21. Lieder, K. W., Booker, S., Ruzicka, F. J., Beinert, H., Reed, G. H., and Frey, P. A. (1998) S-adenosyl-L-methionine-dependent reduction of lysine 2,3-aminomutase and observation of the catalytically functional iron-sulfur centers by electron paramagnetic resonance, *Biochemistry 37*, 2578-2585.

22. Walsby, C. J., Hong, W., Broderick, W. E., Cheek, J., Ortillo, D., Broderick, J. B., and Hoffman, B. M. (2002) Electron-nuclear double resonance spectroscopic evidence that S-adenosyl-L-methionine binds in contact with the catalytically active [4Fe-4S]+ cluster of pyruvate formate-lyase activating enzyme., *J. Am. Chem. Soc. 124*, 3143-3151.

23. Cicchillo, R. M., Tu, L., Stromberg, J. A., Hoffart, L. M., Krebs, C., and Booker, S. J. (2005) *Escherichia coli* quinolinate synthetase does indeed harbor a [4Fe-4S] cluster, *J. Am. Chem. Soc. 127*, 7310-7311.

24. Saunders, A. H., Griffiths, A. E., Lee, K.-H., Cicchillo, R. M., Tu, L., Stromberg, J. A., Krebs, C., and Booker, S. J. (2008) Characterization of quinolinate synthases from *Escherichia coli*, *Mycobacterium tuberculosis*, and *Pyrococcus horikoshii* indicates that [4Fe-4S] clusters are common cofactors throughout this cass of enzymes., *Biochemistry 47*, 10999-11012.

25. Berkovitch, F., Nicolet, Y., Wan, J. T., Jarrett, J. T., and Drennan, C. L. (2004) Crystal structure of biotin synthase, an *S-adenosyl-L-methionine*-dependent radical enzyme, *Science 303*, 76-79.

26. Layer, G., Moser, J., Heinz, D. W., Jahn, D., and Schubert, W.-D. (2003) Crystal structure of coproporphyrinogen III oxidase reveals cofactor geometry of Radical SAM enzymes, *EMBO J. 22*, 6214-6224.

27. Lepore, B. W., Ruzicka, F. J., Frey, P. A., and Ringe, D. (2005) The x-ray crystal structure of lysine-2,3-aminomutase from *Clostridium subterminale*, *Proc. Natl. Acad. Sci. USA 102*, 13819-13824.

28. Hanzelmann, P., and Schindelin, H. (2004) Crystal structure of the S-adenosyl-L-methionine-dependent enzyme MoaA and its implications for molybdenum cofactor deficiency in humans, *Proc. Natl. Acad. Sci. USA 101*, 12870-12875.

29. Vey, J. L., Yang, J., Li, M., Broderick, W. E., Broderick, J. B., and Drennan, C. L. (2008) Structural basis for glycyl radical formation by pyruvate formate-lyase activating enzyme, *Proc. Natl. Acad. Sci. USA 105*, 16137-16141.

30. Marinoni, I., Nonnis, S., Monteferrante, C., Heathcote, P., Hartig, E., Bottger, L. H., Trautwein, A. X., Negri, A., Albertini, A. M., and Tedeschi, G. (2008) Characterization of L-aspartate oxidase and quinolinate synthase from Bacillus subtilis, *FEBS J 275*, 5090-5107.

31. Rekittke, I., Wiesner, J., RoÌˆhrich, R., Demmer, U., Warkentin, E., Xu, W., Troschke, K., Hintz, M., No, J. H., Duin, E. C., Oldfield, E., Jomaa, H., and Ermler, U. (2008) Structure of (E)-4-hydroxy-3-methyl-but-2-enyl diphosphate reductase, the terminal enzyme of the non-mevalonate pathway, *J. Am. Chem. Soc. 130*, 17206-17207.

32. Walsby, C. J., Ortillo, D., Broderick, W. E., Broderick, J. B., and Hoffman, B. M. (2002) An anchoring role for FeS clusters: Chelation of the amino acid moiety of S-adenosyl-L-methionine to the unique iron site of the [4Fe-4S] custer of pyruvate formate-lyase activating enzyme., *J. Am. Chem. Soc. 124*, 11270-11271.

33. Krogan, N. J., Cagney, G., Yu, H., Zhong, G., Guo, X., Ignatchenko, A., Li, J., Pu, S., Datta, N., Tikuisis, A. P., Punna, T., PeregrÃ-n-Alvarez, J. M., Shales, M., Zhang, X., Davey, M., Robinson, M. D., Paccanaro, A., Bray, J. E., Sheung, A., Beattie, B., Richards, D. P., Canadien, V., Lalev, A., Mena, F., Wong, P., Starostine, A., Canete, M. M., Vlasblom, J., Wu, S., Orsi, C., Collins, S. R., Chandran, S., Haw, R., Rilstone, J. J., Gandi, K., Thompson, N. J., Musso, G., St Onge, P., Ghanny, S., Lam, M. H. Y., Butland, G., Altaf-Ul, A. M., Kanaya, S., Shilatifard, A., O'Shea, E., Weissman, J. S., Ingles, C. J., Hughes, T. R., Parkinson, J., Gerstein, M., Wodak, S. J., Emili, A., and Greenblatt, J. F. (2006) Global landscape of protein complexes in the yeast Saccharomyces cerevisiae, *440*, 637.

34. Gavin, A.-C., Aloy, P., Grandi, P., Krause, R., Boesche, M., Marzioch, M., Rau, C., Jensen, L. J., Bastuck, S., Dumpelfeld, B., Edelmann, A., Heurtier, M.-A., Hoffman, V., Hoefert, C., Klein, K., Hudak, M., Michon, A.-M., Schelder, M., Schirle, M., Remor, M., Rudi, T., Hooper, S., Bauer, A., Bouwmeester, T., Casari, G., Drewes, G., Neubauer, G., Rick, J. M., Kuster, B., Bork, P., Russell, R. B., and Superti-Furga, G. (2006) Proteome survey reveals modularity of the yeast cell machinery, *Nature 440*, 631-636.

35. Collins, S. R., Kemmeren, P., Zhao, X.-C., Greenblatt, J. F., Spencer, F., Holstege, F. C. P., Weissman, J. S., and Krogan, N. J. (2007) Toward a comprehensive atlas of the physical Interactome of *Saccharomyces cerevisiae*, *Mol. Cell. Proteomics 6*, 439-450.

36. Proudfoot, M., Sanders, S. A., Singer, A., Zhang, R., Brown, G., Binkowski, A., Xu, L., Lukin, J. A., Murzin, A. G., Joachimiak, A., Arrowsmith, C. H., Edwards, A. M., Savchenko, A. V., and Yakunin, A. F. (2008) Biochemical and structural characterization of a novel family of cystathionine [beta]-synthase domain proteins fused to a Zn ribbon-like domain, *J. Mol. Biol. 375*, 301-315.

37. Johnson, D. C., Dean, D. R., Smith, A. D., and Johnson, M. K. (2005) Structure, function, and formation of biological iron-sulfur clusters, *Annu. Rev. Biochem. 74*, 247-281.

38. Lill, R., and Muhlenhoff, U. (2008) Maturation of iron-sulfur proteins in eukaryotes: mechanisms, connected processes, and diseases, *Annu. Rev. Biochem. 77*, 669-700.

39. Otwinowski, Z., and Minor, W. (1997) Processing of x-ray diffraction data collected in oscillation mode, *Methods Enzymol. 276*, 307-326.

40. Sheldrick, G. M. (2008) A short history of SHELX, *Acta Crystallogr. A 64*, 112-122.

41. Collaborative Computational Project-Number 4. (1994) The CCP-4 suite: programs for protein crystallography, *Acta. Crystallogr. D 50*, 760-763.

42. Terwilliger, T. C. (1999) Reciprocal-space solvent flattening., *Acta Crystallogr. D Biol. Crystallogr. 55*, 1863-1871.

43. Terwilliger, T. C. (2000) Maximum-likelihood density modification., *Acta Crystallogr. D Biol. Crystallogr. 56*, 965-972.

44. Emsley, P., and Cowtan, K. (2004) Coot: model-building tools for molecular graphics, *Acta Crystallogr. D Biol. Crystallogr. 60*, 2126-2132.

45. Murshudov, G. N., Vagin, A. A., and Dodson, E. J. (1997) Refinement of macromolecular structures by the maximum-likelihood method, *Acta Crystallogr. D Biol. Crystallogr. 53*, 240-255.

46. Adams, P. D., Grosse-Kunstleve, R. W., Hung, L. W., Ioerger, T. R., McCoy, A. J., Moriarty, N. W., Read, R. J., Sacchettini, J. C., Sauter, N. K., and Terwilliger, T. C. (2002) PHENIX: building new software for automated crystallographic structure determination, *Acta Crystallogr. D Biol. Crystallogr. 58*, 1948-1954.

47. Brünger, A. T., Adams, P. D., Clore, G. M., DeLano, W. L., Gros, P., Grosse-Kunstleve, R. W., Jiang, J. S., Kuszewski, J., Nilges, M., Pannu, N. S., Read, R. J., Rice, L. M., Simonson, T., and Warren, G. L. (1998) Crystallography & NMR system: A new software suite for macromolecular structure determination, *Acta Crystallogr. D Biol. Crystallogr. 54*, 905-921.

CHAPTER 3

MECHANISTIC UNDERSTANDING OF PYROCOCCUS HORIKOSHII DPH2, A [4Fe-4S] ENZYME REQUIRED FOR DIPHTHAMIDE BIOSYNTHESIS*

Abstract

Diphthamide, the target of diphtheria toxin, is a unique posttranslational modification on eukaryotic and archaeal translation elongation factor 2 (EF2). The proposed biosynthesis of diphthamide involves three steps and we have found that in *Pyrococcus horikoshii* (*P. horikoshii*), the first step uses a S-adenosyl-L-methionine (SAM)-dependent [4Fe-4S] enzyme, PhDph2, to catalyze the formation of a C-C bond. Crystal structure shows that PhDph2 is a homodimer and each monomer contains three conserved cysteine residues that can bind a [4Fe-4S] cluster. In the reduced state, the [4Fe-4S] cluster can provide one electron to reductively cleave the bound SAM molecule. However, different from classical radical SAM family of enzymes, biochemical evidence suggests that a 3-amino-3-carboxypropyl radical is generated in PhDph2. In this chapter I present evidence supporting that the 3-amino-3-carboxypropyl radical does not undergo hydrogen abstraction reaction, which is observed for the deoxyadenosyl radical in classical radical SAM enzymes. Instead, the 3-amino-3-carboxypropyl radical is added to the imidazole ring in the pathway towards the formation of the product. Furthermore, the data suggest that the chemistry requires only one [4Fe-4S] cluster to be present in the PhDph2 dimer.

Introduction

Diphthamide, found in both eukaryotes and archaea (*1-3*), is a unique posttranslational modification on a histidine residue of translational elongation factor 2 (EF2). EF2 is a GTPase required for ribosomal protein synthesis (*4*). Diphthamide is the target of diphtheria toxin(*5*), which ADP-ribosylates diphthamide and inhibits protein synthesis, leading to host cell death(*6*). Diphthamide was reported to help prevent -1 frame shift mutation during protein synthesis(*7*). The biosynthesis of the modification is still not completely understood(*8*), despite the fact that the modification has been identified for over three decades.(*1*) Genetic studies have identified five genes, Dph1, Dph2, Dph3, Dph4, and Dph5, in eukaryotes required for the biosynthesis of diphthamide and a three-step biosynthesis pathway involving these genes has been proposed(*9, 10*). The first step is the transfer of the 3-amino-3-carboxypropyl group from *S*-L-adenosylmethionine (SAM) to the C-2 position of the imidazole ring of the target histidine residue in EF2. Dph1-4 are known to be required for the first step (*6, 9, 11-15*). The second step, catalyzed by Dph5 (*16*), is the trimethylation of the amino group to form an intermediate compound called diphthine. The last step is the ATP-dependent amidation of the carboxyl group of diphthine (Figure 3.1). The enzyme that catalyzes the last step has not been identified.

Diphthamide is also found in archaea. However, among the five eukaryotic genes required for diphthamide biosynthesis, only two orthologs can be found in archaea by BLAST search. One of them, Dph2, is homologous to eukaryotic Dph1 and Dph2 (Dph1 and Dph2 are homologous to each other), and the other one is the diphthine synthase, Dph5.

We have successfully reconstituted the first step of diphthamide biosynthesis using the *Pyrococcus horikoshii* Dph2 (PhDph2) and EF2 (PhEF2) (Figure 3.1). PhDph2 forms a homodimer. Each monomer has three conserved cysteine residues

(Cys59, Cys163 and Cys287) that can bind a [4Fe-4S] cluster. Similar to radical SAM enzymes, the [4Fe-4S] cluster in PhDph2 binds SAM and in the reduced state can provide one electron to reductively cleave SAM. However, unlike radical SAM enzymes, our evidence suggest that PhDph2 generates a 3-amino-3-carboxypropyl (ACP) radical, instead of a 5'-deoxyadenosyl radical (*17*).

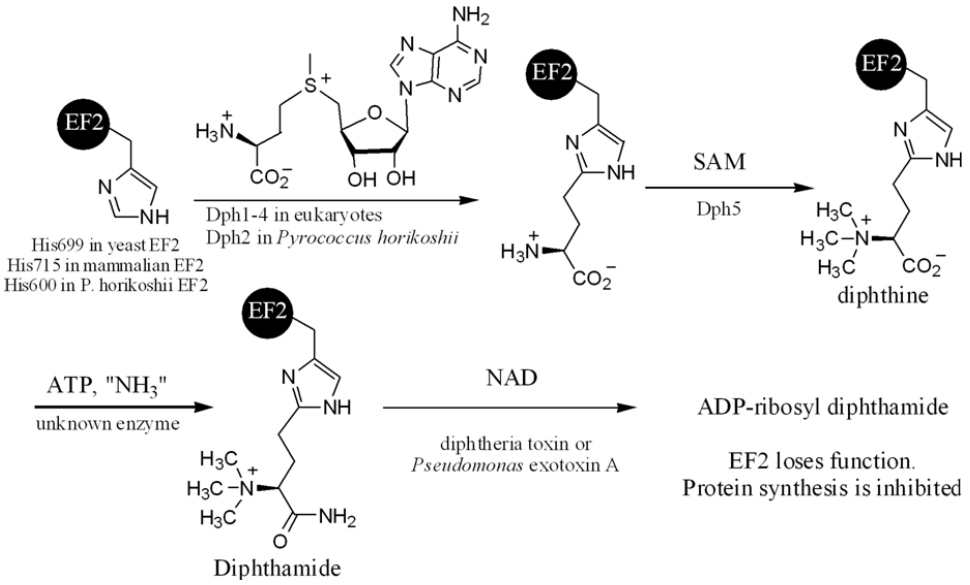

Figure 3.1. Diphthamide biosynthesis pathway

Although our previous study suggests that an ACP radical is responsible for the C-C bond formation reaction(*17*), details of the reaction mechanism still need to be determined. For example, how does the ACP radical react with the imidazole ring to form the C-C bond? Does the reaction require each of the monomers to contain a [4Fe-4S] cluster, or is only one [4Fe-4S] cluster per dimer sufficient? These two questions may be connected to each other, as indicated by the two possible mechanistic proposals shown in Figure 3. 2. Here we report our efforts in trying to differentiate these two mechanisms using mutagenesis to generate a "heterodimer" of PhDph2, with one wild type monomer that contains a [4Fe-4S] cluster while the other mutant

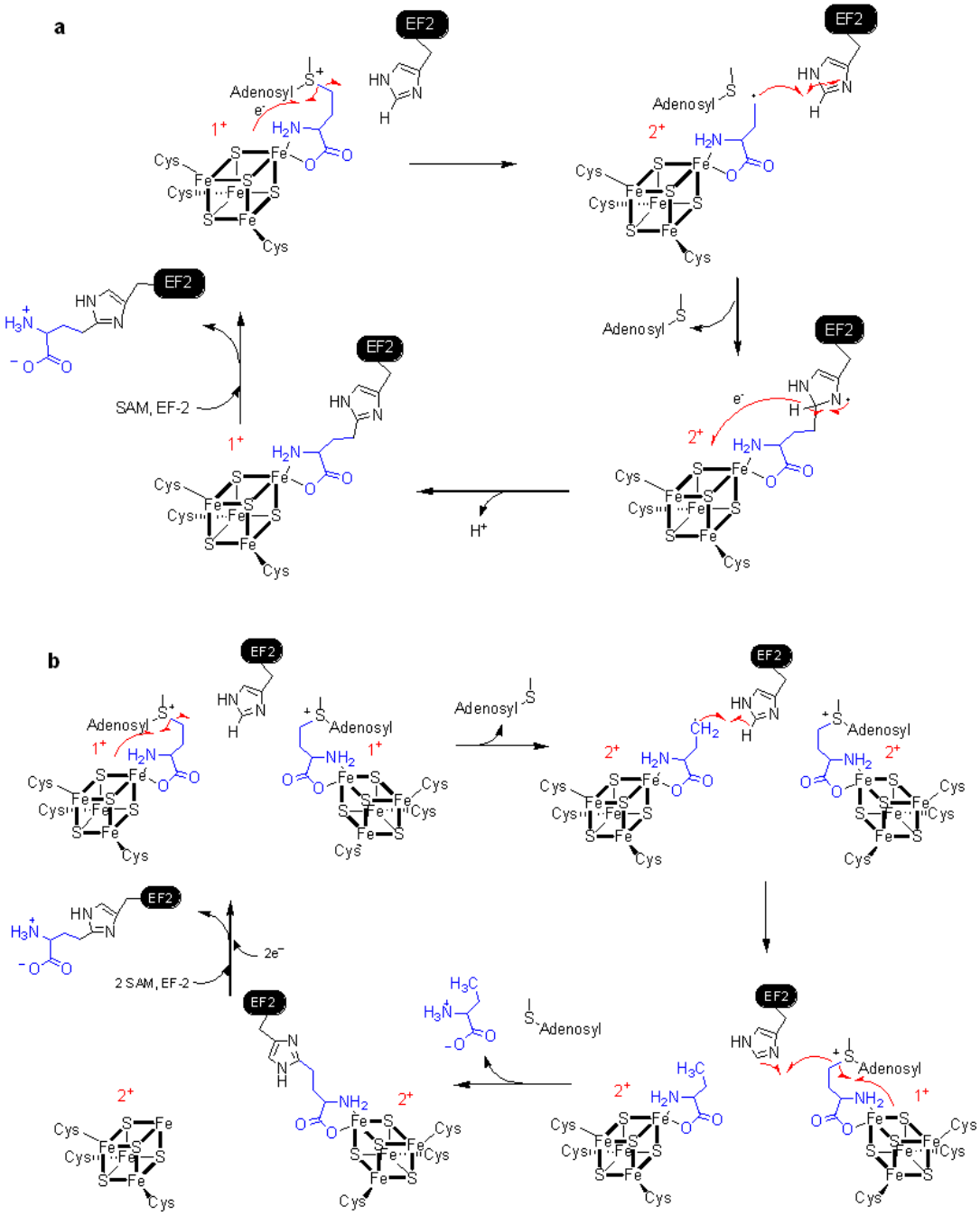

Figure 3.2. Two possible mechanisms for PhDph2-catalyzed reaction. a. One [4Fe-4S] cluster per PhDph2 dimer is sufficient for the reaction and the ACP radical adds to the imidazole ring; b. Two [4Fe-4S] clusters per PhDph2 dimer are required for the reaction. The ACP radical abstracts a hydrogen atom from the imidazole ring. As a consequence, one reaction needs two SAM with one ACP transferred to PhEF2 and the other one released as 2-aminobutyric acid.

monomer is incapable of binding a [4Fe-4S] cluster. Our evidence suggests that the chemistry only requires one [4Fe-4S] cluster to be present per PhDph2 dimer, consistent with the mechanism in Figure 3. 2a. In addition, in the presence of PhEF2, we showed that 2-aminobutyrate is not formed, further supporting the mechanism shown in Figure 3. 2a.

Results

Single cysteine to alanine mutants of PhDph2 can still bind [4Fe-4S] clusters while double mutants cannot.

Our previous work showed that PhDph2 forms a homodimer and each monomer contains three conserved cysteine residues (Cysteine59, Cysteine163 and Cysteine287) that can bind a [4Fe-4S] cluster. In order to make a PhDph2 heterodimer with only one subunit capable of binding a [4Fe-4S] cluster, we decided to mutate these conserved cysteine residues to alanine. All three single mutants (C59A, C163A and C287A) purified anaerobically have a brown color, similar to that of wild type PhDph2, indicative of the binding of a [4Fe-4S] cluster. Ultraviolet-visible (UV-Vis) spectroscopy and electron paramagnetic resonance (EPR) spectroscopy were obtained to further confirm that these single mutants can bind an Fe-S cluster. All three single mutants of PhDph2 have absorption at 400 nm, similar to the wild type PhDph2 (Figure 3.3a). The absorption disappears upon reduction by 0.5 mM dithionite (Figure 3.3b). The 400 nm absorption is consistent with several known radical SAM enzymes, including AtsB(*18*), HemN(*19*), and MoaA(*20*). Upon reduction with dithionite, the wild type PhDph2 shows a strong EPR absorption with an average *g* factor of ~ 1.935 (Figure 3.3c). The temperature dependence of the EPR spectrum, which is best resolved at ~ 12K and becomes unobservable above 30K, is typical for rapidly relaxing $[4Fe - 4S]^{1+}$ clusters. EPR spectra of PhDph2 single mutants are in general

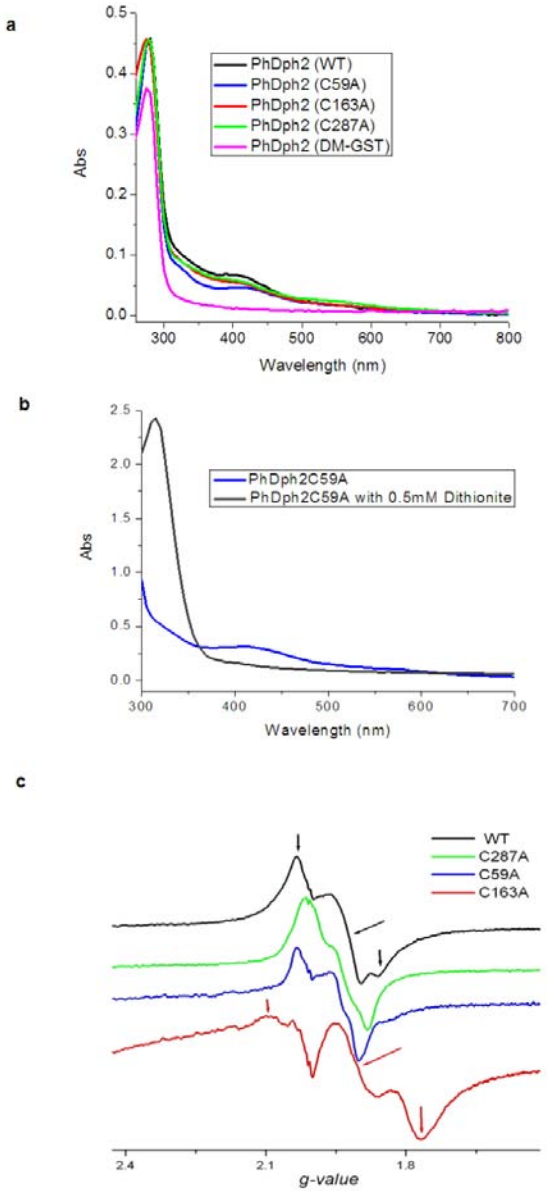

Figure 3.3. Spectroscopic characterization of PhDph2 mutants. a. UV-Vis spectra of purified PhDph2 wild type (black line), single mutants: C59A (blue line), C163A (red line), C287A (green line) and double mutant(pink line); b. UV-Vis spectra of PhDph2 C59A with and without dithionite; c. EPR spectra of wild type PhDph2 and its single mutants in the reduced dithionite reduced state at 12 K. The principal values of g-factor for the main spectral component (shown for wild type and C163A with arrows of corresponding color) are: *WT*: 2.03, 1.92, 1.86*;* C287A: 2.01, 1.94, 1.88. *S59A*: 2.03, 1.94, 1.90; *C163A*: 2.11, 1.91, 1.793;

very similar to wild type (Figure 3.3c), suggesting that they do bind Fe-S cluster. The most remarkable difference in the EPR spectrum of the reduced form is observed for C163A, which exhibits pronounced rhombic main features with greatly increased g-value anisotropy. For both C59A and C287A, the g-tensors are more axial than wild type. The changes in EPR spectra in the mutants probably reflect the changes of the local environment introduced by the mutation.

We next constructed a double cysteine mutant of PhDph2, C59A/C287A. This double mutant, when anaerobically purified, has no color, indicating the lack of Fe-S cluster. UV-Vis spectrum (Figure 3.3a, pink line) confirmed the lack of Fe-S cluster. Thus, the single cysteine mutant can bind Fe-S cluster whereas the double mutant cannot.

Single mutants of PhDph2 have activity and the double mutant does not.

Wild type PhDph2 can catalyze the transfer of 3-amino-3-carboxypropyl group from SAM onto His600 of PhEF2, which can be detected by autoradiography if carboxy-^{14}C-SAM is used. MTA, the small molecule product derived from SAM, can be monitored by HPLC (*17*). Using these two methods, we tested whether the single and double cysteine mutants of PhDph2 have activity or not (Figure 3.4). All three single mutants (C59A, C163A and C287A) were able to transfer the ACP group onto His600 of PhEF2 (Figure 3.4a,) and to produce MTA (Figure 3.4b). However, the single mutants are not as active as the wild type PhDph2, as judged by the amount of MTA formed in the reaction (Figure 3.4b). Unlike the single mutants, the double mutant of PhDph2 (C59A/C287A) has no activity (Figure 3.7a, lanes 11 and 14), consistent with the finding that the double mutant cannot bind a [4Fe-4S] cluster.

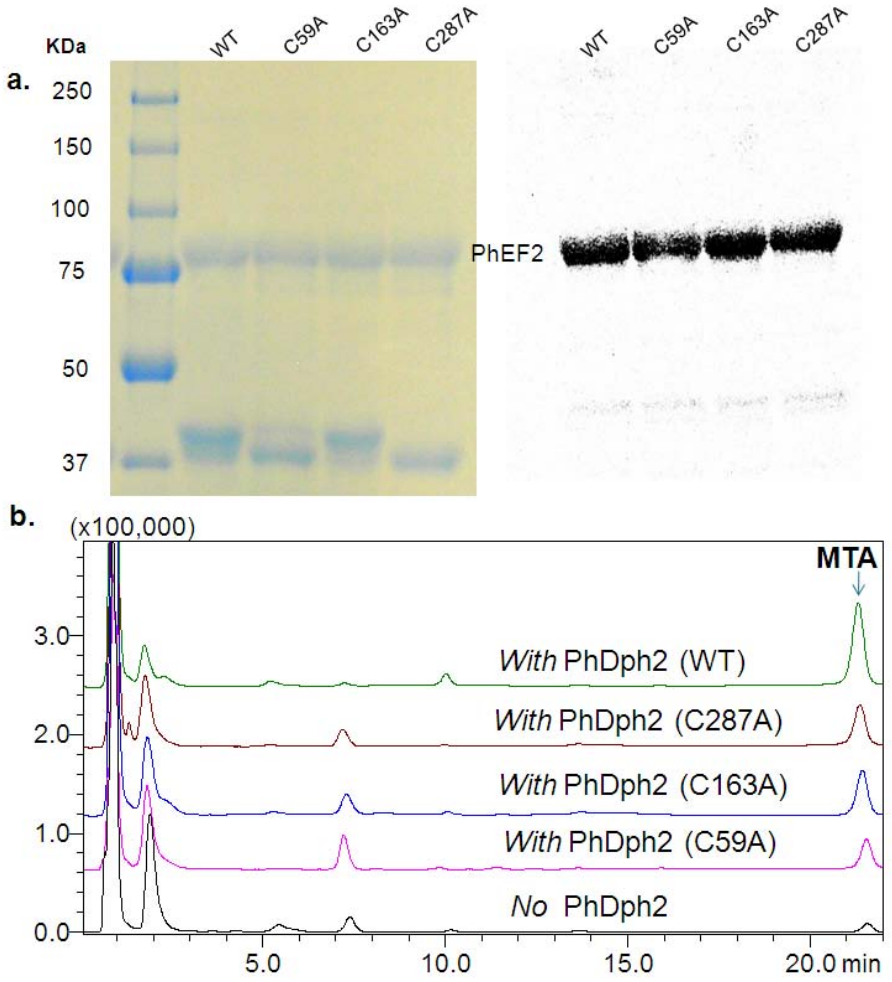

Figure 3.4. Activity assay of PhDph2 single mutants monitored by autoradiography and HPLC. a. ^{14}C- labeling of PhEF2 by PhDph2 wild type and three single mutants. The reactions contain PhEF2, PhDph2 (WT or mutants), SAM, and dithionite. Left panel shows the Coomassie Blue-stained gel and right panel shows the autoradiography. b. Reaction product methylthioadenosine (MTA) formation was detected by HPLC. SAM was eluted at 2 min and MTA was eluted at 21.5 min.

Expression and purification of PhDph2 heterodimer

To obtain a PhDph2 heterodimer with only one subunit capable of binding a [4Fe-4S] cluster to investigate the reaction mechanism, we co-expressed PhDph2 wild type with a His_6 tag (WT-His_6) and the C59A/C287A double mutant with a GST tag

(DM-GST). The proteins were first purified by a Ni affinity purification to give a mixture of PhDph2 WT-His_6: WT-His_6 homodimer and WT-His_6: DM-GST heterodimer. The mixture was then subjected to a glutathione affinity purification to give the DM-GST: WT-His6 heterodimer (Figure 3.5). The homodimers WT-His_6: WT-His_6 and DM-GST:DM-GST can be obtained by further purifying the flow through from the two affinity purification steps(Figure 3.5a). The homodimer and heterodimer after such purifications were checked by SDS-PAGE as shown in Figure 3.5b, which demonstrates that our tandem purification strategy works as outlined in Figure 3.5a.

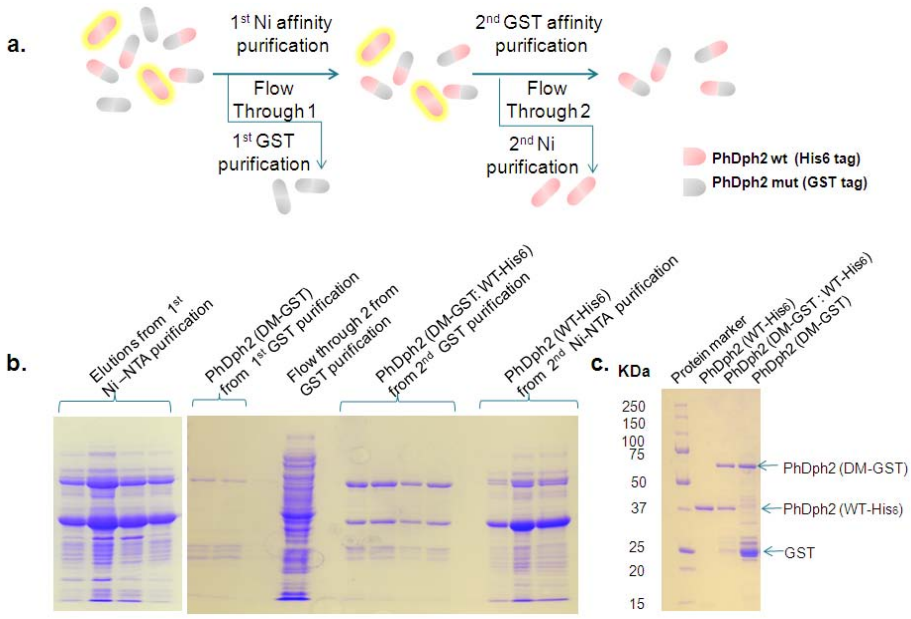

Figure 3.5. Tandem purification to get different PhDph2 dimers. a. Diagram showing the tandem purification strategy to get different PhDph2 dimers; b. Tandem purification of PhDph2 dimers: left, elutions from Ni-NTA purification by using different concentrations of imidazole solutions to get PhDph2 (WT-His_6) and PhDph2 (DM-GST:WT-His_6) mixture; Right, purification of PhDph2 (DM-GST), PhDph2 (DM-GST:WT-His_6), and PhDph2 (WT-His_6). PhDph2 (WT-His_6). c. Purified PhDph2 dimers. The PhDph2 (WT-His_6) shown here was further purified by heating at 95 °C.

PhDph2 heterodimer is stable.

In order to use the PhDph2 heterodimer to study the reaction mechanism, we have to make sure that the heterodimer is stable. If it is not stable and subunits can dissociate and reassociate, then homodimers of WT and double mutant will form in the reaction and complicate the data analysis. The homodimers WT-His_6: WT-His_6 and DM-GST: DM-GST were first mixed to allow subunits exchange, if there was any. The mixture was then incubated with Ni-NTA resin. If subunits exchange occurs, the heterodimer DM-GST: WT-His_6 will form, which will bind to the Ni-resin, leading to the retaining of DM-GST on the resin. If subunits exchange did not occur, only the WT-His_6 will be retained on the Ni-resin. Proteins retained on Ni-resin can then be eluted with imidazole and analyzed by SDS-PAGE. The detection of the GST-tagged protein in the imidazole elutions on SDS-PAGE would indicate that subunits exchange has occurred. Based on this analysis, PhDph2 WT-His_6 (~ 34 kDa per monomer, Figure 3.5c, lane 2) and DM-GST (about 60 kDa per monomer, Figure 3.5c, lane 4) can indeed undergo subunit exchange when mixed together, because DM-GST was detected on SDS-PAGE in the imidazole elutions (Figure 3.6b, lane 2 and 3). By the same analysis, if subunit exchange occurs to the PhDph2 heterodimer (WT-His_6: DM-GST), then the homodimer with GST-tagged double mutant will form which cannot be retained on the Ni-resin. When we carried out the experiment with the heterodimer, no DM-GST was detected in the flow through on SDS-PAGE (Figure 3.6b, lane 5) and both WT-His_6 and DM-GST were found in the elutions from Ni-resin (Figure 3.6b, lane 6). As a control, when we used the homodimer of DM-GST, we can readily detect it in the flow through (Figure 3.6a, lane 1). Taken together, we found that the homodimers are not stable, but the heterodimer is stable.

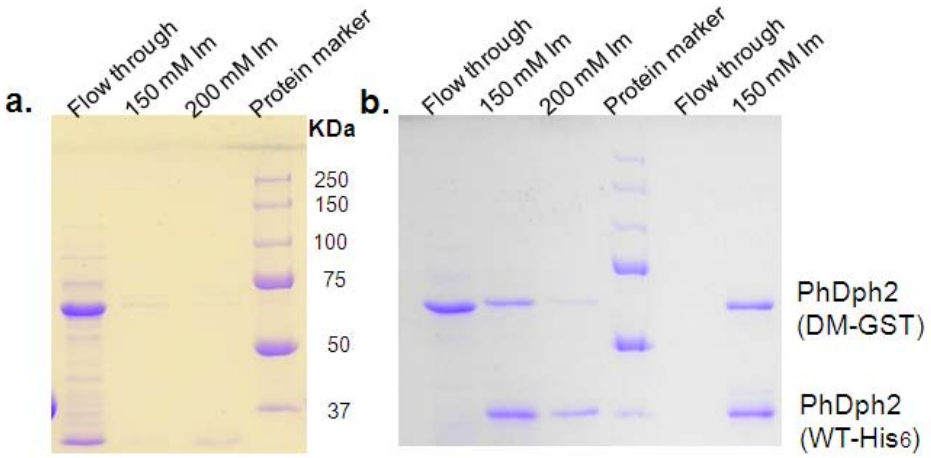

Figure 3.6. Stability of PhDph2 homodimer and PhDph2 (DM-GST:WT-His_6) heterodimer. a. PhDph2 (DM-GST) cannot bind to Ni resin, it was found in the flow through of Ni-affinty purification but not in the elutions. b. Stability test. Left of the protein marker: PhDph2 (WT-His_6) and (DM-GST) were mixed, incubated for 90 min, and then purified with Ni-resin. PhDph2 (DM-GST) was found in flow through; PhDph2 (DM-GST:WT-His_6) and PhDph2 (WT-His_6) were eluted from Ni resin by 150 mM and 200 mM imidazole; Right of the protein marker: PhDph2 (DM-GST:WT-His_6) heterodimer from tandem purification was incubated with Ni-resin then eluted with 150 mM imidazole. No homodimer was found in the flow through.

The PhDph2 heterodimer is active.

To test whether the first step of diphthamide biosynthesis requires the PhDph2 dimer to have two [4Fe-4S] clusters or only one is sufficient, we set up reactions either with the PhDph2 heterodimer (WT-His_6:DM-GST) or with the WT homodimer. The heterodimer, like wild type PhDph2, can catalyze the transfer of 3-amino-3-carboxylpropyl from SAM to EF2, as indicated by the ^{14}C-labeling experiment (Figure 3.7a). Similar results were obtained when we monitored the formation of MTA, by HPLC (Figure 3.7c blue and brown line). In contrast, the DM-GST homodimer has no activity (Figure 3.7c lane4, pink line). In order to make sure that the reaction rates

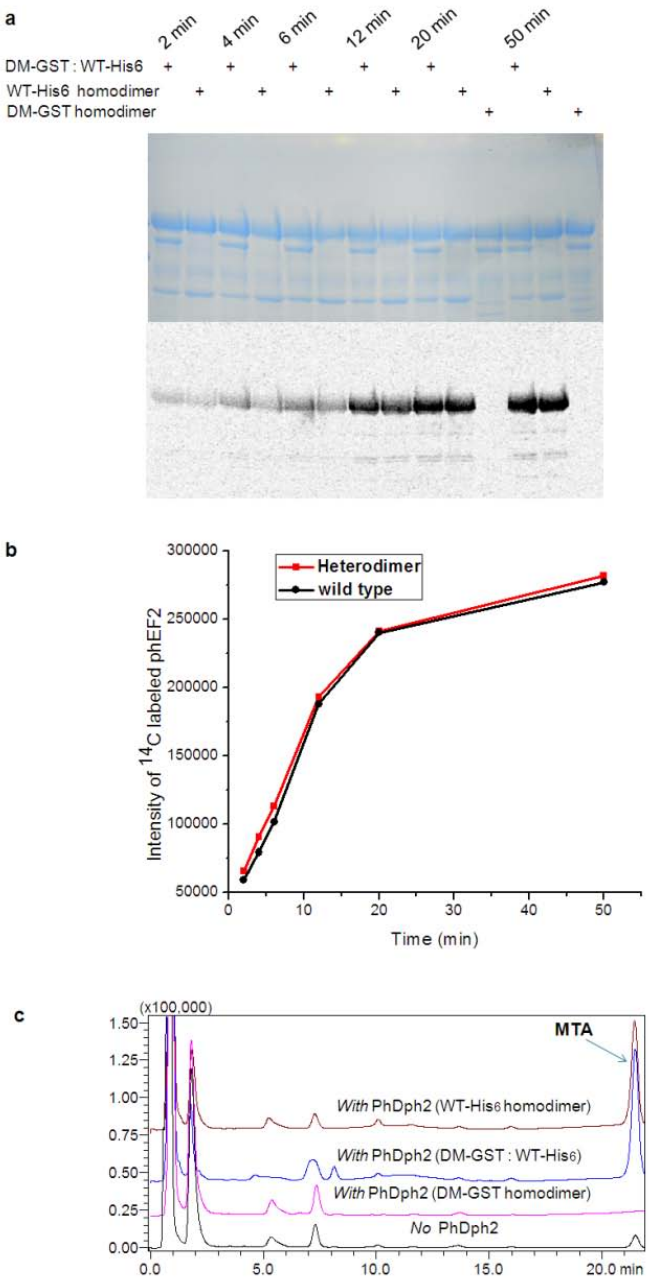

Figure 3.7. Activity assay of PhDph2 heterodimer. a. Time course of reactions catalyzed by PhDph2 wild type (WT-His_6) homodimer, PhDph2 double mutant and wild type heterodimer (DM-GST:WT-His_6) and PhDph2 double mutant (DM-GST) homodimer by using ^{14}C-labeled SAM. The upper panel shows the Coomassie blue-stained gel and the lower panel shows the autoradiography. b. Plot of the intensity of labelled PhEF2 (shown on the autoradiography in a) versus time. c. The formation of MTA catalyzed by different PhDph2 dimers was detected by HPLC.

catalyzed by heterodimer and WT homodimer was the same, we monitored the reaction time. The results shown in Figure 3.7a and Figure 3.7b indicate that the rate catalyzed by heterodimer was essentially the same as that catalyzed by wild type. These results suggest that only one [4Fe-4S] cluster per PhDph2 dimer is required for the reaction, which is consistent with the mechanism shown in Figure 3.2a.

PhEF2 (shown on the autoradiography in **a**) versus time. **c.** The formation of MTA catalyzed by different PhDph2 dimers was detected by HPLC.

No aminobutyric acid is formed when excess PhEF2 is present.

Our previous results showed that in the absence of PhEF2, PhDph2 can catalyze the cleavage of SAM to form 2-aminobutyric acid (ABA) (*17*). However, whether ABA is formed when excess PhEF2 is present will depend on the detailed reaction mechanism. In the mechanism shown in Figure 2a, no ABA will form in the presence of excess PhEF2. In contrast, in the mechanism shown in Figure 2b, ABA will form in the presence of excess PhEF2. To further differentiate the two mechanisms shown in Figure 2, we detected the formation of ABA by LCMS after dansylation. In the absence of PhEF2, ABA was formed, consistent with our previous results (*17*) With excess PhEF2, no ABA was detected (the level is the same as the negative control, Figure 3.8). The data provide further support for the mechanism shown in Figure 3.2a.

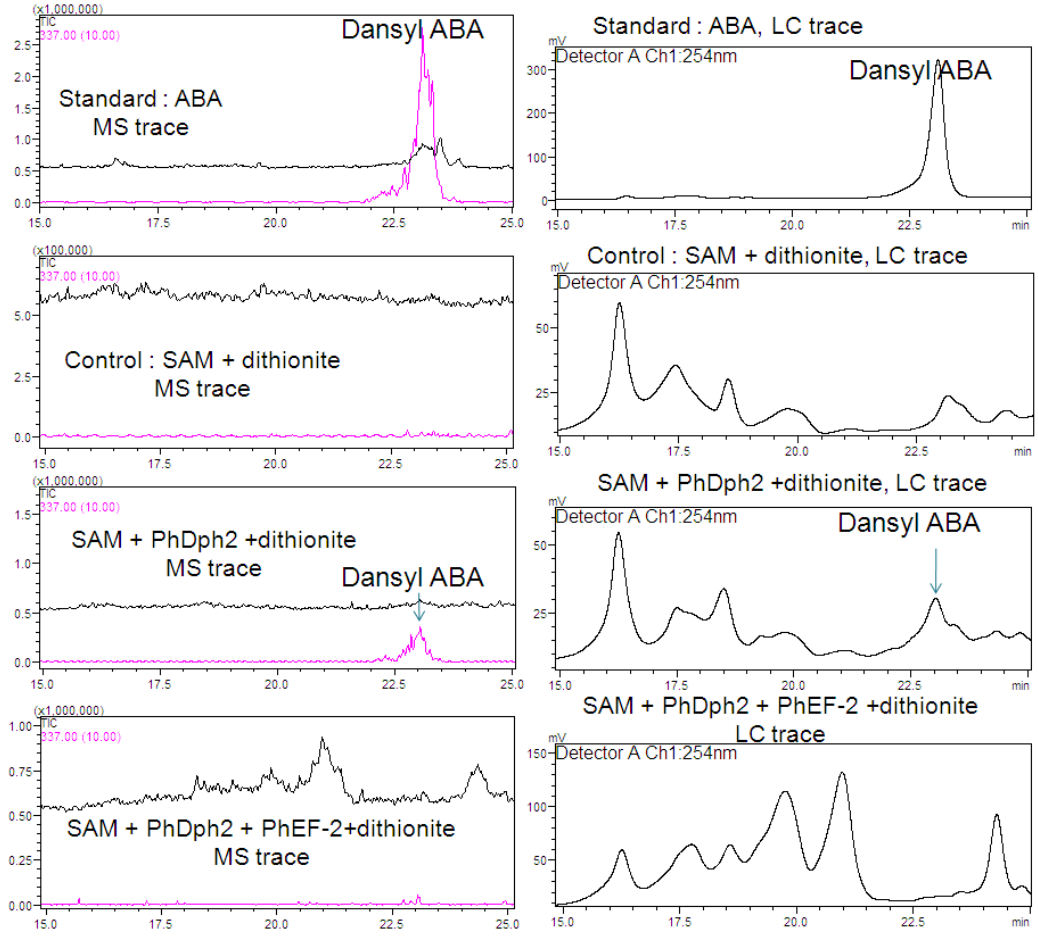

Figure 3.8. Detection of dansylated 2-aminobutyric acid (ABA) by LCMS. Left panel shows the MS traces and right panel shows the LC traces. Components used in different reactions were labeled in the figure. ABA was only formed in the reaction with PhDph2 but without PhEF2.

Discussion

Our previous work showed that PhDph2 forms a homodimer (*17*). Each subunit consists of three domains. Three cysteine residues (Cysteine59, Cysteine163 and Cysteine287), each from a different domain, are clustered in the center of each PhDph2 subunit to bind a [4Fe-4S] cluster. The three cysteine residues are conserved in eukaryotic Dph1 proteins but only two of the three cysteine residues are conserved

in eukaryotic Dph2 proteins. It is intriguing whether all three cysteine residues in archaeal PhDph2 are required for enzyme activity and whether the PhDph2 dimer requires one or both subunits to contain a [4Fe-4S] cluster for activity.

To test whether all the three conserved cysteine residues are required for the activity of PhDph2, we performed site directed mutagenesis to change the three cysteine residues to alanine. We then studied how such mutations affect the enzyme activity by monitoring the reaction products (the modified PhEF2 and MTA). The results showed that mutating one of the three cysteine residues did not affect the activity much (Figure 4). Thus, two conserved cysteine residues are sufficient for the activity of PhDph2. The spectroscopic data also suggest that the single cysteine mutants can still bind a [4Fe-4S] cluster (Figure 3). However, after changing two of the cystein residues to alanine (C59A/C287A), PhDph2 cannot bind to the Fe-S cluster and is inactive.

To gain further insights into the detailed reaction mechanism of PhDph2, we examined the activity of a heterodimer of PhDph2 consisting of one wild type subunit and one C59A/C287A double mutant. In this heterodimer, the wild type subunit can bind a [4Fe-4S] cluster while the double mutant cannot. Our stability measurement suggests that the heterodimer is more stable than the homodimers. The reason for this stability is not clear. It is possible that the PhDph2 dimer with one [4Fe-4S] cluster is thermodynamically more stable. Alternatively, the GST tag on the double mutant may somehow disfavor the formation of the double mutant homodimer. Under the experimental conditions tested, the heterodimer is as active as the wild type PhDph2 homodimer (Figure 7). The results support the mechanism shown in Figure 2a and indicate that only one [4Fe-4S] cluster per PhDph2 dimer is sufficient for the reaction. This conclusion is consistent with our previous structure of PhDph2, in which only one [4Fe-4S] is found to be present in the dimer (*17*). Furthermore, we demonstrated

that when excess PhEF2 was present, no ABA was formed in the reaction (Figure 8). This result indicates that the ACP radical generated does not undergo hydrogen abstraction in the presence of PhEF2 and thus the addition to the imidazole ring is more likely, which further supports the mechanism shown in Figure 2a. It is interesting to note that in classical Radical SAM enzymes, the deoxyadenosyl radical generated always does hydrogen abstraction to carry out the enzymatic reaction.(*21*, *22*) In contrast, in PhDph2, all our evidences suggest that the 3-amino-3-carboxypropyl radical should undergo an addition reaction instead of hydrogen abstraction. Thus, the non-classical Radical SAM enzyme PhDph2 differ not only in the radical species derived from SAM, (*17*),[21] but also in the downstream chemistry that the radical undergoes.

Experimental

Cloning, expression, and purification of PhDph2, PhDph2 mutants and PhEF2.

Cloning, protein expression and purification of PhDph2 and PhEF2 were reported(*17*). PhDph2 site directed mutants (C59A, C163A, C287A and C59A/C287A) were carried out by overlap-extension polymerase chain reaction (PCR) (*23*) with AccuPrime *Pfx* DNA polymerase (Invitrogen). The constructed mutant genes were inserted into pENTR^{TM}/TEV/D-TOPO® entry vector (Invitrogen). The amplified plasmid was purified using QIAprep® Spin Miniprep Kit (QIAGEN) and its sequence was confirmed by DNA sequencing (performed by Cornell University Life Sciences Core Laboratories Center). PhDph2 C59A and C287A single mutants were recombined with destination vector pDESTF1 to create expression clones with an N-terminal His_6 tag. The double mutant was recombined with pDEST15 with an N-terminal GST tag. A different cloning method was used for PhDph2 C163A. The PCR product was digested by *EcoRI* and *SalI* and the mutant

gene was ligated into pET28a vector by T4 DNA ligase.

Construction and tandem purification of PhDph2 heterodimer.

The plasmids containing PhDph2 wild type with His_6 tag (WT-His_6) in pCDFduet vector and PhDph2 C59A/C287A double mutant with GST tag (DM-GST) in pDEST15 vector were co-transformed into the *E. coli* expression strain BL21(DE3) with pRARE2. The cells were grown in LB media with 100 g/ml ampicillin, 25 g/ml chloramphenicol, and 50 g/ml streptomycin at 37°C and induced at OD_{600} of 0.8 with 0.1 mM isopropyl-β-D-thiogalactopyranoside (IPTG). The induced cells were incubated in a shaker (New Brunswick Scientific Excella E25) at 37°C and 200 rpm for 3 h. Cells were harvested by centrifugation at 6,371 g (Beckman Coulter Avanti J-E) and 4°C for 10 min. Cell pellets were transferred into an anaerobic chamber (Coy Laboratory Products) and pellets from 2L of LB culture were re-suspended in 30 ml lysis buffer (500 mM NaCl, 10 mM $MgCl_2$, 5 mM imidazole, and 20 mM Tris-HCl at pH 8.0) with 0.01% lysozyme, which were stored and de-oxygenated in the anaerobic chamber. The resuspended cells were sealed in a polypropylene tube and taken out for freezing with liquid nitrogen and then thawed at 26°C in the anaerobic chamber to lyse the cells. The sealed tube containing the cell lysis were taken out of the anaerobic chamber and centrigued at 48,400 g (Beckman Coulter Avanti J-E) for 30 min and then taken back into the anaerobic chamber for further processing. The supernatant was incubated for 1 hour with 1.2 ml Ni-NTA resin (Qiagen) pre-washed with water and equilibrated with the lysis buffer. The resin was then loaded onto a polypropylene column and washed with 20 ml lysis buffer. PhDph2 heterodimer (WT-His_6:DM-GST) and wild type homodimer (WT-His_6:WT-His_6) were eluted from the column with elution buffers (100 mM, 150 mM and 200 mM imidazole in the lysis buffer, 1.5 ml each). The protein was buffer-exchanged to GST bind/wash buffer (43 mM Na_2HPO_4, 14.7 mM KH_2PO_4, 1.37 M NaCl and 27 mM KCl) using a Bio-Rad 10–DG desalting

column. The heterodimer was further purified by incubating with GST binding resin (Novagen) for 2 hours at 26°C in the anaerobic chamber. The resin was then loaded onto a polypropylene column and washed with 20 ml GST bind/wash buffer. PhDph2 heterodimer was eluted from the column with 4 ml GST elution buffer (10 mM glutathione in 50mM Tris-HCl buffer, pH 8.0). DM-GST in the flow-through from the Ni resin purification was purified with GST binding resin. WT-His_6 from the flow through of the GST purification was incubated with Ni-Resin to concentrated and then further purified by heating at 90 °C for 5 min.

PhDph2 dimer stability test.

PhDph2 homodimers (DM-GST: DM-GST and WT-His_6: WT-His_6) were mixed in 1:1 ratio and incubated at 26°C for 1.5 hours in an anaerobic chamber (Coy Laboratory Products). The mixture was then incubated with Ni-NTA resin for 1 hour at 26°C and loaded onto a polypropylene column, washed with lysis buffer (20 mM Tris-HCl with 500 mM NaCl, 10 mM $MgCl_2$ and 5 mM imidazole, pH 8.0), and eluted with 100 mM, 150 mM and 200 mM imidazole in the lysis buffer. Both flow through and elution fractions were checked by SDS-PAGE. PhDph2 (DM-GST: WT-His_6) from the tandem purification was incubated at both 26 and 37°C for 1.5 hours before incubating with Ni-resin and elution from Ni-resin.

UV-Vis spectroscopy of PhDph2 mutants.

Samples of PhDph2 and mutants (50 µM), with and without dithionite, were prepared anaerobically in 150 mM NaCl solution and 200 mM Tris-HCl at pH 7.4. The sample treated with dithionite was allowed to incubate for 30 min after adding the reducing reagent at a final concentration of 0.5 mM. The samples were sealed in a quartz cell (100 µl each) before taking out from the anaerobic chamber. UV-Vis spectra were obtained on a Cary 50 Bio UV-Visible spectrophotometer (Varian), scanning from 200 nm to 800 nm. The baseline was corrected with the buffer used to

prepare the samples.

EPR spectroscopy of PhDph2 mutants

ESR spectra were recorded on a Bruker EMX (BRUKER, Billerica, MA) spectrometer at a frequency of 9.24 GHz under standard conditions in 4 mm ID quartz tubes. A liquid helium cryostat, ESR-10 (Oxford Instruments Ltd, England) was used to stabilize the temperature in the range of 4-50K. Spectra shown in Figure 2 d are recorded with a modulation amplitude of 8G and microwave power 0.63 mW.

Activity assay of PhDph2 wild type and mutants by autoradiography and HPLC

The reaction components, 12 µM PhEF2, 40 µM PhDph2 mutants (C59A and C287A), and 10 mM dithionite, were mixed in 150 mM NaCl, 1 mM DTT, and 200 mM Tris-HCl at pH 7.4 to a final volume of 15 µl in the anaerobic chamber under strictly anaerobic conditions. The reaction vials were sealed before taking out of the anaerobic chamber. Carboxy-^{14}C-SAM (2 µL, final concentration of 27 µM) was injected into each reaction vial to initiate the reaction. The reaction mixtures were vortexed briefly to mix and incubated at 65°C for 40 min. The reaction was stopped by adding loading buffer to the reaction mixture and subsequent heating at 100°C for 10 min, which was resolved by 12% SDS-PAGE. The dried gel was exposed to a PhosphorImaging screen (GE Healthcare, Piscataway, NJ) and the radioactivity was detected using a STORM860 phosphorimager (GE Healthcare, Piscataway, NJ).

The reactions of PhEF2 and PhDph2 single mutants / double mutant / heterodimer analyzed by HPLC are similar to those of analyzed by radio labeling except that they were scaled up to a final volume of 60 µl and a normal SAM instead of a ^{14}C SAM was used. The reaction mixture was quenched by 5% TFA and centrifuged to separate the precipitated proteins and the supernatant. The supernatant was analyzed by HPLC (Shimadzu) on a C18 column (HαSprite) monitored at 260 nm absorbance, using a linear gradient from 0 to 40% buffer B in 20 min at a flow rate of

0.3 ml min^{-1} (buffer A: 50 mM ammonium acetate, pH 5.4; buffer B, 50% (v/v) methanol/water).

Time course reaction of PhDph2 wild type and heterodimer

PhDph2 wild type (10 μM) / heterodimer (20 μM) / double mutants (10 μM) was incubated with PhEF2 (25 μM), carboxy-^{14}C-SAM (20 μM) and dithionite (5 mM) in a vial sealed with a rubber cap at 37°C. The amount of iron sulfur cluster contained in wild type and heterodimer are the same (based on the absorbance at 400 nm). Eight microliter reaction mixture was taken out at 2 min, 4 min, 6 min, 12 min, 20 min, and 50 min and the reaction was stopped by freezing at -20°C. Reaction with PhDph2 double mutants was monitored at 20 min and 50 min. Reaction mixtures at different time slots were mixed with gel loading dye and subsequent heated at 100°C for 10 min, then resolved by 12% SDS-PAGE. The dried gel was exposed to a PhosphorImaging screen (GE Healthcare, Piscataway, NJ) and the radioactivity was detected using a STORM860 phosphorimager (GE Healthcare, Piscataway, NJ). The signal was quantified by Image Quant TL (Amersham Biosciences). The intensity of ^{14}C-labeled PhEF2 was plotted vs time.

Dansylation of the reaction products and detection by LC-MS.

To differentiate the two possible mechanisms, reactions catalyzed by PhDph2 with excess of PhEF2 or without PhEF2 were set up anaerobically. The reaction products were characterized by dansylation reaction which was monitored by LC-MS as previously described (*17*).

REFERENCES

1. Robinson, E. A., Henriksen, O., and Maxwell, E. S. (1974) Elongation factor 2. amino acid sequence at the site of adenosine diphosphate ribosylation, *J. Biol. Chem. 249,* 5088-5093.

2. Van Ness, B. G., Howard, J. B., and Bodley, J. W. (1980) ADP-ribosylation of elongation factor 2 by diphtheria toxin. NMR spectra and proposed structures of ribosyl-diphthamide and its hydrolysis products, *J. Biol. Chem. 255,* 10710-10716.

3. Van Ness, B. G., Howard, J. B., and Bodley, J. W. (1980) ADP-ribosylation of elongation factor 2 by diphtheria toxin. Isolation and properties of the novel ribosyl-amino acid and its hydrolysis products, *J. Biol. Chem. 255,* 10717-10720.

4. Gomez-Lorenzo, M. G., Spahn, C. M. T., Agrawal, R. K., Grassucci, R. A., Penczek, P., Chakraburtty, K., Ballesta, J. P. G., Lavandera, J. L., Garcia-Bustos, J. F., and Frank, J. (2000) Three-dimensional cryo-electron microscopy localization of EF2 in the *Saccharomyces cerevisiae* 80S ribosome at 17.5 Å resolution, *EMBO J. 19,* 2710-2718.

5. Collier, R. J. (2001) Understanding the mode of action of diphtheria toxin: a perspective on progress during the 20th century, *Toxicon 39,* 1793-1803.

6. Liu, S., Milne, G. T., Kuremsky, J. G., Fink, G. R., and Leppla, S. H. (2004) Identification of the proteins required for biosynthesis of diphthamide, the target of bacterial ADP-ribosylating toxins on translation elongation factor 2, *Mol. Cell. Biol. 24,* 9487-9497.

7. Ortiz, P. A., Ulloque, R., Kihara, G. K., Zheng, H., and Kinzy, T. G. (2006) Translation elongation factor 2 anticodon mimicry domain mutants affect fidelity and diphtheria toxin resistance, *J. Biol. Chem. 281*, 32639-32648.

8. Walsh, C. T. (2006) *Posttranslational modifications of proteins: Expanding nature's inventory*, Roberts and Company Publishers, Englewood, Colorado.

9. Moehring, T. J., Danley, D. E., and Moehring, J. M. (1984) In vitro biosynthesis of diphthamide, studied with mutant Chinese hamster ovary cells resistant to diphtheria toxin, *Mol. Cell. Biol. 4*, 642-650.

10. Dunlop, P. C., and Bodley, J. W. (1983) Biosynthetic labeling of diphthamide in *Saccharomyces cerevisiae*, *J. Biol. Chem. 258*, 4754-4758.

11. Moehring, J. M., Moehring, T. J., and Danley, D. E. (1980) Posttranslational modification of elongation factor 2 in diphtheriatoxin-resistant mutants of CHO-K1 cells, *Proc. Natl. Acad. Sci. USA 77*, 1010-1014.

12. Chen, J. Y., Bodley, J. W., and Livingston, D. M. (1985) Diphtheria toxin-resistant mutants of *Saccharomyces cerevisiae.*, *Mol. Cell. Biol. 5*, 3357-3360.

13. Mattheakis, L. C., Sor, F., and Collier, R. J. (1993) Diphthamide synthesis in *Saccharomyces cerevisiae*: structure of the DPH2 gene, *Gene 132*, 149.

14. Phillips, N. J., Ziegler, M. R., and Deaven, L. L. (1996) A cDNA from the ovarian cancer critical region of deletion on chromosome 17p13.3, *Cancer Lett. 102*, 85.

15. Schultz, D. C., Balasara, B. R., Testa, J. R., and Godwin, A. K. (1998) Cloning and localization of a human diphthamide biosynthesis-like protein-2 gene,DPH2L2, *Genomics 52,* 186.

16. Mattheakis, L. C., Shen, W. H., and Collier, R. J. (1992) DPH5, a methyltransferase gene required for diphthamide biosynthesis in Saccharomyces cerevisiae, *Mol Cell Biol 12*, 4026-4037.

17. Zhang, Y., Zhu, X., Torelli, A. T., Lee, M., Dzikovski, B., Koralewski, R. M., Wang, E., Freed, J., Krebs, C., Ealick, S. E., and Lin, H. Diphthamide biosynthesis requires an organic radical generated by an iron-sulphur enzyme, *Nature 465*, 891-896.

18. Grove, T. L., Lee, K.-H., St. Clair, J., Krebs, C., and Booker, S. J. (2008) *In vitro* characterization of AtsB, a radical SAM formylglycine-generating enzyme that contains three [4Fe-4S] clusters., *Biochemistry 47*, 7523-7538.

19. Layer, G., Verfurth, K., Mahlitz, E., and Jahn, D. (2002) Oxygen-independent coproporphyrinogen-III oxidase HemN from *Escherichia coli*., *J. Biol. Chem. 277*, 34136-34142.

20. Hanzelmann, P., Hernandez, H. L., Menzel, C., Garcia-Serres, R., Huynh, B. H., Johnson, M. K., Mendel, R. R., and Schindelin, H. (2004) Characterization of MOCS1A, an oxygen-sensitive iron-sulfur protein involved in human molybdenum cofactor biosynthesis, *J. Biol. Chem. 279*, 34721-34732.

21. Duschene, K. S., Veneziano, S. E., Silver, S. C., and Broderick, J. B. (2009) Control of radical chemistry in the AdoMet radical enzymes, *Current Opinion in Chemical Biology 13*, 74-83.

22. Frey, P. A., Hegeman, A. D., and Ruzicka, F. J. (2008) The radical SAM superfamily, *Crit. Rev. Biochem. Mol. Biol. 43*, 63 - 88.

23. Ling, M. M., and Robinson, B. H. (1997) Approaches to DNA mutagenesis: an overview, *Anal Biochem 254*, 157-178.

CHAPTER 4

RECONSTITUTION OF DIPHTHINE SYNTHASE ACTIVITY IN VITRO*

Abstract

Diphthamide, the target of diphtheria toxin, is a unique posttranslational modification on eukaryotic and archaeal translation elongation factor 2 (EF2). Although diphthamide modification was discovered three decades ago, *in vitro* reconstitution of diphthamide biosynthesis using purified proteins has not been reported. The proposed biosynthesis pathway of diphthamide involves three steps. Our laboratory has recently showed that in *Pyrococcus horikoshii (P. horikoshii)*, the first step uses an [4Fe-4S] enzyme PhDph2 to generate a 3-amino-3-carboxypropyl radical from S-adenosyl-L-methionine (SAM) to form a C-C bond. The second step is the trimethylation of an amino group to form the diphthine intermediate. This step is catalyzed by a methyltransferase called diphthine synthase or Dph5. In this chapter, I present the *in vitro* reconstitution of the second step using *P. horikoshii* Dph5 (PhDph5). Our results demonstrate that PhDph5 is sufficient to catalyze the mono-, di-, and trimethylation of *P. horikoshii* EF2 *(*PhEF2). Interestingly, the trimethylated product from PhDph5-catalyzed reaction can easily eliminate the trimethylamino group. The potential implication of this unexpected finding on the diphthamide biosynthesis pathway is discussed.

Introduction

Diphthamide, found in both eukaryotes and archaea(*1-3*), is a unique posttranslationally modified histidine residue on translational elongation factor 2 (EF2), a GTPase required for ribosomal protein synthesis (*4*). The histidine residues

* Reproduced with permission from Zhu, X et al. *Biochemistry*, **2010**, *49* (44), pp 9649–9657

that are modified are His699 in yeast EF2, His715 in mammalian EF2, and His600 in *Pyrococcus horikoshii* EF2. Diphthamide is the target of diphtheria toxin(*5*), which ADP-ribosylates diphthamide and inhibits protein synthesis, leading to host cell death(*6*). It has been indicated that diphthamide may prevent the -1 frame shift during protein synthesis(*7*). However, the physiological function and biosynthesis of the modification are still not completely understood(*8*), despite of the fact that the modification has been known for over three decades. Diphthamide modification has been proposed to involve three steps (Figure 4.1)(*9*).

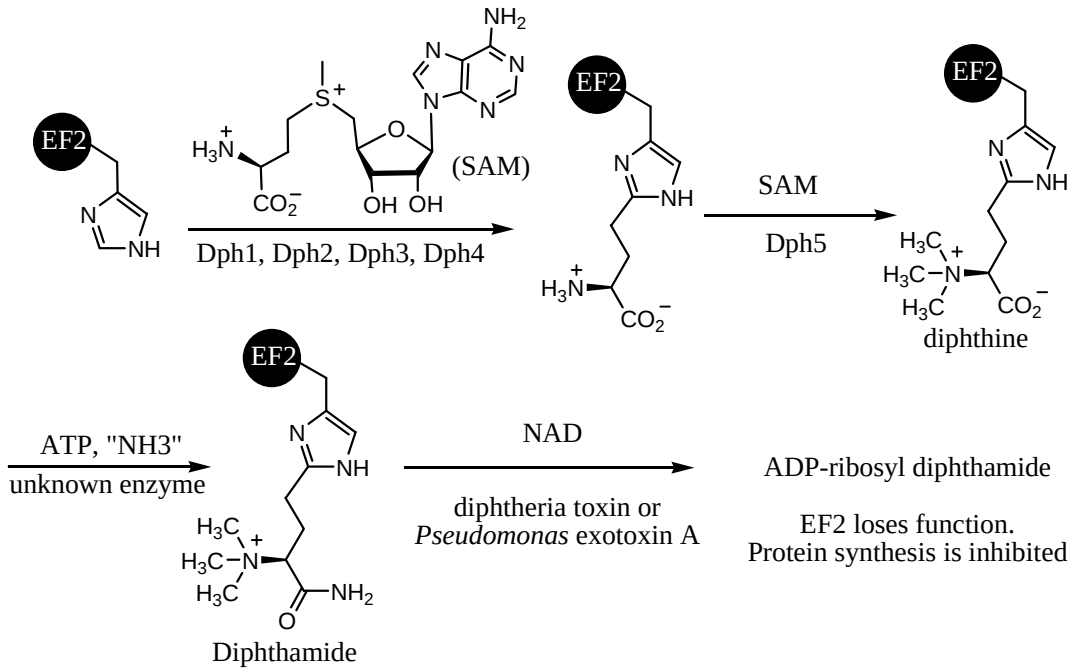

Figure 4.1. Proposed diphthamide biosynthesis pathway. The diphthamide residue is the target of bacterial ADP-ribosyltransferases, such as diphtheria toxin and Pseudomonas exotoxin A. The ADP-ribosylation of diphthamide by these toxins leads to inhibition of protein synthesis in the eukaryotic host cells**.**

The first step is the transfer of the 3-amino-3-carboxypropyl group from *S*-adenosyl-L-methionine (SAM) to the C-2 position of the imidazole ring of the target histidine

residue in EF2. The second step is the trimethylation of the amino group to form an intermediate called diphthine. The last step is the ATP-dependent amidation of the carboxyl group of diphthine. Genetic studies have identified five proteins in eukaryotes required for the biosynthesis of diphthamide, Dph1, Dph2, Dph3, Dph4, and Dph5. Dph1-4 are known to be required for the first step (*6, 10-15*), whereas Dph5 (also called diphthine synthase) is known to be required for the second step(*16*). The enzyme that catalyzes the last step has not been identified yet. Diphthamide is also found in archaea. However, among the five eukaryotic proteins required for diphthamide biosynthesis, only two orthologs can be found in archaea by BLAST search. One of them, Dph2, is homologous to eukaryotic Dph1 and Dph2 (Dph1 and Dph2 are homologous to each other), and the other one is the diphthine synthase, Dph5.

Although five genes are known to be required for the first two steps of diphthamide biosynthesis, it is not clear whether these genes are sufficient. In fact, another gene, WDR85 (*17*), was recently identified to be required for the first step of diphthamide biosynthesis in eukaryotes, further demonstrating the complexity of diphthamide biosynthesis. The same can be said about the second step: one can similarly ask whether Dph5 alone is sufficient to catalyze the trimethylation or additional proteins are needed. Therefore, to fully understand diphthamide biosynthesis, it is important to reconstitute the biosynthesis *in vitro* using purified proteins. Recently, we have successfully reconstituted the first step of diphthamide biosynthesis using the *Pyrococcus horikoshii* Dph2 (PhDph2) and EF2 (PhEF2)(*18*). We found that PhDph2 forms a homodimer and can bind a [4Fe-4S] cluster in each monomer with three conserved cysteine residues. PhDph2 is similar to the radical SAM superfamily(*19*) in that both contain [4Fe-4S] clusters and are SAM-dependent. However, PhDph2 does not contain the CXXCXXXC motif(*20*) that is found in most

radical SAM enzymes. Furthermore, we showed that PhDph2 likely generates a 3-amino-3-carboxypropyl radical in the first step of diphthamide biosynthesis, instead of a 5'-adeoxyadenosyl radical. The successful reconstitution of the first step of diphthamide biosynthesis sets the stage for us to investigate the second step of diphthamide biosynthesis by providing the substrate to test whether PhDph5 is sufficient for the trimethylation step *in vitro*. Herein we report the reconstitution of PhDph5 activity. Our data suggest that PhDph5 is sufficient for the second step of diphthamide biosynthesis and that it catalyzes the trimethylation in a highly processive manner. Interestingly, we found that after the trimethylation step, the resulting diphthine product is not stable and can easily eliminate the trimethylamino group in a reaction similar to Hofmann elimination or Cope elimination(*21*).

Results

Initial PhDph5 activity assay with 14C-labeled SAM gave no labeling.

PhEF2 (83 kDa), PhDph2 (38 kDa) and PhDph5 (30 kDa) were expressed in *E. coli* and purified as described in the Experimental Procedures. Their purity and sizes were checked by SDS-PAGE (Figure 4.2).

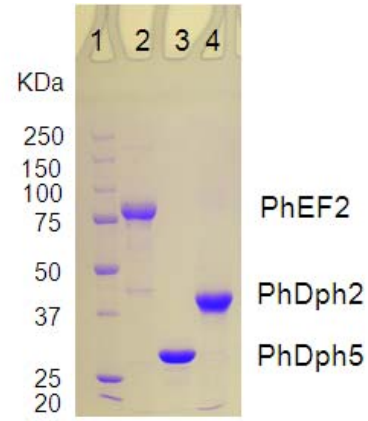

Figure 4.2. Purified PhEF2 (83 kDa), PhDph2 (38 kDa) and PhDph5 (30 kDa).

By incubating PhEF2 with PhDph2 and SAM under anaerobic conditions, we first obtained PhEF2 with the 3-amino-3-carboxypropyl (ACP) group attached to His600.

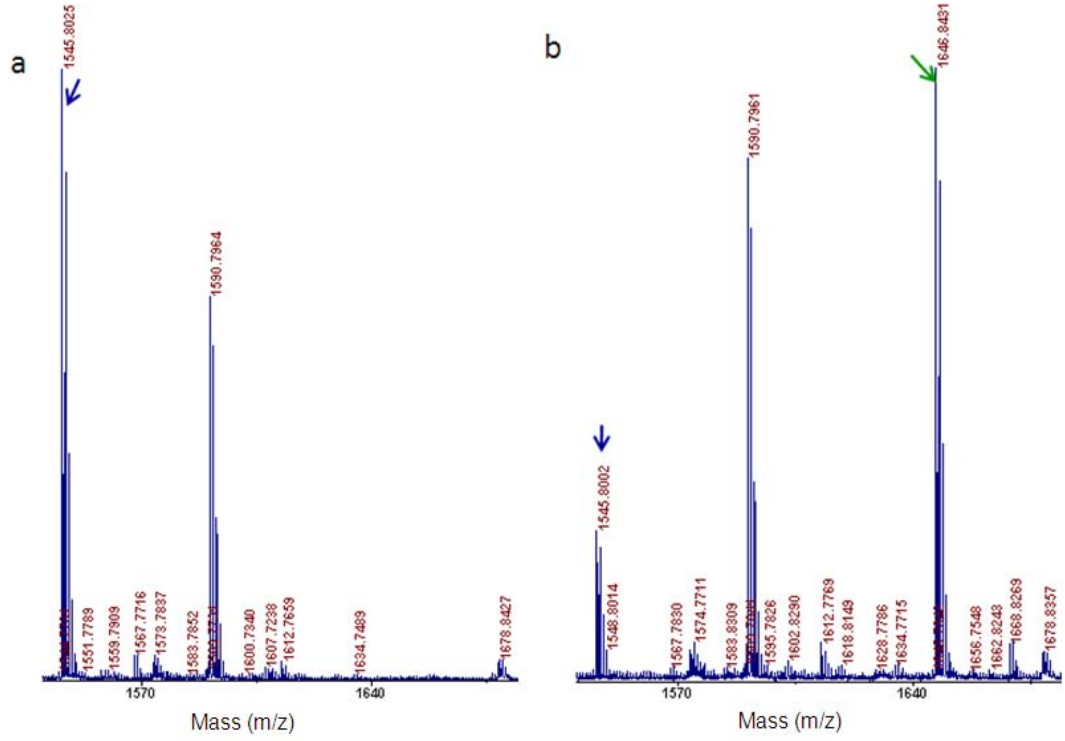

Figure 4.3. Monitoring PhDph2-catalyzed PhEF2 modification using MALDI-MS. a, unmodified PhEF2 peptide residue with m/z 1545.8; b, PhEF2 modified with 3-amino-3-carboxypropyl (ACP) group. Two peaks showed in the spectrum: unmodified PhEF2 peptide with m/z 1545.8; ACP-modified PhEF2 peptide with m/z 1646.8.

The reaction was monitored by MALDI-MS (Figure 4.3). The observed masses of the peptide fragments in Figure 4.3 are consistent with the calculated masses of estimated peptide fragments as shown in Table 4.1. The peptide fragment containing the His600 residue (LLDAQVHEDNVHR) in unmodified PhEF2 has an *m/z* of 1,545.80 (MH^+, calculated 1545.78, Figure 4.3a). This peak was almost gone after reaction with PhDph2 and a new peak with an *m/z* of 1,646.84 appeared (Figure 4.3b), which

corresponds to the product of the PhDph2-catalyzed reaction with the ACP-modified histidine residue (MH^+, calculated 1646.83).

Table 4.1. Calculated masses of peptide fragments are consistent with those observed in PhEF2 MALDI-MS spectra in Figure 4.3

peptide fragment	calculated m/z	observed m/z
LLDAQVHEDNVHR	1545.78	1545.8025
QLVLDFDEQEQAR	1590.78	1590.7964
VPNELAQQIIRQIR	1677.97	1678.8427

To test the activity of the purified PhDph5, the first step reaction mixtures were buffer exchanged to PhDph5 reaction buffer. PhDPh5 and excess methyl-^{14}C SAM were then added to initiate the trimethylation reaction. To our surprise, no labeling on PhEF2 was found (data not shown) by autoradiography. We reasoned that additional proteins or other molecules other than PhDph5 may be needed to reconstitute the second step, since all the reported Dph5 activity assay were performed *in vivo* or by using crude cell lysate (*16*, *23*). However, it is also possible that PhDph5 alone can catalyze the second step, but our reaction conditions need to be optimized to get the reaction to work.

Detection of SAH shows SAM-degrading activity catalyzed by PhDph5.

In the process to find out why no ^{14}C-methyl group can be transferred to PhEF2, we tried other methods to detect the product of the reaction catalyzed by PhDph5. One product of methyl transfer reaction by SAM-dependent methyltransferase is S-adenosylhomocysteine (SAH), which can be used to indicate whether the methyltransfer reaction occurred or not. We monitored the SAH formation with HPLC (Figure 4.4). Standard SAH was eluted at 10 min, as shown in Figure 4.4 (dark blue line). In the reaction without PhDph5, no SAH was detected (Figure 4.4, black line). In contrast, when PhDph5 was present, the SAH peak increased (Figure

4.4, pink line) even when no additional SAM was added (some left-over SAM molecules were present from the first step PhDph2-catalyzed reaction). With increasing concentrations of SAM, the SAH peak increased first then remained unchanged (Figure 4.4, brown and green lines). Taken together, the data suggest that PhDph5 is active since it can remove the methyl group from SAM in the presence of the PhEF2 substrate.

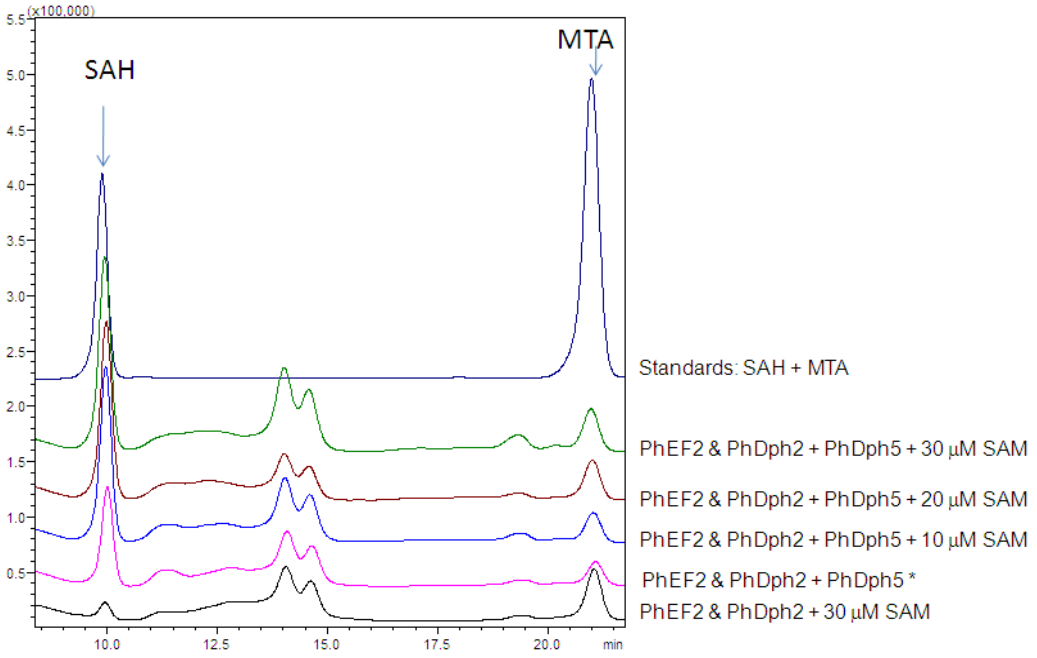

Figure 4.4. HPLC analysis of the reaction product showed that PhDph5 catalyzes the formation of SAH. Absorption was monitored at 260 nm. The description of each overlaid trace is provided on the right, and the identities of major peaks were indicated. In the reaction marked by *, no extra SAM was added. However, some SAM (less than 10 M) was left from the PhDph2-catalyzed reaction to make ACP-modified PhEF2 and led to the formation of SAH when PhDph5 was added.

MALDI-MS/MS of PhEF2 revealed an elimination reaction that occurred to diphthine.

The detection of the SAM-cleavage activity suggests that PhDph5 is active

under the conditions used, although it remained unclear where the methyl group of SAM ends up. To find out whether the methyl group is transferred to PhEF2, we decided to use MALD-MS to monitor the mass of PhEF2. After incubating PhEF2 with PhDph5 and SAM, the reaction mixture was resolved by SDS-PAGE and the PhEF2 band was excised, digested, and analyzed by MALDI-MS. We could not see any peaks for the mono-, di- or tri-methylation products, which is consistent with our previous results obtained with methyl-^{14}C SAM. However, a new peak with an *m/z* of 1629.77 was detected (Figure 4.5b) which was not present in the control, the ACP-modified PhEF2 not subjected to the Dph5 reaction (Figure4.5a). Since the diphthine-containing peptide has a calculated *m/z* of 1688.87 (M^+) and a trimethylamino group has an *m/z* of 59.1, the peak of 1629.77 corresponds to the loss of the trimethylamino group from diphthine, the trimethylated product. The peptide fragment containing the elimination product has a calculated m/z of 1629.80 (MH^+). To confirm that the trimethylamino group was eliminated and a 3-carboxy-2-propenyl group is formed on the histidine residue after elimination (Figure 4.9), we analyzed the 1629.77 peak by tandem MS. The mass difference between Y1 and Y2 ions is 221, which is consistent with the presence of a 3-carboxy-2-propenyl on the histidine residue (Figure 4.6). This result suggested that PhDph5 can catalyze the trimethylation reaction but the diphthine product cannot be detected due to the elimination of the trimethylamino group.

P. horikoshii grows optimally at 98^{o}C. For the *in vitro* reconstitution, we normally carry out the reaction at 65^{o}C, which we found to be optimal for the activity of PhDph2. One concern was that the high temperature may contribute to the elimination. Thus to minimize the elimination reaction, we later carried out the Dph5-catalyzed reactions at 37^{o}C. Similarly, when analyzing the reaction by SDS-PAGE, we did not heat the sample to denature the protein. However, even under these milder conditions, the elimination always occurred based on both MS and the ^{14}C-labeling experiments

(data not shown). The other concern is that the elimination could occur during MALDI-MS from absorbing the energy of laser. This is also unlikely because the elimination also happened in the ^{14}C-labeling experiments in which the reaction was deteted by autoradiography. These observations suggest the elimination occurs readily under the reactions conditions.

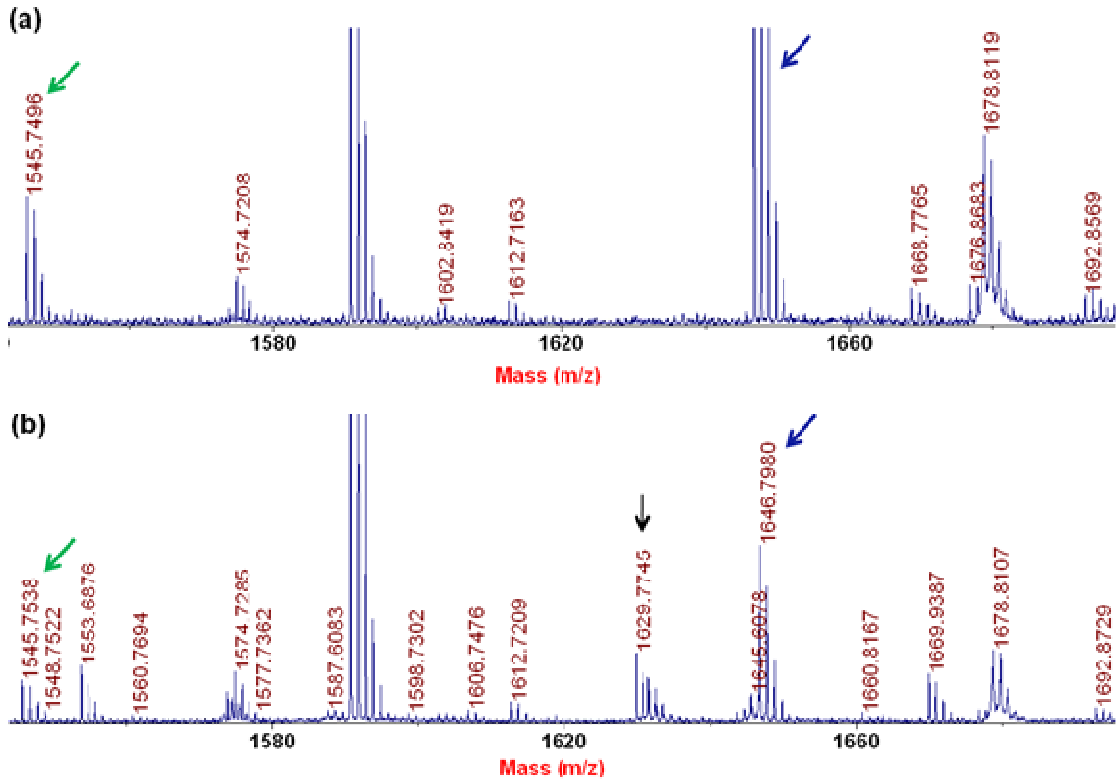

Figure 4.5. The MALDI-MS analysis of PhEF2 in PhDph5-catalyzed reaction. (a) PhEF2 from control reaction with PhDph5; (b) PhEF2 after PhDph5-catalyzed reaction. The peak with m/z 1545.8 corresponds to unmodifed PhEF2 peptide, 1646.8 corresponds to ACP-modified PhEF2 peptide, and 1629.8 corresponds to the elimination product.

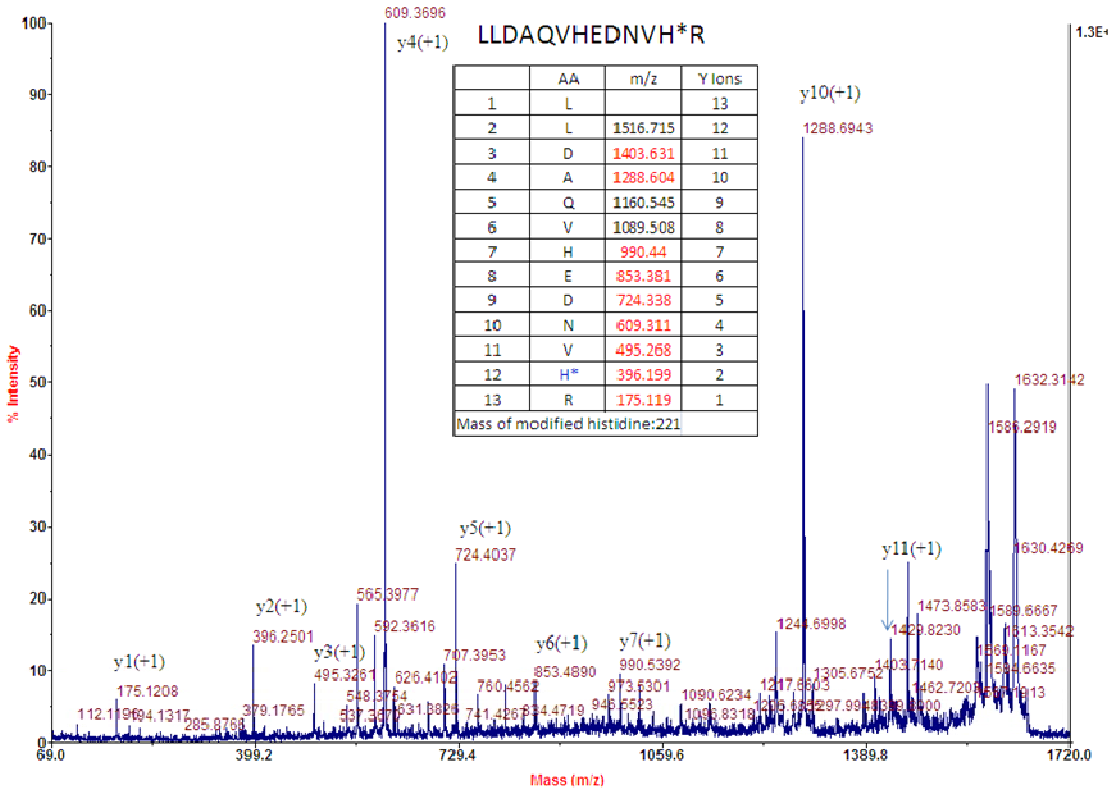

	AA	m/z	Y Ions
1	L		13
2	L	1516.715	12
3	D	1403.631	11
4	A	1288.604	10
5	Q	1160.545	9
6	V	1089.508	8
7	H	990.44	7
8	E	853.381	6
9	D	724.338	5
10	N	609.311	4
11	V	495.268	3
12	H*	396.199	2
13	R	175.119	1
Mass of modified histidine:221			

Figure 4.6. MS/MS of precursor 1629.81, which is from the MALDI spectrum of EF2 modified by PhDph5. The table lists calculated Y ions. Observed Y ions in the spectrum are colored in red.

Decreasing SAM concentrations allows the detection of ^{14}C-labeling on PhEF2.

Although the above result suggested that PhDph5 can catalyze the trimethylation reaction, the actual methyltranfer to PhEF2 still need to be proven. The elimination of the trimethylamino group is similar to the Hofmann elimination reaction that can occur to quaternary ammonium hydroxide salts or the Cope elimination reaction that can happen to tertiary amine oxides(*21*). In Hofmann or Cope elimination, a

quaternary ammonium functional group is required for the elimination to occur. Thus, we reasoned that if we can stop the PhDph5-catalyzed reaction at mono- and di-

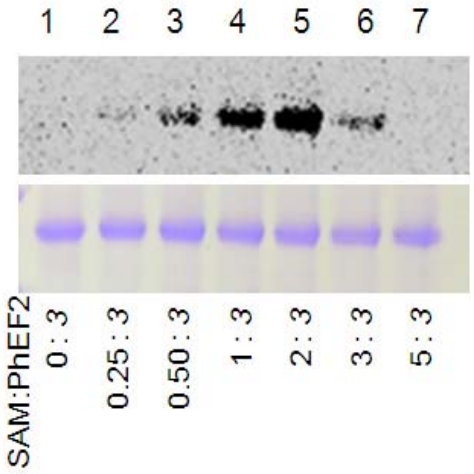

Figure 4.7. PhDph5-catalyzed PhEF2 methylation monitored by methyl-^{14}C SAM. The PhDph5 activity assays were set up with 30 µM ACP-modified PhEF2, 60 µM PhDph5, and different SAM concentrations (0 µM, 2.5 µM, 5 µM, 10 µM, 20 µM, 30 µM and 50 µM). The reactions were incubated at 37°C for 30 min. Bottom panel shows the Coomassie blue-stained gel; top panel shows the autoradiography. The concentration ratios of SAM to PhEF2 were shown at the bottom of the image.

methylation stage, then no elimination reaction will occur and we may be able to detect the methyl transfer to PhEF2. Therefore we revisited the labeling experiment using different concentrations of methyl-^{14}C SAM, hoping to accumulate the mono- and di-methylated PhEF2. After the first modification reaction, the buffer was exchanged to the methylation reaction buffer to make sure the amount of leftover SAM from the previous step was as little as possible. Different concentrations of ^{14}C-SAM and PhDph5 were then added to allow the methylation to occur. The reaction mixtures were resolved by SDS-PAGE and the labeling was detected by autoradiography. When no methyl-^{14}C SAM was added, no labeling was detected (Figure 4.7, lane 1). Labeling of PhEF2 was observed when methyl-^{14}C-SAM was

added and the labeling increased when the ratio of SAM to PhEF2 increased from 0.25:3 to 2:3 (Figure 4.7, lane 2 to lane 5). However, the intensity of labeling decreased when the ratio reached to 3:3 (Figure 4.7, lane 6). Further increasing the ratio of SAM: PhEF2 to 5:3, the labeling disappeared (Figure 4.7, lane 7). These results demonstrated that PhDph5 can transfer the methyl group from SAM to PhEF2. In addition, the loss of the ^{14}C label on PhEF2 at high concentrations of methyl-^{14}C SAM is consistent with the prediction that the trimethylated PhEF2 can undergo the elimination reaction while the mono- and dimethylated PhEF2 cannot.

MALDI-MS of reaction products confirmed the formation of mono- and dimethylated PhEF2.

To confirm the formation of mono- and dimethylated PhEF2, we again relied on MALDI-MS. The peptide fragment containing the ACP-modified His600 residue after PhDph2-catalyzed modification has an *m/z* of 1,646.84 (Figure 4.8a). After the reaction catalyzed by PhDph5 with 2:3 and 3:3 ratio of SAM: PhEF2, two new peaks appeared with *m/z* of 1,660.83 and 1674.84 (Figure 4.8b and 4.8c), corresponding to the masses of PhEF2 with the addition of one (MH^+, calculated *m/z* 1660.84) and two methyl groups (MH^+, calculated *m/z* 1674.86). However, when the concentration of SAM was higher than that of PhEF2 (5:3), no methylated product was observed (Figure 4.8d). These results firmly established that PhDph5 can catalyze the methyltransfer to PhEF2. When one equivalent of SAM is used (Figure 4.8c), the major product is the eliminated product after trimethylation of the ACP group while a significant amount of unmethylated substrate is still present. This result suggests that the trimethylation reaction catalyzed by PhDph5 is highly processive.

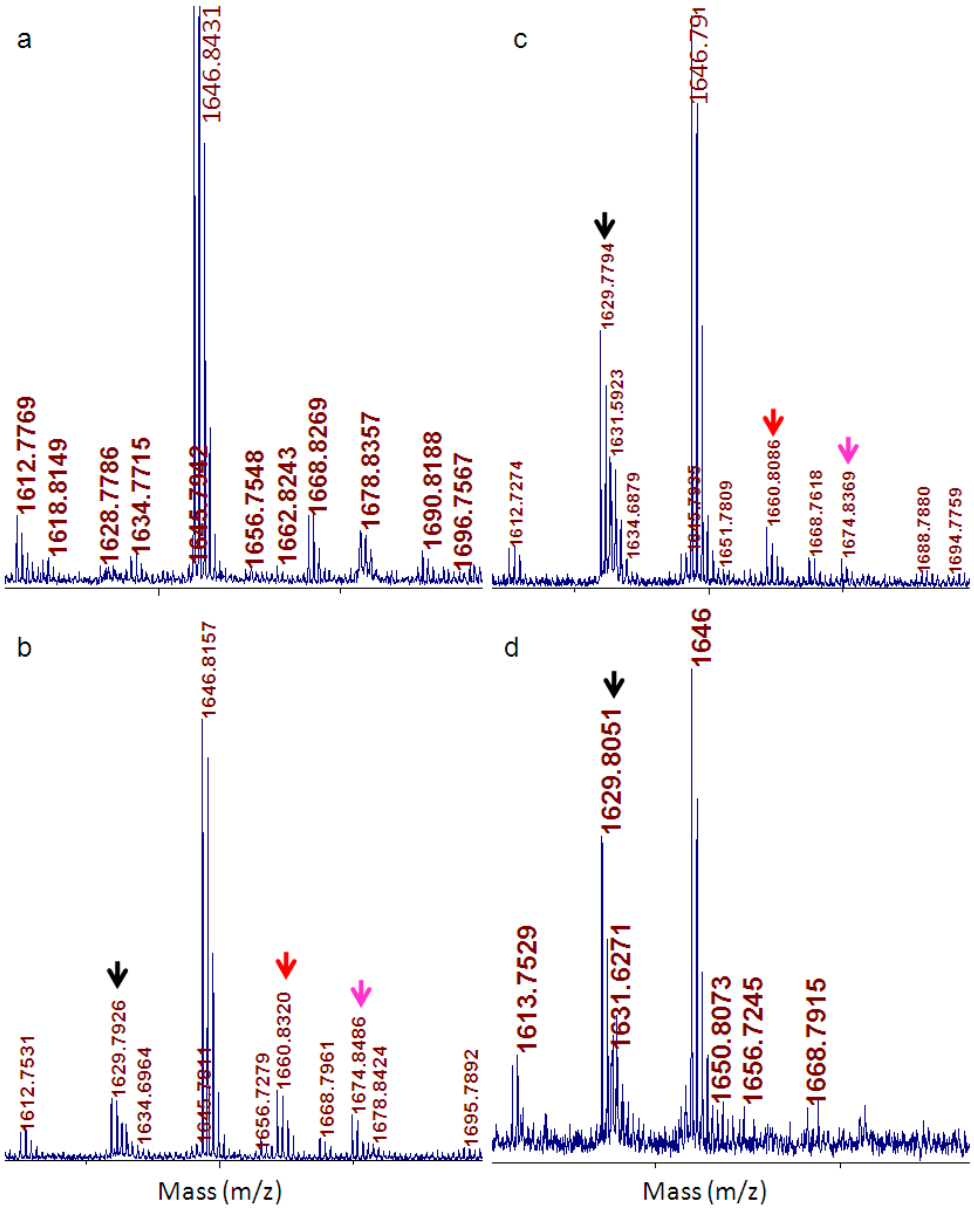

Figure 4.8. Detecting PhDph5-catalyzed PhEF2 methylation using MALDI-MS. Different ratio of PhEF2 to SAM was used to minimize the formation and elimination of the trimethylated product. a, PhEF2 modified with 3-amino-3-carboxypropyl (ACP) group. ACP-modified PhEF2 peptide has an *m/z* of 1646.8. b, PhEF2 modified by PhDph5 with a SAM to PhEF2 ration of 2:3. Three new peaks with *m/z* values of 1629.8; 1660.8; 1674.8 were observed, which correspond to diphthine with the trimethylamino group eliminated, monomethylated, and dimethylated intermediates, respectively. c, PhEF2 modified by PhDph5 with a SAM to PhEF2 ratio of 3:3. d, PhEF2 modified by PhDph5 with a SAM to PhEF2 ratio of 5:3. Only the elimination product with *m/z* of 1629.8 was observed.

Discussion

P. horikoshii Diphthine is not stable in vitro and readily eliminates the trimethylamino group.

Initially, when we used methyl-^{14}C SAM to detect the methylation of PhEF2, no methylation was detected. HPLC analysis of the small molecule product showed that SAH was formed in the reaction, suggesting that PhDph5 is active. Using MALDI-MS, we detected a new product with *m/z* of 1629.77. We attributed this peak to the product resulting from the elimination of the trimethylamino group from diphthine. The structure of the elimination product was further confirmed by MS/MS. The mass difference of the Y2 and Y1 ions is 221, which is consistent with the presence of a 3-carboxy-2-propenyl group on His600, the product of diphthine after elimination of the trimethylamino group. The elimination reaction is similar to the Hofmann elimination reaction or Cope elimination reaction.(*21, 24*) Given that such elimination reaction will require the quaternary ammonium salt, we predicted that the mono- and dimethylated PhEF2 should not undergo the elimination product and thus should be stable and detectable. Indeed, by lowering the concentration of SAM, mono- and dimethylated PhEF2 were detected using methyl-^{14}C-SAM (Figure 4.7) and MALDI-MS (Figure 4.8). This result further confirmed that elimination requires the trimethylamino group and that Dph5 can catalyze the trimethylation reaction. There are two possible mechanisms for the elimination reaction (Figure 4.9). One mechanism uses an external base to attack the proton on the β-carbon (Figure 4.9a) and the other mechanism uses the carboxyl group as the intra-molecular base to deprotonate the β-carbon (Figure 4.9b). At present, it is not known whether a similar elimination reaction also occurs to eukaryotic diphthine. If it does happen to eukaryotic diphthine, we would favor the second mechanism for the elimination

reaction based on the fact that when the carboxylate is converted to the amide as in diphthamide, the trimethylamino group becomes stable given that eukaryotic diphthamide has been isolated and structurally determined(*2*, *25*, *26*).

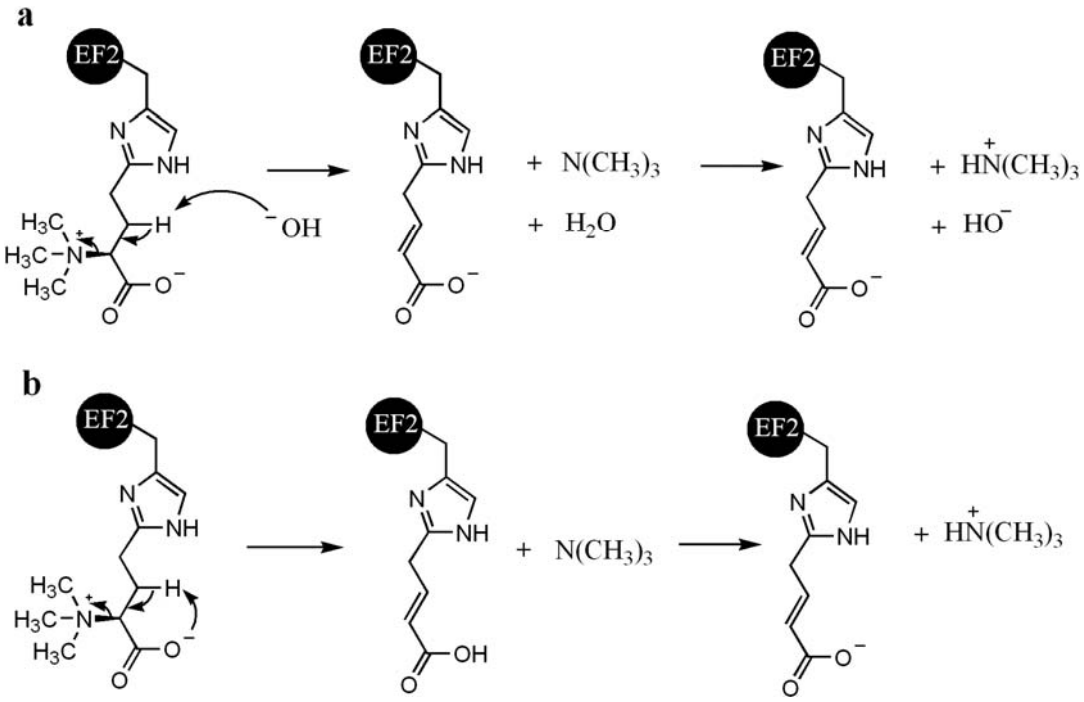

Figure 4.9. Proposed mechanisms for the elimination reaction of diphthine.

PhDph5 is sufficient for the trimethylation step of diphthamide biosynthesis in vitro. Genetic studies have shown that PhDph5 is required for the trimethylation step of diphthamide biosynthesis. However, whether PhDph5 is sufficient for the trimethylation step was not clear(*11*). Our data presented above demonstrated that PhDph5 is sufficient to catalyze the trimethylation step. Mono- and dimethylated PhEF2 was detected by MALDI-MS, while the trimethylated product cannot be detected due to the facile elimination of the trimethylamino group.

The implication of the instability of diphthine on the diphthamide biosynthesis pathway.

Diphthamide structure was determined using eukaryotic EF2 (*2*, *25*, *26*). Whether the final structure in archaea is the same or not is not clear. At this point, we do not know whether the elimination reaction also occurs physiologically. The elimination readily occurs *in vitro* even though we have taken extra care to avoid harsh conditions, such as heat denaturation, to minimize it. However, it is still possible that the elimination reaction only occurs *in vitro* due to the lack of the enzyme for the amidation step in the reaction. If diphthamide is the final structure in *P. horikoshii*, given that *P. horikoshii* diphthine readily eliminate, in order to form the final structure, diphthamide, the last amidation step should occur very quickly in *P. horikoshii* cells to avoid the elimination reaction. Alternatively, it is possible that the amidation step occurs before the trimethylation step.

It would be interesting to know whether a similar elimination reaction also occurs to eukaryotic diphthine, *in vitro* and *in vivo*, and whether the elimination reaction affects the function of EF2 in protein synthesis. The genes required for diphthamide biosynthesis, *dph*1-*dph*5, were identified in yeast and mammalian cells by screening for mutants that are resistant to diphtheria toxin, which can ADP-ribosylate diphthamide and inhibit protein synthesis (*6*, *10*-*15*). The enzyme for the amidation step has not been identified yet using this genetic screening. The explanation for the inability to isolate the amidation enzyme is that diphtheria toxin is able to ADP-ribosylate both diphthamide and diphthine(*11*). The elimination of the trimethylamino group from diphthine may provide an alternative explanation. If EF2 loses its normal function in protein synthesis after the elimination of the trimethylamino group from diphthine, then the disruption of the gene required for the amidation step would lead to the accumulation of diphthine, which will eliminate and

stop protein synthesis, giving a lethal phenotype. The lethality of disrupting the gene may explain why it has not been identified in the genetic screen. This hypothesis, if correct, may help the identification of the gene required for the amidation step in eukaryotes.

Experimental

Cloning, expression, and purification of PhDph2, PhDph5, and PhEF2. The cloning, expression, and purification of PhDph2 and PhEF2 were reported(*22*). PhDph5 was amplified by PCR from *P. horikoshii* genomic DNA (ATCC® 700860D-5TM) with AccuPrime *Pfx* DNA polymerase (Invitrogen) and the primers (AGTCAGCATATGATGGTTTTGTACTTTATTGGATTG &AGTCAGCTCGAGTTAAACATTAACCC TTAATATCTC). Amplified PhDph5 was digested by NdeI and XhoI (New England BioLabs) and then ligated into the pET-28a (+) vector by T4 DNA ligase (Invitrogen). The recombinant plasmid was transformed to TOP10 competent cells (Invitrogen), and colonies containing the plasmid were selected by colony PCR with EconoTaq® DNA polymerase (Lucigen). The amplified plasmid was purified using QIAprep® Spin Miniprep Kit (QIAGEN) and its sequence was confirmed by DNA Sequencing (performed by Cornell University Life Sciences Core Laboratories Center).

The plasmid containing PhDph5 was transformed into the *E. coli* expression strain BL21 (DE3) with pRARE2. The cells were grown in LB media with 100 g/ml ampicillin at 37 °C and induced at an OD_{600} of 0.8 with 0.1 mM isopropyl-β-D-thiogalactopyranoside (IPTG). The induced cells were incubated in a shaker (New Brunswick Scientific Excella E25) at 37 °C and 200 rpm for 3 h. Cells were harvested by centrifugation at 6,371 ×g (Beckman Coulter Avanti J-E) and 4 °C for 10 min. Cell pellets from 2L of LB culture were re-suspended in 30 ml lysis buffer (500 mM NaCl,

10 mM $MgCl_2$, 5 mM imidazole, and 20 mM Tris-HCl at pH 8.0). Cells were lysed using a cell disruptor (EmulsiFlex). Cell debris was removed by centrifugation at 48,400 ×g (Beckman Coulter Avanti J-E) for 30 min. The supernatant was incubated for 1 hour with 1.2 ml Ni-NTA resin (Qiagen) that was pre-washed and equilibrated with the lysis buffer. The resin was then loaded onto a polypropylene column and washed with 20 ml lysis buffer. PhDph5 was eluted from the column with 1.5 mL aliquots of buffers containing 100 mM, 150 mM and 200 mM imidazole in the lysis buffer. The protein was buffer-exchanged to 50mM Tris-HCl, pH 8.0, with 50 mM NaCl using a Bio-Rad 10–DG desalting column. The protein was further purified by heating at 65 °C for 10 min and centrifugation at 39,191 ×g to remove the precipitate. Purified PhDph5 was concentrated using an Amicon Ultra-4 centrifugal filter device (Millipore).

Reconstitution of PhDph5 activity in vitro and detection of formation of S-adenosyl-L- homocystein (SAH) by HPLC.

The first step of PhEF2 modification was performed in an anaerobic chamber (5% Hydrogen, 95% Nitrogen) (Coy Laboratory Products). PhDph2 (240 µM) was incubated with 10 mM dithionite for 10 min first. PhEF2 (100 µM) and SAM (200 µM) were added and reaction was incubated at 65 °C for 40 mins. After the first step of modification, the reaction mixture was buffer exchanged to PhDph5 reaction buffer (*23*) (100 mM Tris-HCl, pH 8.0, 75 mM NaCl, 50 mM KCl, 1 mM EDTA, 5 mM DTT, 5 mM $MgCl_2$, with or without 2 mM ADP, 10 mM creatine phosphate and 80 pg/ml phosphocreatine kinase) with a 10 kDa Amicon (Millipore) filter and then with a Micro Bio-Spin 6 column (BioRad) to get rid of the leftover SAM from the last step reaction. The PhDph5 activity assay was carried out with 30 µM modified PhEF2, 60 µM PhDph5, and SAM at different concentrations (0 µM, 5 µM, 10 µM, 20 µM, 30 µM and 50 µM) in a total volume of 50 µl and incubating the reaction mixtures at

37°C for 30 min. The reactions were stopped by 5% TFA. The precipitated proteins were separated from the reaction mixture by centrifugation. The supernatant was analyzed by HPLC (Shimadzu) on a C18 column (HαSprite) monitored at 260 nm absorbance, using a linear gradient from 0 to 40% buffer B in 20 min at a flow rate of 0.3 mL/min (buffer A: 50 mM ammonium acetate, pH 5.4; buffer B, 50% (v/v) methanol/water).

Detection of PhEF2 modification by methyl-^{14}C-SAM.

Enzymatic reactions with methyl-^{14}C SAM followed the similar procedure as described above. Reactions were incubated at at 37°C for 30 min. The reaction mixtures were resolved by sodium dodecyl sulfate polyacrylamide gel electrophoresis (SDS-PAGE, 12% acrylamide gel) without preheating to denature protein. The dried gel was exposed to a PhosphorImaging screen (GE Healthcare, Piscataway, NJ) which were then scanned by a STORM860 phosphorimager (GE Healthcare, Piscataway, NJ).

Characterization of PhEF2 modification with matrix-assisted laser desorption/ionization mass spectrometry (MALDI-MS) and MS/MS.

PhDph5 activity assay with normal SAM were carried out following the same procedure as that used for the activity assay with ^{14}C-labeled SAM. The mixtures were separated by SDS-PAGE (12% acrylamide gel) without heating to denature protein. The PhEF2 band from the Coomassie blue-stained gel were cut out and washed with water, 50% Ambic/acetonitrile and pure acetonitrile. Gel pieces dried in ventilated fume hood were digested by trypsin (10μg/mL) overnight in a 30°C incubator (Fisher Scientific Inc.) to cleave protein at carboxyl side of lysine or arginine into peptide fragments. Digested products were extracted and cleaned up by Ziptip C4 (Millipore). MALDI-MS was performed at the Proteomics and Mass Spectrometry Facility of Cornell University on an Applied Biosystems 4700 which was operated in positive ion

reflector mode (20kV). The matrix used was alpha-cyano-4-hydroxycinnamic acid at 3mg/ml in 60%ACN/0.1%TFA with 1mM ammonium phosphate added to suppress low m/z matrix adducts. The instrument was calibrated using calibration mix obtained from the instrument manufacturer. 1200 laser shots (80 shots/location, 15 different locations and uniform firing pattern) were used to acquire the survey spectrum from m/z 700-4000 Da. The zoomed spectrum was from m/z 1500-1700 Da. The peak of 1629.8 was further analyzed by MS/MS.

REFERENCES

1. Robinson, E. A., Henriksen, O., and Maxwell, E. S. (1974) Elongation factor 2. amino acid sequence at the site of adenosine diphosphate ribosylation, *J. Biol. Chem. 249,* 5088-5093.

2. Van Ness, B. G., Howard, J. B., and Bodley, J. W. (1980) ADP-ribosylation of elongation factor 2 by diphtheria toxin. NMR spectra and proposed structures of ribosyl-diphthamide and its hydrolysis products, *J. Biol. Chem. 255,* 10710-10716.

3. Van Ness, B. G., Howard, J. B., and Bodley, J. W. (1980) ADP-ribosylation of elongation factor 2 by diphtheria toxin. Isolation and properties of the novel ribosyl-amino acid and its hydrolysis products, *J. Biol. Chem. 255,* 10717-10720.

4. Gomez-Lorenzo, M. G., Spahn, C. M. T., Agrawal, R. K., Grassucci, R. A., Penczek, P., Chakraburtty, K., Ballesta, J. P. G., Lavandera, J. L., Garcia-Bustos, J. F., and Frank, J. (2000) Three-dimensional cryo-electron microscopy localization of EF2 in the *Saccharomyces cerevisiae* 80S ribosome at 17.5 Å resolution, *EMBO J. 19,* 2710-2718.

5. Collier, R. J. (2001) Understanding the mode of action of diphtheria toxin: a perspective on progress during the 20th century, *Toxicon 39,* 1793-1803.

6. Liu, S., Milne, G. T., Kuremsky, J. G., Fink, G. R., and Leppla, S. H. (2004) Identification of the proteins required for biosynthesis of diphthamide, the target of bacterial ADP-ribosylating toxins on translation elongation factor 2, *Mol. Cell. Biol. 24,* 9487-9497.

7. Ortiz, P. A., Ulloque, R., Kihara, G. K., Zheng, H., and Kinzy, T. G. (2006) Translation elongation factor 2 anticodon mimicry domain mutants affect fidelity and diphtheria toxin resistance, *J. Biol. Chem. 281*, 32639-32648.

8. Walsh, C. T. (2006) *Posttranslational modifications of proteins: Expanding nature's inventory*, Roberts and Company Publishers, Englewood, Colorado.

9. Dunlop, P. C., and Bodley, J. W. (1983) Biosynthetic labeling of diphthamide in *Saccharomyces cerevisiae*, *J. Biol. Chem. 258*, 4754-4758.

10. Moehring, J. M., Moehring, T. J., and Danley, D. E. (1980) Posttranslational modification of elongation factor 2 in diphtheriatoxin-resistant mutants of CHO-K1 cells, *Proc. Natl. Acad. Sci. USA 77*, 1010-1014.

11. Moehring, T. J., Danley, D. E., and Moehring, J. M. (1984) In vitro biosynthesis of diphthamide, studied with mutant Chinese hamster ovary cells resistant to diphtheria toxin, *Mol. Cell. Biol. 4*, 642-650.

12. Chen, J. Y., Bodley, J. W., and Livingston, D. M. (1985) Diphtheria toxin-resistant mutants of *Saccharomyces cerevisiae.*, *Mol. Cell. Biol. 5*, 3357-3360.

13. Mattheakis, L. C., Sor, F., and Collier, R. J. (1993) Diphthamide synthesis in *Saccharomyces cerevisiae*: structure of the DPH2 gene, *Gene 132*, 149.

14. Phillips, N. J., Ziegler, M. R., and Deaven, L. L. (1996) A cDNA from the ovarian cancer critical region of deletion on chromosome 17p13.3, *Cancer Lett. 102*, 85.

15. Schultz, D. C., Balasara, B. R., Testa, J. R., and Godwin, A. K. (1998) Cloning and localization of a human diphthamide biosynthesis-like protein-2 gene,DPH2L2, *Genomics 52,* 186.

16. Mattheakis, L. C., Shen, W. H., and Collier, R. J. (1992) DPH5, a methyltransferase gene required for diphthamide biosynthesis in Saccharomyces cerevisiae, *Mol Cell Biol 12*, 4026-4037.

17. Carette, J. E., Guimaraes, C. P., Varadarajan, M., Park, A. S., Wuethrich, I., Godarova, A., Kotecki, M., Cochran, B. H., Spooner, E., Ploegh, H. L., and Brummelkamp, T. R. (2009) Haploid genetic screens in human cells identify host factors used by pathogens, *Science 326*, 1231-1235.

18. Zhang, Y., Zhu, X., Torelli, A. T., Lee, M., Dzikovski, B., Koralewski, R. M., Wang, E., Freed, J., Krebs, C., Ealick, S. E., and Lin, H. (2010) Diphthamide biosynthesis requires an organic radical generated by an iron-sulphur enzyme, *Nature 465*, 891-896.

19. Frey, P. A., Hegeman, A. D., and Ruzicka, F. J. (2008) The radical SAM superfamily, *Crit. Rev. Biochem. Mol. Biol. 43*, 63 - 88.

20. Sofia, H. J., Chen, G., Hetzler, B. G., Reyes-Spindola, J. F., and Miller, N. E. (2001) Radical SAM, a novel protein superfamily linking unresolved steps in familiar biosynthetic pathways with radical mechanisms: functional characterization using new analysis and information visualization methods, *Nucl. Acids Res. 29*, 1097-1106.

21. Bruice, P. Y. (2007) *Organic Chemistry*, Pearson Prentice Hall, Upper Saddle River, NJ.

22. Zhang, Y., Zhu, X., Torelli, A. T., Lee, M., Dzikovski, B., Koralewski, R. M., Wang, E., Freed, J., Krebs, C., Ealick, S. E., and Lin, H. Diphthamide biosynthesis requires an organic radical generated by an iron-sulphur enzyme, *Nature 465*, 891-896.

23. Chen, J. Y., and Bodley, J. W. (1988) Biosynthesis of diphthamide in Saccharomyces cerevisiae. Partial purification and characterization of a specific S-adenosyl-L-methionine:elongation factor 2 methyltransferase, *J Biol Chem 263*, 11692-11696.

24. Cope, A. C., and Trumbull, E. R. (1960) Olefins from Amines: The Hofmann Elimination Reaction and Amine Oxide Pyrolysis, *Organic Reactions 11*, 317-493.

25. Jorgensen, R., Yates, S. P., Teal, D. J., Nilsson, J., Prentice, G. A., Merrill, A. R., and Andersen, G. R. (2004) Crystal structure of ADP-ribosylated ribosomal translocase from *Saccharomyces cerevisiae*, *J. Biol. Chem. 279*, 45919-45925.

26. Jorgensen, R., Merrill, A. R., Yates, S. P., Marquez, V. E., Schwan, A. L., Boesen, T., and Andersen, G. R. (2005) Exotoxin A-eEF2 complex structure indicates ADP ribosylation by ribosome mimicry, *Nature 436*, 979-984.

APPENDIX A

PERMISSIONS FOR REPRODUCTION

Figure 1.7. X-ray crystal structure of Biotin synthase and HydE

Reuse Figure with permission from Duschene, K.S., Veneziano, S.E., Silver, S.C., Broderick, J.B. *Current Opinion in Chemical Biology* **2009**; *13(1):74-83* Copyright 2009, Elsevier

The order details and publisher terms and conditions are available by clicking the link below:

https://s100.copyright.com/CustomerAdmin/PLF.jsp?lID=2010120_1291577960159

Chapter 2: Reproduced in part with permission from Zhang, Y. & Zhu, X. et al. *Nature.* **2010,** *465,* 891-896

Copyright 2010 Nature Publishing Group.

The order details and publisher terms and conditions are available by clicking the link below:

http://s100.copyright.com/CustomerAdmin/PLF.jsp?lID=2010111_1291060738303

Chapter 3: Reproduced by permission of The Royal Society of Chemistry via email; Zhu, X. et al. Mol Biosyst. 2011 Jan 1;7(1):74-81. Epub 2010 Oct 8.Copyright 2011 © Royal Society of Chemistry 2010.

Chapter 4: Reproduced with permission from Zhu, X et al. *Biochemistry*, **2010**, *49* (44), pp 9649–9657

Copyright © 2010 American Chemical Society

The order details and publisher terms and conditions are available by clicking the link below:

https://s100.copyright.com/CustomerAdmin/ViewLicense.jsp